Fundamental study of small-scale processes in the atmosphere and in the ocean

Caroline Muller

Mémoire présenté pour obtenir l'Habilitation à Diriger des Recherches HDR

Caroline Muller

Laboratoire de Météorologie Dynamique
Institut Pierre-Simon Laplace
muller@lmd.ens.fr

Fundamental study of small-scale processes in the atmosphere and in the ocean

Étude fondamentale de processus à petite échelle dans l'atmosphère et dans l'océan

---

September 18th, 2019, 2pm
École Normale Supérieure de Paris

Jury:

Chantal Staquet (reviewer)
Bjorn Stevens (reviewer)
Frank Roux (reviewer)
Hélène Chepfer
Christopher Holloway
Philippe Drobinski

Acknowledgments

I would first like to thank members of the jury for their time. This work would not have been possible without the precious contributions from many talented students, postdoctoral researchers, and collaborators. I learn from them every day, which is what makes this job so exciting and rewarding. I would particularly like to thank my friends and colleagues from LadHyX and LMD, including Océane Richet, Sara Shamekh, Adrien Lefauve, Keshav Raja, Nicolas Da Silva, Jean-Marc Chomaz, Sandrine Bony, Sabrina Speich, Philippe Drobinski... Our numerous discussions, on science and on other topics, are invaluable to me and to my research. Finally I would like to thank Venance Journe, Jean-Yves Grandpeix, and Alain Lahellec whom we miss, for allowing me to work in their office when I am in jussieu (aka UPMC aka SU). I thank my family, Emmanuel, Margot, Adèle, and the guy who discovered coffee for their support along the way.

I will end with a Shadok proverb, which I have always found quite inspiring:

Shadok proverb: "If there is no solution, then there must be no puzzle."

French abstract: "Résumé"

De manière générale, mes activités de recherche portent sur la dynamique des fluides géophysiques et les fluides stratifiés. Je suis particulièrement intéressée par l'étude des phénomènes aux échelles trop petites pour permettre leur résolution explicite dans les modèles climatiques globaux actuels (**GCMs**). Deux exemples importants sur lesquels je travaille sont les ondes internes océaniques, et la convection nuageuse atmosphérique. Ces phénomènes aux petites échelles doivent être paramétrés dans les GCMs, afin d'améliorer les prévisions climatiques.

Le but de mes recherches est d'utiliser des outils théoriques et numériques, aussi bien les modèles haute résolution en configuration idéalisée que les GCMs globaux, pour une meilleure compréhension fondamentale de ces phénomènes, en vue d'améliorer les prévisions climatiques actuelles.

Plus précisément, les questions auxquelles je me suis intéressée ces dernières années sont :

- Quel est le rôle de la topographie sous-marine dans la génération d'ondes internes dans l'océan? Quelle est la contribution de ces ondes au mélange océanique, et quel impact sur la circulation océanique grande échelle?
  Les ondes internes sont omniprésentes dans l'océan et participent donc du bilan énergétique global des océans. Mais leurs échelles sont trop petites pour être explicitement résolues dans les GCMs. Leur effet sur les masses d'eau et sur la circulation globale doit donc être paramétré. La circulation océanique n'est pas seulement un sujet fascinant, c'est aussi un ingrédient essentiel de la prévision climatique. Le but de mes recherches est de clarifier les processus physiques menant à l'instabilité et au déferlement de ces ondes, ainsi que de quantifier le mélange induit par ce déferlement.

- Quelle est la réponse du cycle hydrologique (précipitations moyennes et précipitations extrêmes) au changement climatique?
  Comprendre la réponse du cycle hydrologique au réchauffement climatique est une question cruciale, avec d'importants impacts sociétaux. De nombreuses études, utilisant des modèles régionaux à haute-résolution aussi bien que des modèles globaux à basse résolution, prédisent une augmentation de l'intensité des précipitations extrêmes avec le réchauffement climatique. L'origine physique de cette augmentation est bien comprise, grâce à de nombreuses études théoriques, notamment son lien étroit avec une contrainte thermodynamique (liée à l'augmentation de vapeur d'eau atmosphérique). Mais si cette contribution thermodynamique est bien comprise, des incertitudes persistent concernant les contributions dynamique (liée aux vitesses verticales dans les nuages) et microphysique (liée à l'efficacité des pluies). Mes travaux s'intéressent à quantifier ces différentes contributions, dans des simulations idéalisées, sans et avec organisation spatiale des nuages.

- Quelle est l'origine physique de l'organisation spatiale des nuages dans les tropiques? L'exemple le plus spectaculaire d'organisation spatiale de la convection nuageuse est sans nul doute le cyclone tropical, avec son oeil entouré d'un mur nuageux abrupt, où l'on trouve les vents parmi les plus violents sur notre planète. Il existe d'autres types de convection spatialement

organisée (convection fait référence aux mouvements de l'air dans lesquels les nuages sont insérés); en effet la convection organisée est omniprésente dans les tropiques. Mais elle est encore mal comprise et mal représentée dans les paramétrisations convectives des GCMs, malgré son fort impact sociétal et climatique. Un des buts de mes recherches est de clarifier les processus physiques à l'origine de cette organisation spatiale des nuages, et d'étudier leur réponse au réchauffement climatique.

Ces questions sont aujourd'hui clefs pour mieux comprendre les conséquences du changement climatique et les événements extrêmes, tels que les cyclones tropicaux. Elles sont également très importantes pour comprendre le rôle des phénomènes petites échelles dans la circulation océanique à grande échelle, et donc l'évolution du climat et des écosystèmes. Mon document d'HDR décrit en détail les résultats scientifiques majeurs de mes recherches sur ces trois questions obtenus depuis mon arrivée au CNRS en 2012.

Content

Chapter I

Introduction: general overview, context, and goal of my research activities

"If we knew what it was we were doing, it would not be called research, would it?"
Albert Einstein

My research interests lie in the fields of geophysical fluid dynamics and climate science. I am particularly interested in the study of processes which are too small in space and time to be explicitly resolved in coarse-resolution Global Climate Models (GCMs) used for climate prediction. Important examples that I work on are internal wave breaking in the ocean and cloud processes in the atmosphere. These small-scale, subgrid processes need to be parametrized in GCMs in order to improve current model projections of climate change.

The overall goal of my research activities is to use theoretical and numerical models, from idealized high-resolution simulations to global GCMs in realistic configuration, in order to improve our fundamental understanding of these small-scale processes. My ultimate goal is to help guide and improve GCM parameterizations, for better climate projections.

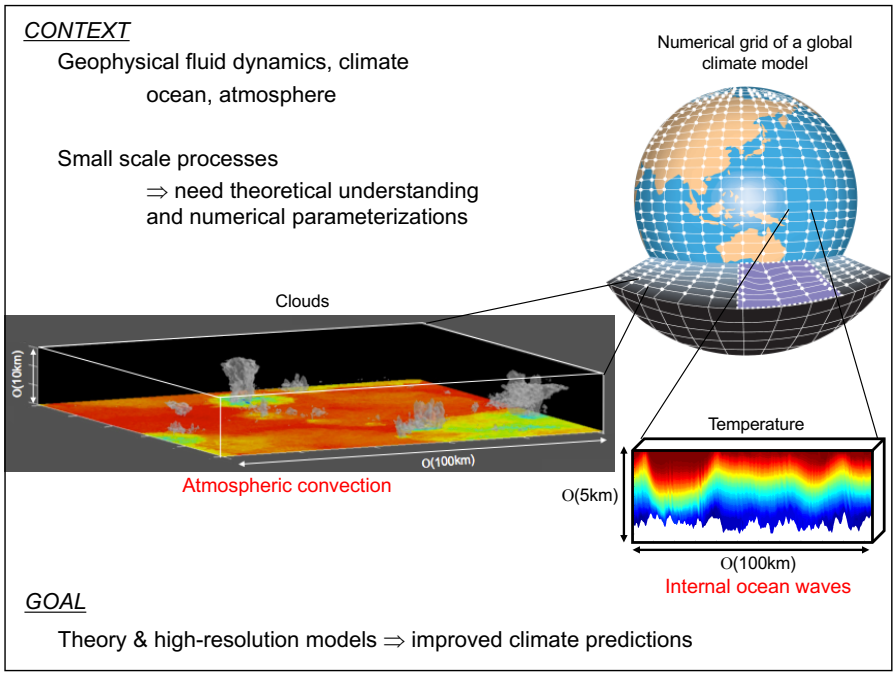

Figure I.1: *The overall goal of my research activities is to improve our fundamental understanding of climate processes with scales smaller than a typical GCM resolution (tens to hundreds of kilometers). Important examples of such subgrid-scale processes that I work on are internal waves in the ocean, and convective clouds in the atmosphere.*

More specifically, my research activities focus on three main topics:

- What role does the small-scale seafloor topography play in the generation of internal waves in the abyssal ocean? What is the contribution of those internal waves to ocean mixing, and what impact on the ocean large-scale circulation?
  Internal waves are ubiquitous in the ocean, and contribute significantly to the ocean global energetics. But their scales are too small, both in space and time, to be explicitly resolved in GCMs. Thus their effect on water masses and on the large-scale ocean circulation must be parameterized. The goal of my research is to clarify the physical mechanisms leading to

the instability, overturning and breaking of those waves, as well as to quantify the mixing induced by wave breaking events.

- What is the response of the hydrological cycle (both mean precipitation and extreme precipitation) to global warming?
  Understanding the response of precipitation extremes to climate change is a crucial question, with important societal impacts. Numerous studies, using both regional high-resolution models and global coarse-resolution models, predict an increase of the intensity of precipitation extremes with warming. The physical origin of this increase is well understood, thanks to numerous theoretical studies, notably its link with a strong thermodynamic constraint (related to water vapor). But if the thermodynamic contribution to precipitation extremes is well understood, a large uncertainty remains regarding the dynamic contribution linked to vertical velocities in updrafts, and the microphysics contribution related to precipitation efficiency. My work aims at quantifying these contributions, in idealized simulations without and with convective organization.

- What are the physical processes responsible for the organization of tropical clouds?
  Arguably, the most spectacular example of organized convection is the tropical cyclone, with its eye devoid of deep convection, surrounded by a cloudy eyewall where extreme winds are found. There are other types of organized convection, (convection refers to the overturning of air within which clouds are embedded). In fact, organized convection is ubiquitous in the tropics. But it is still poorly understood and typically not accounted for in global climate models, despite strong societal and climatic impacts. One of the goals of my research is to clarify the physical processes responsible for organizing convection, and to investigate their response to climate change.

These questions have important societal impacts. They are key to improving our understanding of the consequences of climate change, notably on extreme events such as tropical cyclones. Clarifying the role of small-scale processes on the large-scale ocean circulation is also crucial to help determine the evolution of ecosystems in our warming climate.

In the following three chapters (II, III and IV), I describe in detail the major scientific outcomes of my research activities in those three topics. Each of these three chapters starts with a summary of the main scientific results and main collaborations/supervisions of students/postdocs relevant to each topic. This summary is followed by an introduction describing the scientific context and state-of-the-art, and then by my scientific contributions to the field. Unless otherwise noted, in this report I will focus on results that were obtained since I joined the CNRS in 2012.

This manuscript ends with a chapter (V) on my perspectives and future research directions, as well as outstanding open questions.

Chapter II

Dissipation of internal tides in the abyssal ocean: linear and nonlinear processes

"How inappropriate to call this planet Earth when it is quite clearly Ocean."
Arthur C. Clarke

II.1 Summary of key results, main collaborations and relevant supervisions

- *Key results: linear study*

  Internal tides are internal waves generated by the interaction of the barotropic tide with the seafloor topography. The breaking of those waves, and the concomitant dissipation of their energy, is believed to provide a large part of the power needed to mix the abyssal ocean and sustain the meridional overturning circulation. State-of-the-art topographic products barely resolve scales smaller than $\approx$ 10 km in the deep ocean. On these small scales, abyssal hills dominate ocean floor roughness.

  In **[Melet et al., 2013b]**, we use linear wave theory to evaluate the impact of abyssal hill roughness on internal-tide generation. We find that globally, internal tide generation by abyssal hills integrates to $\approx 10\%$ of the energy flux due to larger topographic scales resolved in standard topographic products. Locally, the abyssal hill contribution to the internal tide energy flux can exceed 100%, notably above the Mid-Atlantic ridge. Therefore, abyssal hills, unresolved in state-of-the-art topographic products, can have a strong impact on internal tide generation, especially over mid-ocean ridges.

  This analysis of internal tides generation at small-scale topography, is extended further in **[Lefauve et al., 2015]**, where we use an ad-hoc parameterization of wave breaking developed during my PhD [Muller and Bühler, 2009] to quantify the mixing induced by breaking internal tides. We show that a large fraction of abyssal-hill generated internal tide energy is locally dissipated over mid-ocean ridges in the southern hemisphere. Significant dissipation occurs above ridge crests, and, upon rescaling by the local stratification, follows a monotonic exponential decay with height off the bottom, with a nonuniform decay scale.

  Overall, these results from linear theory imply stronger internal-tide induced mixing than previously estimated from larger-scale bathymetry. This additional tidal mixing has been implemented in a GCM parametrization of ocean mixing [De Lavergne et al., 2016].

- *Key results: nonlinear study*

  Beyond linear predictions, internal tides (and internal waves in general) are known to be subject to nonlinear processes, which can lead to wave instability and overturning, and thus to the mixing ultimately relevant to the large-scale ocean circulation. Notably, previous numerical studies of the dissipation of internal tides in idealized settings, highlight the importance of nonlinear transfer of energy to small-scale secondary waves via the parametric subharmonic instability, or PSI. This triadic instability is favored at a specific resonant latitude, known in the literature as the critical latitude. Consistently, these numerical studies exhibit a large enhancement of internal tide dissipation at the critical latitude.

  In **[Richet et al., 2018]**, we clarify the physical processes at the origin of this strong latitudinal dependence of tidal energy dissipation. We find that different mechanisms are involved equatorward and poleward of the critical latitude. Triadic resonant instabilities are responsible for the dissipation of internal tides equatorward of the critical latitude. In particular, a dominant triad involving the primary internal tide and near-inertial waves is key. At the critical latitude, the peak of energy dissipation is explained by both increased instability growth rates, and smaller scales of secondary waves thus more prone to break

and dissipate their energy. Surprisingly, poleward of the critical latitude, the generation of evanescent waves appears to be crucial. Triadic instabilities have been widely studied, but the transfer of energy to evanescent waves has received comparatively little attention. Our work suggests that the nonlinear transfer of energy from the internal tide to evanescent waves, corresponding to the 2f-pump mechanism described by [Young et al., 2008] is an efficient mechanism to dissipate internal tide energy near and poleward of the critical latitude.

Observations instead indicate a more modest enhancement at the critical latitude. We address this issue in **[Richet et al., 2017]** by investigating the impact of a weak background mean current in numerical simulations. The dissipation and its variation with latitude without the mean current are consistent with earlier studies. But adding a weak mean current has a major impact on the latitudinal distribution of dissipation. This behavior can be attributed to the Doppler shift of the internal tides frequency, which hinders the energy transfer to secondary waves of the unstable triads. Thus, although nonlinear transfers of energy between waves are efficient at dissipating internal tides, the exact location of the dissipation is sensitive to large-scale oceanic conditions, including the presence of large-scale currents or mesoscale eddies, which can impact the propagation and dissipation of internal tides.

- *Main collaborations and relevant supervisions*

  The linear study was performed by **Adrien Lefauve** during his Masters internship under my supervision at LadHyX. Adrien is now doing a PhD at the University of Cambridge UK with Paul Linden. This work was also done in collaboration with **Angélique Melet**, postdoctoral researcher at LEGOS Toulouse at the time, now researcher at MERCATOR.

  The nonlinear study was performed by **Océane Richet** during her PhD at LadHyX. This PhD was co-supervised by myself and my collaborator **Jean-Marc Chomaz**, senior researcher at LadHyX. Océane is now doing a three-year postdoc at the University of Tasmania with Bernadette Sloyan and Maxim Nikurashin.

In this chapter, we summarize the key results obtained in these studies, with a particular focus on the nonlinear process study [Richet et al., 2018].

II.2 Introduction to internal tides induced mixing: what we know, what we dont know

II.2.a What are internal tides?

The presence of celestial bodies (in particular the moon and the sun) induces a barotropic current in the ocean, known as the barotropic tide. Without topography, this flow represents the usual solution to the tidal equation. In the presence of topography, this barotropic tide interacts with the seafloor resulting in the radiation of internal waves, known as the *internal tides* (see e.g. [Garrett and Kunze, 2007] for a review).

Internal waves are waves within stably-stratified fluids. In the case of a rotating stratified fluid with Brunt-Väisälä frequency N (> 0 for stable stratification) and Coriolis parameter f assumed constant, those waves of the form $\propto e^{i(\mathbf{k}.\mathbf{x}-\omega t)}$ satisfy the well-known dispersion relation (obtained from the linearized equations under the Boussinesq approximation, see e.g., [Staquet and Sommeria,

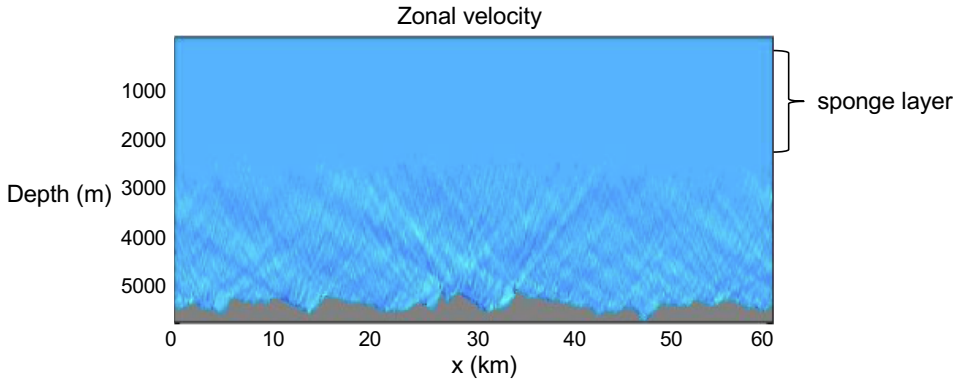

Figure II.1: *Illustration of internal waves in the high-resolution model used in the nonlinear study (§II.4), namely the MITgcm [Marshall et al., 1997]. The waves are generated as an imposed barotropic current* $\mathbf{U(t)} = (U_0 \sin \omega_0 t, 0)$ *interacts with the bottom rough bathymetry (adapted from [Richet et al., 2017]). We investigate the generation of internal tides at the seafloor, and thus neglect the effect of waves reflecting at the ocean surface and radiating back down towards the topography. Thus a sponge layer is imposed in upper levels in order to absorb upward propagating waves (following [Nikurashin and Legg, 2011]).*

2002, Bühler and Muller, 2007]):

$$\omega^2 = N^2 \cos^2 \theta_k + f^2 \sin^2 \theta_k, \tag{II.1}$$

where θ_k denotes the angle between the wave vector $\mathbf{k} = (k_x, k_y, k_z)$ and the horizontal. This dispersion relation yields several interesting properties to internal waves.

First the group velocity and phase velocity have opposite vertical components. In other words, for internal waves, if the phase goes down, the energy goes up, and vice-versa. Second, the frequency of internal waves has magnitude between f and N. In typical oceanic conditions, $|f| < N$, so that $|f| < |\omega| < N$. Third, the angle of propagation of the wave depends solely on their frequency - the higher the frequency, the steeper (more vertical) the slope of the group velocity rays.

Figure II.1 illustrates the generation of internal tides in high-resolution simulations, when an imposed barotropic tide $\mathbf{U(t)} = (U_0 \sin \omega_0 t, 0)$ interacts with the seafloor topography. In this simulation, $\mathbf{U(t)}$ is the semi-diurnal lunar tide, so that ω_0 is the semi-diurnal tidal frequency (approximately twice a day). As predicted by linear theory [Bell, 1975], this interaction generates waves at this fundamental tidal frequency, as well as harmonics at higher frequency $(2\omega_0, 3\omega_0...)$, seen by some steeper rays corresponding to waves with higher frequencies on figure II.1.

II.2.b Why do we care?

The dissipation of internal tides through wave breaking and concomitant three-dimensional turbulence contributes to vertical mixing in the deep ocean, and hence plays a role in the large-scale ocean circulation. Indeed, the turbulent mixing associated with breaking waves makes a significant contribution to the diffusion of fluid particles across density surfaces [Staquet and Sommeria, 2002], which is important for the maintenance of the stratification in the deep ocean (e.g., [Wunsch and Ferrari, 2004]).

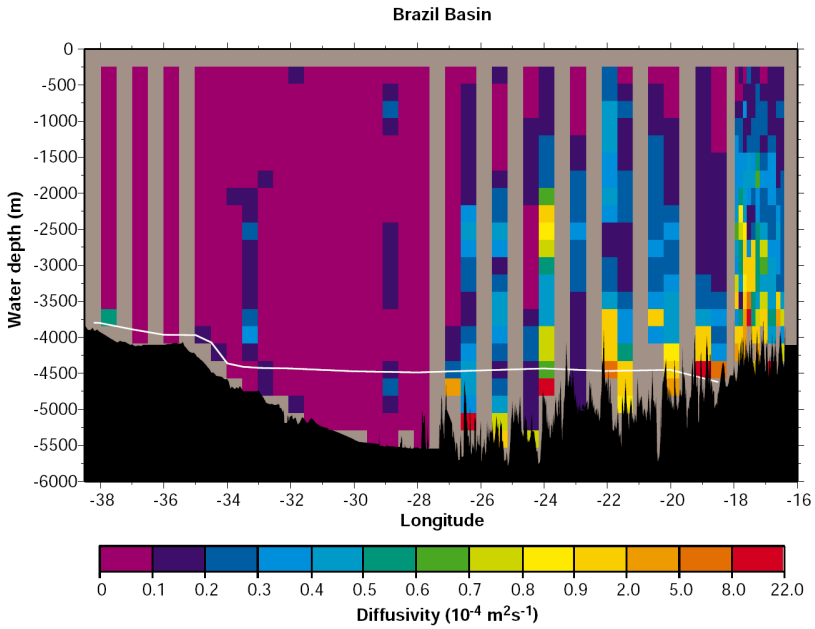

Figure II.2: *Depth-longitude section of diapycnal diffusivity in the Brazil Basin from [Polzin et al., 1997]. There is a clear signal of enhanced vertical mixing over rough topography.*

Consistently, greatly elevated values of diapycnal diffusivities are found over the rough bathymetry of the Mid-Atlantic ridge, where bottom values can reach several orders of magnitude higher than the pelagic value 0.1 $cm^2\ s^{-1}$ (figure II.2). These observed enhanced mixing rates were attributed to the dissipation of the internal tides, although other mechanisms could also contribute to high bottom diffusivities, such as lee waves generated by mesoscale eddies interacting with the bathymetry [Nikurashin et al., 2013, Sommeria et al., 2016], or the hydraulic flow of dense bottom waters through constrictive passages at the seafloor [Legg, 2014].

In recent years, the emerging consensus is that this tidally-induced mixing is important for the dynamics of the large-scale ocean circulation in the deep abyssal ocean, below 1500 m depth or so (e.g., [Munk and Wunsch, 1998], [Wunsch, 2000], and the reviews in [Wunsch and Ferrari, 2004] and [Thorpe, 2005]). As schematically depicted in figure II.3, the dense Antarctic bottom water, or AABW, sinks at high latitudes in the southern Ocean. Mixing processes, to which internal tides contribute significantly, lift up deep waters to mid-depths, likely to 1000 - 2000 m above the seafloor (the red line indicates maximum height of topographic features below which mixing is strong). These deep waters return to the surface at these depths via the southern Ocean [Ferrari, 2014, Waterhouse et al., 2014].

Numerical models have been shown to be sensitive to diffusivity values, from simple idealized models [Nikurashin and Vallis, 2012] to state-of-the-art GCMs [Melet et al., 2013a]. But as mentioned in the introduction, these internal wave processes are far too small in spatial and/or temporal scale to be resolved in climate models. Thus theory, high-resolution modeling and observations must be used to parametrize their effects in such models. One of our goals is to get a better understanding of the role of internal tides dissipation in ocean mixing, and how it relates to the bathymetry. Of particular interest is the degree of spatial inhomogeneity of the mixing induced by breaking internal tides. This spatial variability in the mixing, both horizontally and vertically,

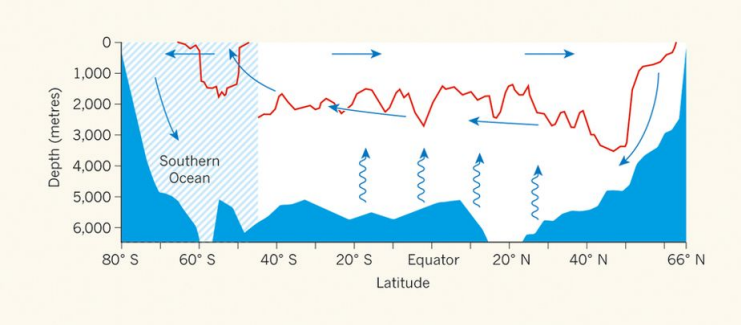

Figure II.3: *Emerging model of the deep-ocean circulation from models and observations. The red line represents the height of the tallest topographic features below which mixing is strong (adapted from [Ferrari, 2014]).*

could imply a radically different interior circulation in models than that obtained with uniform mixing schemes.

II.2.c Ocean mixing: questions addressed

Quantitatively, very large uncertainties remain, notably on the amount of local (near the generation site at the seafloor) versus remote dissipation of internal tides. Observations indicate that the local dissipation of internal tides near their generation site could be up to 70 - 100 % in regions with small-scale rough topography, but is believed to be smaller without small-scale topographic roughness [Waterhouse et al., 2014]. Large uncertainties also remain regarding the remotely dissipating internal tides, which could contribute to Antarctic bottom water consumption between 1 and 28 Sv depending on the amount and vertical structure of the corresponding wave-induced mixing [De Lavergne et al., 2016].

In this work, we address the following questions:

- What is the fraction of wave energy dissipated locally near the generation site?
- How is this dissipation distributed spatially?
- What mechanisms lead to internal tides instability, breaking and dissipation (convective instability? nonlinear effects?...)?

Our focus is thus on the local dissipation of internal tides near their generation site. The ultimate fate of the remaining fraction of wave energy which propagates away is an important question, but is beyond the scope of this work.

II.3 My research: local dissipation of internal tides via convective instability, results from linear theory

II.3.a Wave energy carried by internal tides

This section is based on the paper

A. Melet, M. Nikurashin, C. Muller, S. Falahat, J. Nycander, P. Timko, B. Arbic, J. Goff
Internal tide generation by abyssal hills using analytical theory
J. Geophys. Res. - Oceans, 118 (2013).

We first quantify the amount of energy carried by the internal tides upon generation at small-scale topography. One of the main results of my Ph.D. thesis is that the wave breaking and concomitant mixing are extremely sensitive to small topographic scales, smaller that 10 km or so [Muller and Bühler, 2009]. These scales are smaller than the current resolution of global bathymetry from satellites [Smith and Sandwell, 1997]. We thus need to take a statistical approach to investigate the contribution from small topographic scales to the generation of internal tides.

Taking this statistical approach to represent the small-scale seafloor (mainly abyssal hills at those scales), we quantify the energy carried by the internal tides generated at small-scale topography, using the linear wave theory. Internal tide generation by abyssal hills integrates to 0.1 TW globally, or 0.03 TW when the energy flux is empirically corrected for supercritical slope (i.e., 10 % of the energy flux due to larger topographic scales resolved in standard topographic products in both cases). The abyssal hill driven energy flux is dominated by mid-ocean ridges, where abyssal hill roughness is large. Focusing on two regions located over the Mid-Atlantic ridge and the East Pacific rise, it is shown that regionally linear theory predicts an increase of the energy flux due to abyssal hills of up to 100 % or 60 % when an empirical correction for supercritical slopes is attempted. Therefore, abyssal hills, unresolved in state-of-the-art topographic products, can have a strong impact on internal tide generation, especially over mid-ocean ridges. These results have been implemented in an ocean mixing parametrization [De Lavergne et al., 2016], and the variability of the mixing that it entails affects the large-scale ocean circulation.

II.3.b Local dissipation of internal tides via convective instability

This section is based on the paper

A. Lefauve, C. Muller, A. Melet
A three-dimensional map of tidal dissipation over abyssal hills
J. Geophys. Res. - Oceans, 120 (2015).

Here we investigate the fraction of the internal tide energy which gets dissipated near their generation site at the seafloor by convective instability. Both the fraction of internal tide energy that is dissipated locally and the resulting vertical mixing distribution are crucial for the ocean state, but remain poorly quantified. Current parameterizations in GCMs typically assume that a constant fraction of the energy carried by the internal tides is dissipated through wave breaking (for instance 50 % in the parameterization mentioned above [De Lavergne et al., 2016]), and that the induced mixing decays exponentially from topography where the waves are generated.

In order to more precisely quantify the fraction of tidal energy dissipated through wave breaking, as well as its vertical distribution over topography, we use a heuristic model for wave breaking developed during my Ph.D. thesis [Muller and Bühler, 2009]. This model uses the wave amplitude (also known as wave steepness in the literature e.g. [Staquet and Sommeria, 2002]) estimated from linear theory, to predict regions of convective instability and wave breaking. Combined with a nonlinear parameterization for wave breaking, it also yields an estimate of the amount of wave energy dissipated by the wave breaking events. This heuristic model can be applied to various topographies, idealized [Bühler and Muller, 2007] or realistic [Muller and Bühler, 2009], to obtain an estimate of the tidal dissipation.

We extend this model to account for stratification variations within the WentzelKramersBrillouin, or WKB, approximation, and derive the first global map of mixing due to internal tides generated at small-scale abyssal hills (figure II.4). Our estimate is based on quasi-global small-scale abyssal hill bathymetry, stratification, and tidal data. We show that a large fraction of abyssal-hill generated internal tide energy is locally dissipated over mid-ocean ridges in the southern hemisphere. Significant dissipation occurs above ridge crests, and, upon rescaling by the local stratification, follows a monotonic exponential decay with height off the bottom, with a nonuniform decay scale. We however show that a substantial part of the dissipation occurs over the smoother flanks of mid-ocean ridges, and exhibits a middepth maximum due to the interplay of wave amplitude with stratification.

We link the three-dimensional map of dissipation to abyssal hills characteristics, ocean stratification, and tidal forcing, and discuss its potential implementation in time-evolving parameterizations for GCMs. Although linear theory, on which our heuristic model is based, may overestimate the occurrence of convective instability, we believe that qualitatively the non-homogeneous spatial distribution of wave energy dissipation that it predicts is robust. Our results suggest that the presence of small-scale, mostly unresolved abyssal hills could significantly enhance the spatial inhomogeneity of tidal mixing, particularly above mid-ocean ridges in the southern hemisphere.

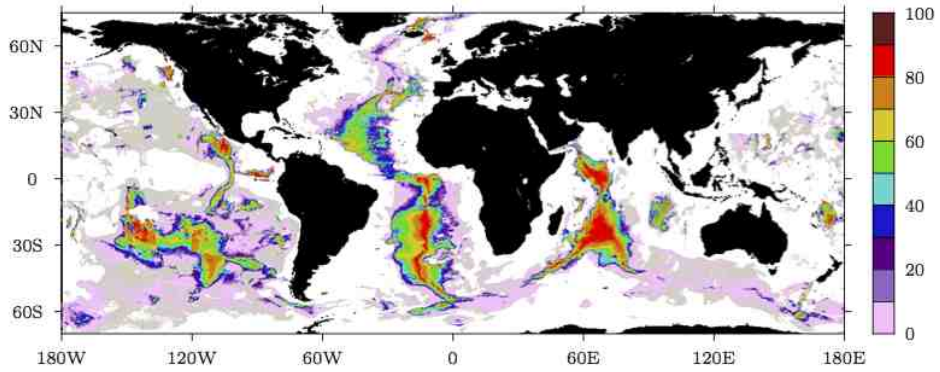

Figure II.4: *Fraction (in %) of energy carried by the internal tides generated at small-scale seafloor topography, which is dissipated by wave breaking (from [Lefauve et al., 2015]).*

II.4 My research: local dissipation of internal tides via nonlinear effects, catastrophic dissipation via Parametric Subharmonic Instability (PSI)?

II.4.a Dissipation by nonlinear wave-wave interactions

This section is based on the paper

O. Richet, J.-M. Chomaz, C. Muller

Internal tide dissipation at topography: triadic resonant instability equatorward and evanescent waves poleward of the critical latitude

J. Geophys. Res. - Oceans, 123 (2018).

Beyond the linear evolution of the internal tides investigated in the previous section, vigorous nonlinear interactions can transfer energy from the internal tides into secondary waves. In this section, we investigate these energy transfers in detail. In the case of internal tides, this transfer depends on latitude in a non trivial way, with a critical latitude where dissipation is maximum ($\approx$ 30° latitude, see figure II.5). This critical latitude corresponds to the latitude where the Coriolis frequency f matches half the semi-diurnal tidal frequency $\omega_0/2$ (without loss of generality, we set the tidal frequency $\omega_0 > 0$ and we place ourselves in the northern hemisphere so that $f \geq 0$; the same applies in the southern hemisphere with $|f| = \omega_0/2$). It has thus been suggested that triadic resonant instabilities are responsible for the transfer of energy from the primary internal tide into smaller-scale secondary waves. More precisely, the parametric subharmonic instability is believed to play a key role.

A triadic resonant instability is an instability leading to energy transfer from a primary wave (frequency ω_0, wavenumber vector $\mathbf{k_0}$) to secondary waves (with frequencies ω_1, ω_2 and wavenumber vectors $\mathbf{k_1}$, $\mathbf{k_2}$) satisfying the resonance condition:

$$\omega_0 = \omega_1 + \omega_2 \tag{II.2}$$

$$\mathbf{k_0} = \mathbf{k_1} + \mathbf{k_2}. \tag{II.3}$$

When both secondary waves have their frequencies equal to $\omega_0/2$, we call this specific triadic resonant instability, the Parametric Subharmonic Instability ([Staquet and Sommeria, 2002, Bourget et al., 2013, Maurer et al., 2016]). At the critical latitude, where $\omega_0/2 = f$, the secondary waves are near-inertial waves with same frequency $\omega_1 = \omega_2 = \omega_0/2 = f$. In this study, we investigate in detail the physical process behind this enhanced mixing at the critical latitude, and its link with the generation of secondary waves.

Methodology

To that end, we use linear stability analysis and two-dimensional direct numerical simulations with the model MITgcm, as illustrated in figure II.1. The use of high resolution ($dx = 30$ m, $dz = 10$ m) allows to resolve waves and overturning, and part of the inertial range. The resolution is not sufficient though to reach dissipative scales, and following [Nikurashin and Legg, 2011] we use slightly enhanced viscosity and diffusivity values ($\nu_h = \nu_v = 2 \times 10^{-3}$ m s^{-1} and $\kappa = 10^{-4}$ m s^{-1} respectively). Results are found to be insensitive to reasonable changes of those values (as long as part of the inertial range is resolved).

Internal tides are generated by a barotropic flow (at the semi-diurnal frequency ω_0) interacting with an idealized sinusoidal topography. The choice of a simple idealized sinusoidal topography is motivated by the fact that the dissipation profiles and magnitudes are found to be similar to those obtained with a realistic topography spectrum, as long as the vertical and horizontal Froude numbers are the same [Richet et al., 2017]. We therefore use realistic horizontal and vertical Froude numbers representative of small-scale seafloor bathymetry of the Brazil basin. With this choice, the sensitivity of dissipation to latitude and the physical processes involved in our simulations are relevant, at least qualitatively, to more realistic conditions representative of the deep ocean in the region of the Brazil basin. The simulations are repeated at different latitudes, i.e. at different values of the Coriolis frequency f.

Results equatorward of the critical latitude

We start by analyzing the wave energy frequency distribution as a function of latitude (figure II.6). Equatorward of the critical latitude, we find that dominant frequencies in the domain are ω_0,

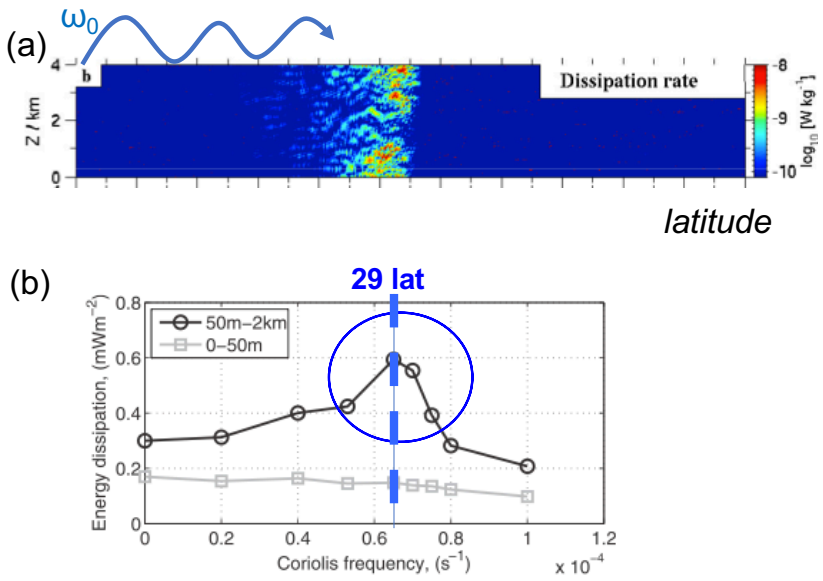

Figure II.5: *(a) Numerical simulation of a low vertical mode (i.e. $1/k_z$ comparable to the ocean depth) internal tide at frequency ω_0 propagating from low latitudes (blue arrow). Colors show the wave energy dissipation rate at a function of water depth. Enhanced dissipation is seen to occur at a critical latitude of about 30° latitude (adapted from [MacKinnon and Winters, 2005]). (b) This enhanced dissipation is confirmed in another set of simulations using the MITgcm for small scale internal tides (i.e. $1/k_z$ small compared to the ocean depth, simulations similar to the one shown figure II.1). Shown in black is the wave energy dissipation integrated from 50 m to 2 km above the seafloor. Simulations at different Coriolis frequency f, and thus at different latitudes, are performed. Once again enhanced dissipation at the critical latitude is found (adapted from [Nikurashin and Legg, 2011]).*

the primary internal tide, but also waves at frequency close to f, i.e., near-inertial waves, and at frequencies close to $(\omega_0 - f)$. These results suggest that the physical mechanism responsible for the energy transfer from internal tides to smaller-scale secondary waves is the formation of resonant triads between the primary internal tide, near-inertial waves and waves at frequencies $(\omega_0 - f)$.

The growth rate of resonant triadic instabilities as a function of the frequency of secondary waves ω_1 is shown figure II.7. We find that for all f, the growth rate is strictly positive, thus the dissipation of energy of the primary tidal wave at ω_0 is indeed the result of triadic resonant instabilities. But it does not help explain the leading triad $(\omega_0, f, \omega_0 - f)$, as the magnitude of the growth rate is not very different (between 1 and 1.5 s^{-1}) for all secondary wave frequencies between f and $\omega_0 - f$, and does not have a maximum at f or $\omega_0 - f$. We interpret the accumulation of wave energy at f and $\omega_0 - f$ as being the consequence of the small vertical group velocity of near-inertial waves. Further analysis of the wave energy spectrum ([Richet et al., 2018]) shows that the leading order triad involves downward propagating near-inertial waves and upward propagating waves at frequency $\omega_0 - f$, consistent with the accumulation of near-inertial wave energy in the domain near the topography.

The enhanced dissipation at the critical latitude can be attributed to changing properties of the secondary waves as f increases towards $\omega_0/2$ (figure II.7). The vertical wavenumber of secondary

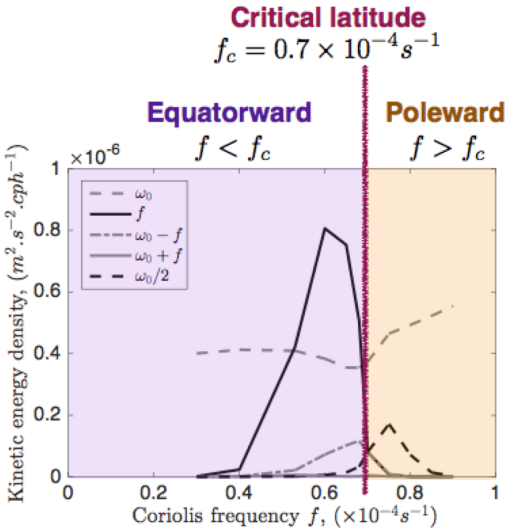

Figure II.6: *Latitudinal evolution of the kinetic energy density for the leading frequencies in the domain, including the primary internal tide ω_0 (gray dashed), inertial waves f (black plain) and waves at frequencies $(\omega_0 - f)$ (gray point-dashed) and $\omega_0/2$ (black dashed). The vertical purple line materializes the critical latitude (adapted from [Richet et al., 2018]).*

waves increases, yielding smaller and smaller scales more prone to wave breaking and dissipation. The growth rate of the corresponding resonant triad also increases as f approaches the critical latitude. Both effects lead to enhanced dissipation, consistent with the latitudinal profiles of figure II.5.

Results poleward of the critical latitude

Poleward of the critical latitude, on the other hand, the dominant frequencies in the kinetic energy spectrum (figure II.6) are the primary internal tide at ω_0 and evanescent waves at $\omega_0/2$ (these are evanescent since $\omega_0/2 < f$). This result suggests the transfer of energy to smaller-scale evanescent near-inertial waves as the dominant physical process leading to the dissipation of the primary internal tide poleward of the critical latitude.

Recently, [Young et al., 2008] extended the parametric subharmonic instability poleward of the critical latitude. In their theory, the dissipation of a primary wave at frequency $\omega_0 = 2f + \epsilon$ is investigated for small positive and negative ϵ. Briefly, the Boussinesq equations are linearized about a "pump wave" whose frequency is close to twice the inertial frequency. A multiple-timescales approach yields an amplitude equation describing how this pump wave energizes a vertical continuum of near-inertial oscillations. Qualitatively, in our simulations, the generation of secondary waves at $\omega_0/2$ beyond the critical latitude is consistent with their theoretical expectation. Furthermore, quantitatively, they predict a cut-off latitude beyond which the mechanism halts, corresponding with our parameter values to $f \approx 0.8$, matching the extent of enhanced dissipation (figure II.5b) and $\omega_0/2$ secondary waves (figure II.6).

Discussion

Thus, triadic resonant instabilities are found to be a powerful mechanism to extract tidal energy. The increase of energy dissipation from the equator toward the critical latitude is due to increased

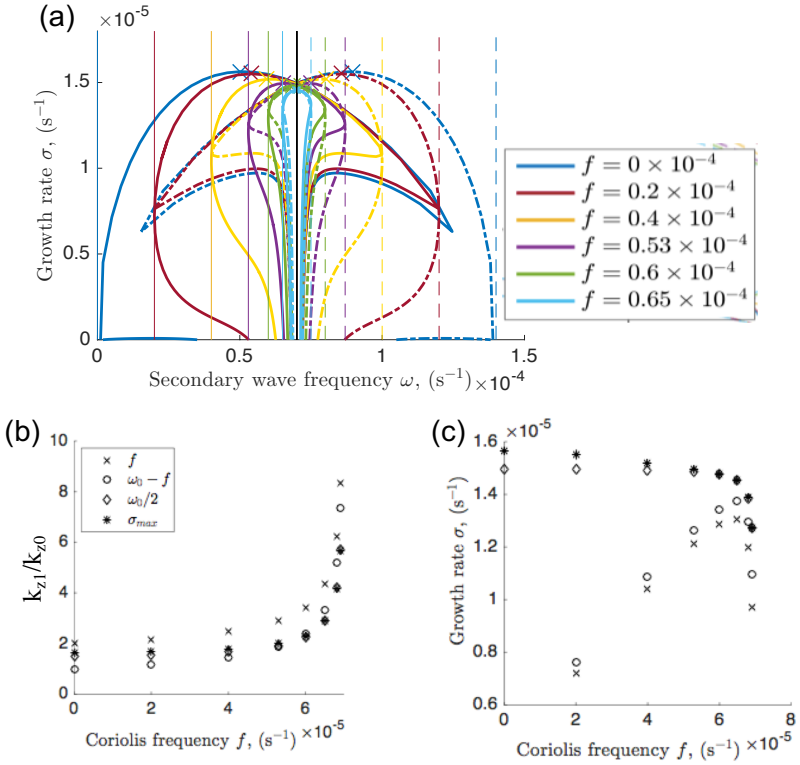

Figure II.7: *(a) Theoretical estimate of the growth rate of resonant triadic instabilities as a function of the frequency of secondary waves. The computation is performed at different latitudes (i.e. at different values of the Coriolis frequency f). (b) Evolution of the vertical wavenumber of the secondary wave (normalized by that of the primary wave) as f approaches the critical latitude, for the secondary waves at frequency f, $\omega_0 - f$, $\omega_0/2$, and frequency of the maximum growth rate (shown with crosses in panel a). (c) Same as panel b but showing the evolution of the growth rate of the corresponding triadic resonant instability (adapted from [Richet et al., 2018]).*

instability growth rates, as well as to the smaller and smaller vertical scales of the secondary waves (figure II.7), hence more likely to break and dissipate their energy. Poleward of the critical latitude, the "2f-pump" mechanism described in [Young et al., 2008] seems to be the leading-order mechanism by which internal tides lose energy. In this case, the internal tide transfers energy nonlinearly to evanescent waves at frequencies $\omega_0/2$, which dissipate internal tide energy as efficiently as the parametric subharmonic instability equatorward of the critical latitude. In fact, the 2f-pump is an extension of the parametric subharmonic instability poleward of the critical latitude when we consider near-inertial waves $f + \epsilon/2$ for small values of ϵ of both signs. The dissipation poleward of the critical latitude has implications for the possible consumption of Antarctic bottom water. These results suggest that evanescent waves could play a leading-order role in the dissipation of tidal energy in the deep ocean poleward of the critical latitude, and could contribute significantly to the diapycnal mixing relevant to the large-scale ocean circulation and to water masses.

II.4.b Robustness to a mean current

This section is based on the paper

O. Richet, C. Muller, J.-M. Chomaz

Impact of a mean current on the internal tide energy dissipation at the critical latitude

J. Phys. Oceanog., 47 (2017).

This work investigates the impact of a background mean current on the aforementioned enhanced dissipation at the critical latitude. Indeed the latter is not clearly confirmed in observations [MacKinnon et al., 2013], which only seem to indicate a modest enhancement at this latitude. For low modes (large-scale waves), the enhanced dissipation found in numerical simulations (figure II.5a) seems to be sensitive to resolution and diffusion, thus potentially explaining this discrepancy with observations. But for the higher modes (smaller scales) discussed in the previous section, the enhanced dissipation (figure II.5b) does not appear to be sensitive to changes in the diffusion or resolution [Nikurashin and Legg, 2011]. Here we investigate whether the presence of a mean current could reduce the enhanced dissipation at the critical latitude. Indeed, the ocean is not a quiescent medium; the presence of large-scale currents or mesoscale eddies can impact the propagation and dissipation of internal tides.

We use high-resolution simulations (figure II.8) similar to the ones used in the previous section, with an additional mean background current αU_0, where $0 \leq \alpha \leq 1$ and U_0 is the amplitude of the tidal forcing (figure II.1). The current is only applied above topography, to minimize its impact on the generation of the internal tides at the topography, and instead focus on its impact on the propagation of those waves.

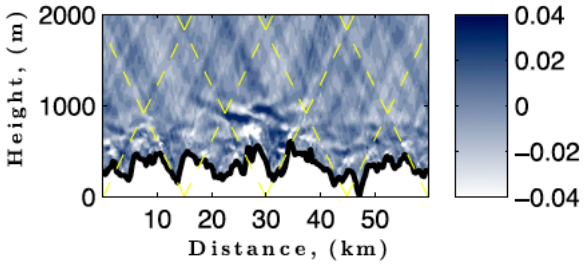

Figure II.8: *Snapshot from a nonlinear high-resolution MITgcm simulation without a mean current (shown is the anomalous horizontal velocity in m s^{-1}). The yellow lines show wave characteristics computed from linear wave theory (adapted from [Richet et al., 2017]).*

Adding a weak mean current has a major impact on the latitudinal distribution of dissipation. The peak at the critical latitude disappears, and the dissipation is closer to a constant. This disappearance results from the Doppler shift of the internal tides frequency (figure II.9), which hinders the nonlinear transfer of energy to small-scale secondary waves via the parametric subharmonic instability. The two new weak peaks correspond to the Doppler-shifted critical latitudes of the left- and right-propagating waves. The results are confirmed in simulations with simple sinusoidal topography $h \propto \sin(k_t x)$, keeping the Froude numbers consistent with realistic deep ocean values. This simple monochromatic topography makes clear the disappearance of the enhanced dissipation at the critical latitude $\omega_0/2$, and the appearance of two weaker peaks of dissipation at the Doppler-shifted critical frequencies $(\omega_0 \pm U_0 k_t)/2$ (figure II.10). Thus, although nonlinear transfers via the

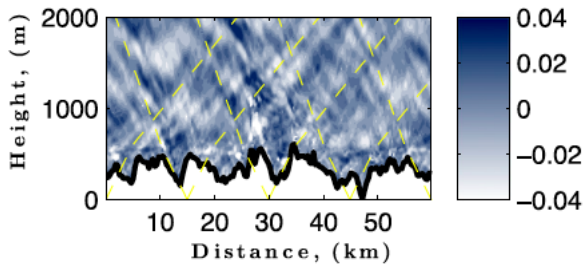

Figure II.9: *Same as figure II.8 but with a mean current imposed above topography. The change of slope of the characteristic lines (yellow lines) helps visualize the Doppler effect on the propagation of the waves (adapted from [Richet et al., 2017]).*

parametric subharmonic instability are efficient at dissipating internal tides, the exact location of the dissipation is sensitive to large-scale oceanic conditions.

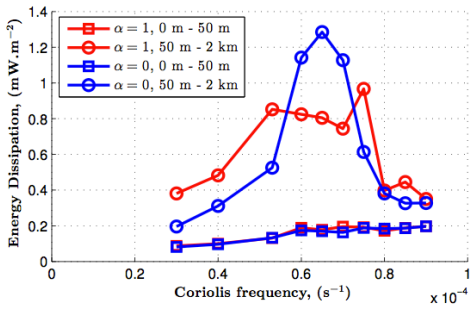

Figure II.10: *Wave energy dissipation in simulations without mean current (blue) and with mean current (red) for internal tides generated at sinusoidal topography* $h \propto \sin(k_t x)$. *Without mean current, the dissipation integrated from 50 m to 2 km above the seafloor shows a maximum at the critical latitude* $\omega_0/2$ *consistent with earlier studies (e.g. figure II.5b). With a mean current, the dissipation maxima are weaker and moved to Doppler-shifted latitudes of* $(\omega_0 \pm U_0 k_t)/2$ *(adapted from [Richet et al., 2017]).*

This suggests that under realistic conditions, where waves are unlikely to propagate through a quiescent ocean, the local dissipation of the internal tide is not a strong function of latitude. The reduced dissipation near the critical latitude implies that more wave energy than previously thought may propagate away from topography and hence may be available to dissipate in remote locations. This has implications for the transformation of deep water masses and the abyssal circulation. Recent estimates of internal waves impact on the overturning circulation point out the large uncertainty associated with remote dissipation of tides, which do not dissipate locally near their generation site. As mentioned in the introduction, depending on where this dissipation and the concomitant mixing occur, in particular its vertical structure, such mixing could drive 1 to 28 Sv of Antarctic bottom water upwelling [De Lavergne et al., 2016]. More work is desirable to help better constrain estimates of remote internal tide energy propagation and dissipation.

Chapter III

Precipitation extremes and their response to warming

"There was an ocean above us, held in by a thin sac that might rupture and let down a flood at any second."
Stephen King

III.1 Summary of key results, main collaborations and relevant supervisions

- *Key results: theoretical scaling*

  In recent decades, there have been important fundamental advances in our understanding of the response of precipitation extremes to warming. GCMs disagree on the amplitude of the response of precipitation extremes, especially in the tropics where they largely rely on convective parameterizations to represent deep cloud dynamics and deep convection [Kharin et al., 2007]. Thus, progress on this question must also rely on observations, theory, and high-resolution numerical simulations which resolve deep convection, instead of parameterizing it.

  In [**Muller and Takayabu, 2019**], a review article invited by the World Climate Research Program, or WCRP, on weather and climate extremes, we review recent advances in our understanding of the response of precipitation extremes to warming from theory and from idealized cloud-resolving simulations. Notably, a theoretical scaling for precipitation extremes has been proposed in the past decades, and refined including during my postdoctoral work, allowing to address separately the contributions from the thermodynamics, the dynamics and the microphysics. In this review, we discuss the theoretical constraints, as well as remaining uncertainties, associated with each of these three contributions to precipitation extremes. Notably, to leading order, precipitation extremes seem to follow the thermodynamic theoretical expectation, i.e. the scaling given by the Clausius-Clapeyron equation. But considerable uncertainty remains regarding the response of the dynamics and of the microphysics to warming.

  In [**Drobinski et al., 2016a**], we use this scaling to analyze the sensitivity of precipitation extremes to temperature using observations and regional modeling in the south of France. The relationship between precipitation extremes and temperature in our current climate has been widely investigated in observations. But difficulties arise when this relationship is extrapolated to the relationship between precipitation extremes and temperature changes due to global warming. Indeed, the response of precipitation extremes to temperature changes due to climate natural variability is not necessarily the same as the response due to climate change. In this study, we highlight the importance of strong seasonal effects in the south of France, where strong so-called "Cevenole" events in the fall dominate the precipitation extremes - temperature curve at warm temperatures in our current climate.

  In [**Drobinski et al., 2016b**], this study is extended to the whole Mediterranean region. We find that the relationship found in the south of France is robust throughout the Mediterranean basin, exhibiting a hook shape with negative slope at high temperatures and a slope following Clausius-Clapeyron scaling at low temperatures. In future climate scenario simulations, the temperature at which the slope breaks, shifts to higher temperatures by a value which is on average the mean regional temperature change due to global warming.

- *Key results: impact of organized convection*

  Convective organization can strongly impact the distribution of precipitation, and a large fraction of precipitation extremes occurs in organized convection.

  In [**Muller, 2013**], we investigate the response of tropical precipitation extremes to a sea-surface temperature increase in a cloud-resolving model with organized convection. Background vertical shear is used to organize the convection into squall lines. The shear is main-

tained throughout the simulations, which are run to radiative-convective equilibrium. We find that, despite very different precipitation values with different degrees of convective organizations, the response to warming is similar for a given shear. The highest percentiles of precipitation extremes increase at a fractional rate similar to that of surface water vapor.

Convective organization can also arise in the absence of vertical shear, solely due to internal feedbacks. One such mode of convective organization is convective self-aggregation, which will be the topic of next chapter (IV). In **[Da Silva et al., 2019]** (also an article invited by the World Climate Research Program on weather and climate extremes) we investigate the impact of convective self-aggregation on precipitation extremes. Precipitation extremes are very sensitive to the degree of convective aggregation, with stronger extremes in the more organized climate. When convection is organized, the precipitation is also more localized, leading to more rainfall accumulation in addition to larger instantaneous rainfall rates. Extreme rainfall intensity, frequency and duration (e.g. instantaneous, hourly or daily extreme rainfall rates) are all important for floods and risks.

- *Main collaborations and relevant supervisions*

  The observational study of the theoretical scaling in the south of France [Drobinski et al., 2016a] and in the Mediterranean region [Drobinski et al., 2016b] was part of a collaboration with **Philippe Drobinski**, senior researcher at LMD, and **Nicolas Da Silva** and **Bastien Alonzo**, who were at the time Masters students under the main supervision Philippe Drobinski, project on which I collaborated. Both Nicolas and Bastien then pursued a PhD at LMD with Philippe Drobinski.

  The latest work [Da Silva et al., 2019] was performed as part of a short postdoctoral project (ongoing) by **Nicolas Da Silva** at the end of his PhD under my supervision, also in collaboration with **Sara Shamekh**, currently doing her PhD at LMD supervised by myself and my collaborators **Fabio D'Andrea** and **Jean-Philippe Duvel**, senior scientists at LMD.

  The review on the theoretical scaling [Muller and Takayabu, 2019] is a collaboration with **Yakari Takayabu** senior scientist at the university of Tokyo.

In this chapter, we summarize the key results obtained in these studies, with a particular focus on the theoretical scaling [Muller and Takayabu, 2019].

We note also that for some aspects of the context and state-of-the-art, we will rely on the chapter on clouds [Muller, 2019] from the book of lecture notes of the graduate school, "Les Houches 2017 Summer School: Fundamental Aspects of Turbulent Flows in Climate" - Editors: F. Bouchet, C. Salomon, T. Schneider, A. Venaille.

III.2 Introduction: response of the hydrological cycle to global warming

In this section, we address the important question of the response of precipitation extremes to global warming. We focus on tropical convection, as tropical precipitation extremes are particularly challenging for climate models. The "pop-corn" small-scale nature of convection there (compared the mid-latitudes where clouds and convection are embedded in large-scale low and high pressure frontal systems) implies that coarse-resolution GCMs have to rely on convective parameterizations to represent convective processes in the tropics.

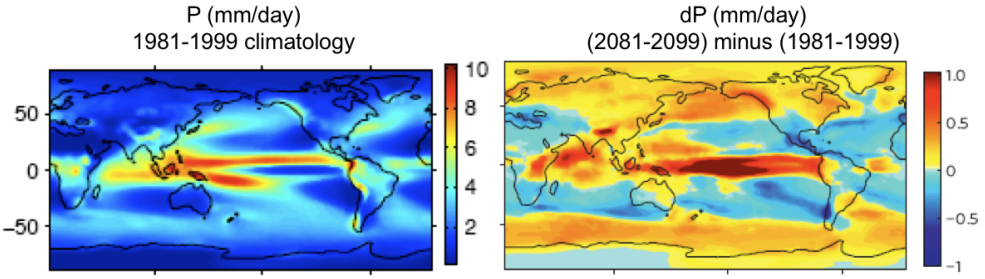

Figure III.1: *Mean precipitation climatology (left) and change in mean precipitation with global warming (right), illustrating the "rich-get-richer" pattern. High-precipitation regions (tropics and extratropics) have enhanced precipitation, and low-precipitation regions (subtropics) have decreased precipitation (after [Muller and O'Gorman, 2011]).*

Despite uncertainties in those parameterizations, GCMs robustly predict a pattern of mean precipitation changes with warming now known as the "rich-get-richet" pattern. Rainy regions (tropics and extratropics figure III.1) become rainier, and regions with little precipitation (subtropics figure III.1) receive even less rain. This can be understood via simple thermodynamics [Held and Soden, 2006, Muller and O'Gorman, 2011]. If changes in relative humidity are small, as is the case in climate models, we expect atmospheric water vapor to increase with warming following the Clausius-Clapeyron equation. Furthermore, if the atmospheric circulation does not change significantly, to leading order we expect regions with moisture convergence (and thus precipitation) to have increased moisture convergence due to the increased moisture. Similarly, regions with moisture divergence are expected to have stronger moisture divergence, and hence decreased precipitation. (Actually moisture divergence and convergence are linked to precipitation minus evaporation; but the changes in precipitation have considerably more structure than the changes in evaporation, so that the above results on patterns of precipitation changes hold. Note also that the large-scale tropical circulation does change, it weakens slightly, see [Held and Soden, 2006] for more details.)

The global mean precipitation does not follow the Clausius-Clapeyron increase though, as it is constrained by global energetics. Atmospheric energy balance implies that the global mean precipitation must balance the global mean radiative cooling (neglecting changes in the Bowen ratio), which increases at a slower rate of about 2% K^{-1} [Held and Soden, 2006].

These results for mean precipitation are extremely robust between climate models, and well understood. But large-scale constraints have little direct relevance to precipitation extremes in tropical storms, and there is a large uncertainty of precipitation extremes in climate models (figure III.2, [Kharin et al., 2007]). This uncertainty is largest in the tropics due to uncertainties in convective parameterizations. Since simulations of tropical precipitation extremes with current GCMs are unreliable, progress on the problem of changing tropical precipitation extremes must rely on either theory, observations, or simulations that resolve the convective-scale processes. Here we will use theory and cloud-resolving simulations to address this question, in disorganized "popcorn" convection at first, and then assessing the impact of convective organization on the results.

What can we expect for the amplification of precipitation extremes with warming from physical considerations? If the dynamics do not change with warming, precipitation extremes can be expected to scale with the moisture convergence into deep convective updrafts, which would then

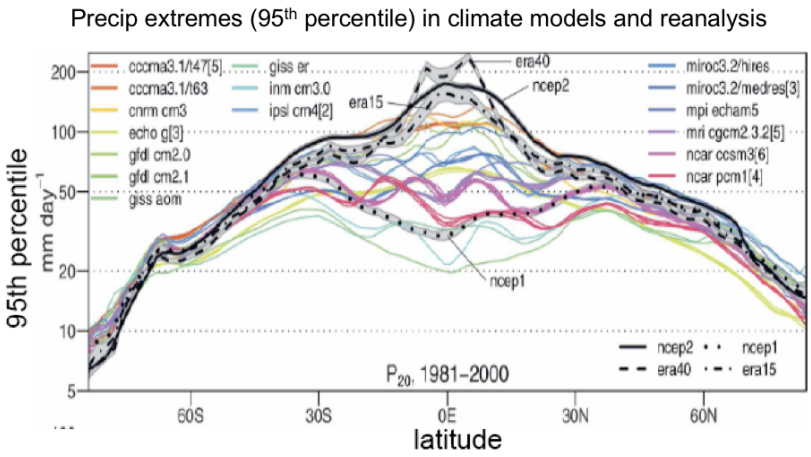

Figure III.2: *Precipitation extremes (95^{th} percentile) in the different IPCC climate models (after [Kharin et al., 2007]). There is a large uncertainty in tropical precipitation extremes, due to uncertainties in convective parameterizations.*

scale with water vapor following the Clausius-Clapeyron equation [Trenberth, 1999]. In the tropics, this equation predicts an increase of water vapor larger than 8% K^{-1} [O'Gorman and Muller, 2010]. We will assess the accuracy of this thermodynamic expectation for precipitation extremes in cloud-resolving simulations. The next section §III.3 describes the idealized settings of the numerical simulations. Then §III.4 introduces a theoretical scaling for the amplification of precipitation extremes with warming, which is then applied to idealized simulations and to observations in the Mediterranean region. Finally the impact of organized convection is investigated in §III.5.

III.3 Some notes on the methodology: idealized cloud-resolving simulations in radiative-convective equilibrium

This section is based on the book chapter

C. Muller

Clouds in current and in a warming climate

Chapter contribution to the book of lecture notes from

Les Houches 2017 Summer School: Fundamental Aspects of Turbulent Flows in Climate,

Oxford University Press (2019).

Most of my work described in this chapter and the next, relies on theory and on idealized, high-resolution cloud-resolving simulations of the tropical atmosphere, run in radiative-convective equilibrium, or RCE. In this section, we discuss briefly the setting and properties of this radiative-convective equilibrium, and the cloud-resolving simulations; readers familiar with it can skip this discussion and go directly to the results sections.

III.3.a Radiative-convective equilibrium

Non-rotating (Coriolis parameter $f = 0$) radiative-convective equilibrium is an idealization of the tropical atmosphere, in which the rotation of the earth is neglected (a reasonable approximation

in the tropics where the Coriolis parameter f is small), and in which the large-scale motion (larger than the domain) is neglected. Thus there is no import or export of moist-static energy into or out of the domain, and the net atmospheric radiative cooling (top of atmosphere minus surface) must balance the input of energy into the atmosphere at the surface, namely latent and sensible heat fluxes.

Over oceans, surface fluxes are largely dominated by the latent heat flux, so that in radiative-convective equilibrium over oceans, the net atmospheric radiative cooling is approximately equal to surface evaporation. From water conservation, the latter is equal to precipitation. In other words in radiative-convective equilibrium, the net atmospheric radiative cooling is in balance with the latent heating associated with the condensation of water vapor into precipitation by convection. It is this equilibrium between radiative cooling and convective heating which is referred to as radiative-convective equilibrium. The rest of this section is devoted to describing the fundamental properties of the radiative-convective equilibrium in more detail.

Radiative-convective equilibrium is most easily understood by first looking at radiative equilibrium. Radiative equilibrium is the equilibrium state of the atmosphere and surface in the absence of non-radiative fluxes. In that case, radiative cooling and heating drive the atmosphere towards a state of radiative equilibrium. At radiative equilibrium, the incoming shortwave solar heating $\pi R^2 S_0(1-a)$, where R denotes the Earth radius, S_0 incoming solar flux, and a albedo, exactly balances the outgoing longwave radiation $4\pi R^2 \sigma T_e^4$ where σ is the Stefan-Boltzman constant and T_e the emission temperature (temperature with which a planet needs to emit in order to achieve energy balance), yielding:

$$\sigma T_e^4 = S_0 \frac{1-a}{4}. \tag{III.1}$$

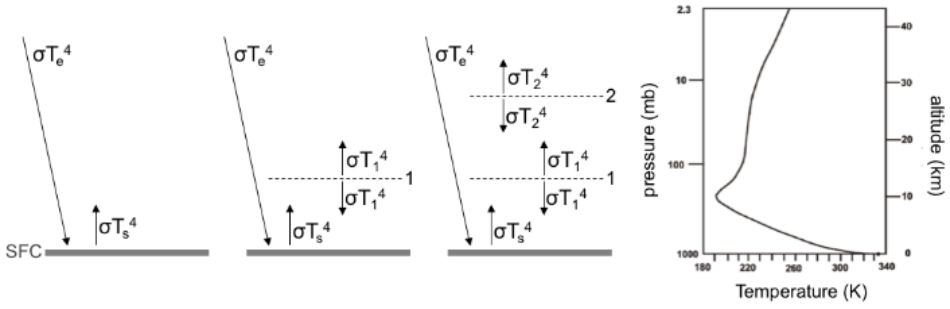

Figure III.3: *Radiative equilibrium without, with one or with two atmospheric levels (three left panels). The last panel shows the full calculation of radiative equilibrium (after [Manabe and Strickler, 1964]).*

In the absence of atmosphere (left panel figure III.3), the surface energy balance implies

$$\sigma T_e^4 = \sigma T_s^4 = S_0 \frac{1-a}{4} \Rightarrow T_s = T_e = 255 \text{ K } = -18^\circ \text{ C},$$

which is much colder that the observed mean surface temperature ≈ 288 K $= 15^\circ$ C. This warmer surface temperature is due to the presence of the atmosphere, and can be understood by adding a level to our simple conceptual model figure III.3. We assume that the atmosphere is transparent to solar radiation, opaque to infrared radiation, and we assume black-body emission from the surface

and each level (though the computation can easily be extended to account for emissivities smaller than 1). Energy balance at the surface and level 1 imply

$$\text{Level 1: } 2\sigma T_1^4 = \sigma T_s^4 \tag{III.2}$$
$$\text{SFC: } \sigma T_s^4 = \sigma T_e^4 + \sigma T_1^4, \tag{III.3}$$

yielding $T_s = 2^{1/4} T_e = 303$ K, warmer than before.

If we add an additional atmospheric level (figure III.3),

$$\text{Level 2: } 2\sigma T_2^4 = \sigma T_1^4 \tag{III.4}$$
$$\text{Level 1: } 2\sigma T_1^4 = \sigma T_s^4 + \sigma T_2^4 \tag{III.5}$$
$$\text{SFC: } \sigma T_s^4 = \sigma T_e^4 + \sigma T_1^4, \tag{III.6}$$

yielding $T_s = 3^{1/4} T_e$, even warmer.

The full calculation of radiative equilibrium was done by [Manabe and Strickler, 1964] and yields the temperature profile shown on the right panel of figure III.3. Compared with observations, this profile is too hot near the surface, too cold near the tropopause, yielding a lapse rate of temperature which is too large in the troposphere (but the stratosphere temperature is close to the observed). In other words, the radiative equilibrium profile is unstable to moist convection.

The observed temperature profile in the troposphere is closer to a radiative-convective equilibrium profile. Physically, what happens is that radiation destabilizes the atmosphere by cooling the interior of the troposphere, thus making the lapse rate steeper. But the radiation time scale $\approx$ tens of days is much slower than the convective adjustment time scale $\approx$ minutes for dry and hours for moist convection. Thus in the competition between radiation and convection, convection "wins", and the observed state is much closer to convective neutrality than to radiative equilibrium. In other words, the vertical temperature profile is close to neutral to dry convection below the lifted condensation level (i.e. on a dry adiabat: θ = constant), and close to neutral to moist convection above (i.e. on a moist adiabat: θ_e = constant). Here $\theta = T\,(p/p_0)^{R/c_p}$ denotes potential temperature, variable conserved in dry adiabatic motion, and $\theta_e = \theta \exp\left(L_v q/(c_p T)\right)$ denotes equivalent potential temperature, variable (approximately) conserved in moist adiabatic motion (p_0 denotes a constant reference pressure, R the gas constant, c_p isobaric heat capacity, L_v latent heat of vaporization, and q specific humidity of water vapor; see [Emanuel, 1994, Muller, 2019] for more details).

III.3.b Cloud-resolving simulations

Cloud-resolving models, or CRMs, are models with fine, kilometer-scale resolution, i.e. simulations with sufficiently high spatial resolution to explicitly resolve the deep convection and deep clouds, instead of parameterizing them. The cloud-resolving model used in most of my work is the System for Atmospheric Modeling, or SAM, see [Khairoutdinov and Randall, 2003] for more details. Briefly, this model solves the anelastic momentum, continuity and scalar conservation equations.

In my work, it is typically run with fixed sea-surface temperature (close to current tropical values, 300 K), on a square domain with doubly periodic geometry. The horizontal resolution is on the order of one or a few kilometers, in order to resolve deep cloud processes. The domain size varies from tens to a few hundreds of kilometers, with larger domains aimed at allowing the mesoscale organization of convection (notably in chapter IV). The vertical resolution is finer, tens

of meters in the low troposphere increasing to 500 m in the mid-troposphere. A sponge layer is added in the upper third of the domain (18 km to 27 km altitude) in order to absorb gravity waves which would otherwise unrealistically fill the domain (see e.g. [Muller and Bony, 2015] for more details).

In simulations of radiative-convective equilibrium, illustrated in figure III.4, convection is somewhat randomly distributed in space, resembling "pop-corn" convection. Such simulations are occasionally referred to as disorganized radiative-convective equilibrium, in contrast with simulations where the convection becomes spatially organized (which will be discussed e.g. in §III.5 and chapter IV).

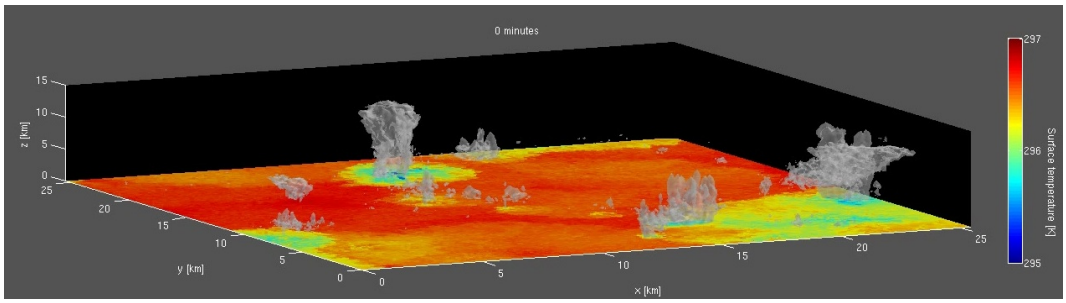

Figure III.4: *Illustration of the cloud-resolving simulations used in chapters III and IV. Shown in gray are isosurfaces of condensates indicating clouds, and colors show near-surface temperature (first atmospheric level temperature). The cloud-resolving model used is SAM [Khairoutdinov and Randall, 2003], typically run here in homogeneous, unforced conditions. Such models reach radiative-convective equilibrium in a few tens of days. In this equilibrium, radiative cooling is in balance with convective heating, and convection is somewhat randomly distributed, resembling "pop-corn" convection, also referred to as disorganized convection (animation available on my website http://www.lmd.ens.fr/muller/).*

III.4 My research: theoretical scaling for the amplification of precipitation extremes with warming

This section is based on the paper

C. Muller, Y. Takayabu

Response of precipitation extremes to warming: what have we learned from theory and idealized cloud-resolving simulations?

Environ. Res. Lett., to be submitted (2019).

III.4.a Theoretical scaling

Theory and high-resolution simulations have helped clarify the physics relevant to the change of precipitation extremes with warming temperatures. Notably, a theoretical scaling for precipitation extremes has been introduced [Betts and Harshvardhan, 1987, O'Gorman and Schneider, 2009] and refined to account for microphysics [Muller et al., 2011]. It relates the changes of precipitation extremes to three contributions: a thermodynamic contribution related to water vapor, a dynamic

contribution related to vertical mass flux in extreme updrafts, and a microphysic contribution related to precipitation efficiency. The latter is defined as the fraction of the condensation in a convective updraft which eventually reaches the surface as precipitation. It is typically less than one as some of the condensates are either advected away as clouds, or evaporate as they precipitate through unsaturated air below the cloud before reaching the surface. Each of these three contributions is subject to different theoretical constraints, and may respond differently to warming.

In this section, we provide a brief overview of the origin of this theoretical scaling. It can be derived from energetics, or from the water budget. We will review the former approach, and its link to the water budget. We focus on tropical precipitation extremes, where the disagreement between GCMs is largest (figure III.2), due to the small-scale nature of tropical convection. The focus on tropical precipitation extremes is also motivated by the fact that it allows comparison with cloud-resolving simulations in non-rotating radiative-convective equilibrium. As we will see, such idealized simulations have proven extremely useful in improving our understanding of the physical processes at stake.

Derivation of the scaling

A scaling for precipitation extremes can be derived from energetics, using the vertically-integrated dry static energy budget [Muller et al., 2011]. An energy rather than a water budget is used because an energy budget allows to more easily define a thermodynamic component (no dependence on relative humidity), and because the weak horizontal temperature gradients in the tropics allow to eliminate the horizontal advection terms. Following [Muller et al., 2011], we use the thermodynamic formulation consistent with the cloud-resolving model SAM (see [Khairoutdinov and Randall, 2003] for a detailed description), and using standard notations this budget becomes:

$$\int \frac{Ds}{Dt}\rho\, dz = L_v \int \frac{D(q_r+q_c)}{Dt}\rho\, dz + L_s \int \frac{D(q_s+q_g+q_i)}{Dt}\rho\, dz + L_v P \tag{III.7}$$

where $s = c_p T + gz$ denotes dry static energy, $\rho(z)$ the mean density profile, P surface precipitation (only involving the liquid phase at typical tropical temperatures) and q_r, q_c, q_s, q_g, q_i denote the mixing ratios of respectively liquid rain, liquid cloud condensates, snow, graupel and cloud ice (the five species are all the water condensates in SAM). The Lagrangian derivative is given by

$$\frac{D}{Dt} = \frac{\partial}{\partial t} + u_i \frac{\partial}{\partial x_i} \tag{III.8}$$

with u_i resolved wind speed along the x_i direction, $1 \leq i \leq 3$ (note that the total vertical flux of condensates includes both the resolved vertical velocity, included in the D/Dt term, and the terminal fall speed of hydrometeors, included in the precipitation term, see [Khairoutdinov and Randall, 2003] for details). The mass weighted integral $\int(...)\rho\, dz$ is taken from the surface to the tropopause.

Note that this is a pointwise energy budget, i.e. at small, convective scales. So the terms are meant to be evaluated at locations and times of extreme rainfall. The subgrid-scale fluxes and radiative cooling contributions have been neglected in this dry static energy budget, anticipating that those terms are negligible compared to the latent heat terms at times and locations of extreme rainfall.

Also, at times of extremes, the time rate of change of dry static energy is largely dominated by

the vertical advection (due to both strong updrafts and weak horizontal temperature gradients):

$$\frac{Ds}{Dt} \approx w\frac{\partial s}{\partial z}.$$

If we further neglect the difference between L_v and L_s for the purpose of deriving a simple approximate expression, and if we assume that the tropical atmosphere is close to a moist adiabat $ds \approx -L_v dq_{sat}$ where q_{sat} denotes saturation mixing ratio, then

$$\frac{\partial s}{\partial z} \approx -L_v\frac{\partial q_{sat}}{\partial z},$$

and (III.7) becomes

$$P_e \approx \int \rho w \left(-\frac{\partial q_{sat}}{\partial z}\right) dz - \int \rho \frac{D(q_r + q_c + q_s + q_g + q_i)}{Dt} dz, \tag{III.9}$$

where the subscript e stands for extremes.

This yields the following scaling for precipitation extremes

$$P_e = \epsilon \int \rho w \left(-\frac{\partial q_{sat}}{\partial z}\right) dz, \tag{III.10}$$

where ϵ denotes a precipitation efficiency. Although this scaling has been derived from energetics, it resembles a water budget and can be interpreted as such. The first integral on the right hand side of (III.9) represents the total net condensation (and deposition) in the updraft (assumed saturated), including condensation from upward motion as well as evaporation of condensates maintaining a moist adiabat in downdrafts. A fraction ϵ of this net condensation reaches the surface as precipitation, thus we refer to ϵ as precipitation efficiency. In the limit $\epsilon = 1$, all the net condensates precipitate out; in the limit $\epsilon = 0$, all condensates are advected from or accumulate in the column over the time scaling in question (second term on the right hand side of (III.9)).

As mentioned earlier, this is a pointwise scaling, i.e. meant to be evaluated at times and locations of precipitation extremes. One worry then is the potential sensitivity to spatial and temporal averaging. [Muller et al., 2011] investigate hourly versus daily precipitation extremes (their figure 4, see also figure III.6 below), as well as coarse grained results (from 2km to 24 km horizontal extent, their figure 6). The results are extremely robust and the scaling shows excellent agreement with precipitation extremes amplification with warming in all cases. Therefore, although the value of precipitation extremes is sensitive to spatial/temporal averaging, its amplification with warming seems to be robust and to be well captured by this scaling, at least in idealized radiative-convective equilibrium simulations, as will be discussed in more detail in the next section.

As it involves net condensation (condensation minus evaporation), ϵ differs slightly from the conventional precipitation efficiency defined as the fraction of total condensation reaching the surface as precipitation. Alternatively, if the integration in (III.10) is limited to heights where $w > 0$ as is sometimes the case in the literature, then ϵ represents the conventional precipitation efficiency.

We note that similar scalings were derived prior to [Muller et al., 2011] for precipitation extremes [Betts and Harshvardhan, 1987, Iribarne and Godson, 1981, O'Gorman and Schneider, 2009, Sugiyama et al., 2010], except that in (III.10) w is now at the convective scale, and there is the additional factor involving precipitation efficiency. We also note that in pressure coordinates, the scaling becomes

$$P_e = -\epsilon \int \omega \frac{\partial q_{sat}}{\partial p} \frac{dp}{g} \tag{III.11}$$

where ω denotes pressure vertical velocity (in hPa s^{-1}). In the extratropics, where the atmosphere is not necessarily on a moist adiabat, the scaling can still be extended, replacing the vertical derivative by a derivative along a moist adiabat, i.e. with constant saturation equivalent potential temperature $\theta_{e,sat}$ [O'Gorman, 2015, O'Gorman and Schneider, 2009]

$$\left.\frac{\partial q_{sat}}{\partial p}\right|_{\theta_{e,sat}}. \tag{III.12}$$

Using the scaling to split precipitation extremes into three contributions

The scaling in (III.10) can be used to relate changes of precipitation extremes, to changes of the dynamics through the mass flux ρw, of the thermodynamics through $\partial q_{sat}/\partial z$, and of the microphysics through ϵ

$$\frac{\delta P_e}{P_e} \approx \underbrace{\frac{\delta\left(\epsilon \int \rho w \left(-\frac{\partial q_{sat}}{\partial z}\right) dz\right)}{\epsilon \int \rho w \left(-\frac{\partial q_{sat}}{\partial z}\right) dz}}_{\text{scaling}} \tag{III.13}$$

$$\approx \underbrace{\frac{\delta\epsilon}{\epsilon}}_{\text{microphysic}} + \underbrace{\frac{\int \delta(\rho w) \left(-\frac{\partial q_{sat}}{\partial z}\right) dz}{\int \rho w \left(-\frac{\partial q_{sat}}{\partial z}\right) dz}}_{\text{dynamic}} + \underbrace{\frac{\int \rho w \, \delta\left(-\frac{\partial q_{sat}}{\partial z}\right) dz}{\int \rho w \left(-\frac{\partial q_{sat}}{\partial z}\right) dz}}_{\text{thermodynamic}}, \tag{III.14}$$

where δ denotes a difference between a warm and a cold climate, and following [Muller, 2013, Muller et al., 2011] we neglected second-order terms.

Assuming that changes in precipitation efficiency are small with warming, changes in precipitation extremes can be related to changes in the dynamics and in the thermodynamics (second and third terms on the right hand side of (III.14)). This simple scaling is found to be in very good agreement with cloud-resolving simulations in non-rotating radiative-convective equilibrium, as discussed in more detail in the next section.

III.4.b Comparison with cloud-resolving simulations

Numerical results

As mentioned in the introduction of this chapter, if the dynamics do not change with warming, precipitation extremes can be expected to increase with warming following water vapor, thus at a rate larger than 8% K^{-1} in the tropics. We will assess the accuracy of this thermodynamic expectation for precipitation extremes in cloud-resolving simulations, addressing the following questions:

- By how much do precipitation extremes increase with warming?
- How does it compare with the change in water vapor?
- How do vertical velocities in updrafts change, and how does it impact precipitation extremes?
- Can we use the theoretical scaling derived in the previous section to relate changes in precipitation extremes to mean quantities?

The cloud-resolving model used here is SAM [Khairoutdinov and Randall, 2003]. Two simulations are performed, one with a sea-surface temperature of 300 K and another warmer simulation with a sea-surface temperature of 305 K. The radiative cooling profiles are imposed but are different for the two sea-surface temperatures, computed from short small-domain runs with the corresponding sea-surface temperatures (see [Muller et al., 2011] for more details). A weak background vertical shear is added, with horizontal wind decreasing from 5 m s^{-1} at low levels to zero at upper levels in the x direction. Note that this shear is too deep and too weak to generate a squall line, so that convection resembles somewhat randomly distributed pop-corn convection in these simulations.

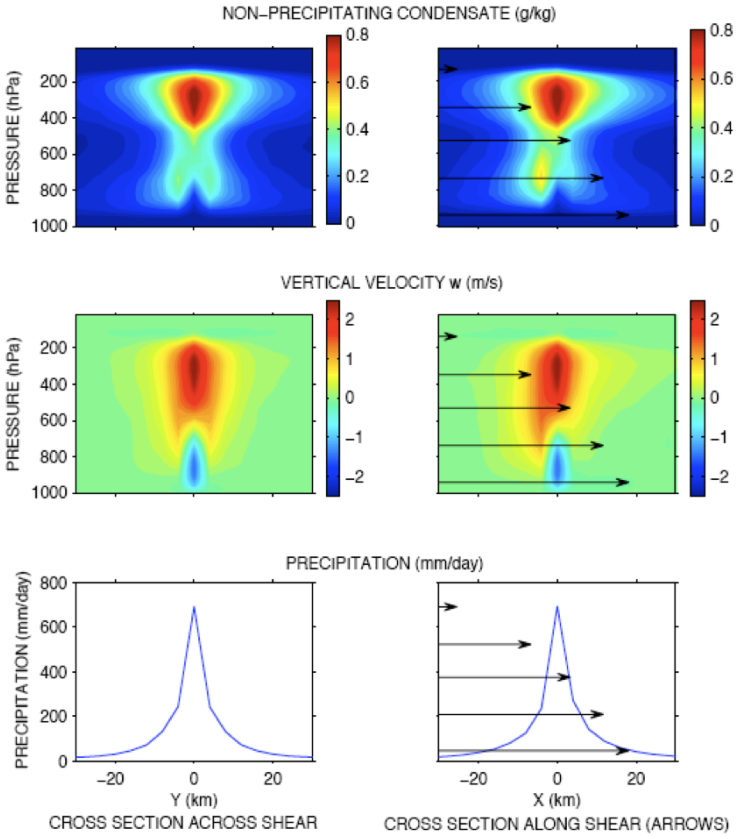

Figure III.5: *Composites in y (left) and x (right) directions around the location of extreme precipitation (placed at the origin). The top panels show non-precipitating condensates, the middle panels vertical velocity, and the bottom panels precipitation (after [Muller et al., 2011]).*

Figure III.5 shows composites around the location of extreme precipitation. We see that, as expected, precipitation is strongest in the dissipating stage of a cloud life cycle, as indicated by the downdrafts seen below the cloud. Also, as expected, there is preferred upward motion and cloud formation in the direction upshear (see §IV.2.b for more on shear-convection interactions). The extremes, i.e. high percentiles, of daily precipitation are shown in the left panel of figure III.6. We see that for a given percentile, the corresponding rainfall rate is always larger in the warmer simulation. Consistently, the ratio between the precipitation in the warm and in the cold runs is above 1. This ratio is shown in the middle panel for daily precipitation, and in the right panel for hourly precipitation. Although the values of precipitation extremes are sensitive to the temporal

average, the *ratio* is not. In other words, the fractional increase in precipitation extremes is robust to the time scale used. The fractional increase in precipitation extremes is found to asymptote at the highest percentiles, to ≈ 7 % K^{-1}.

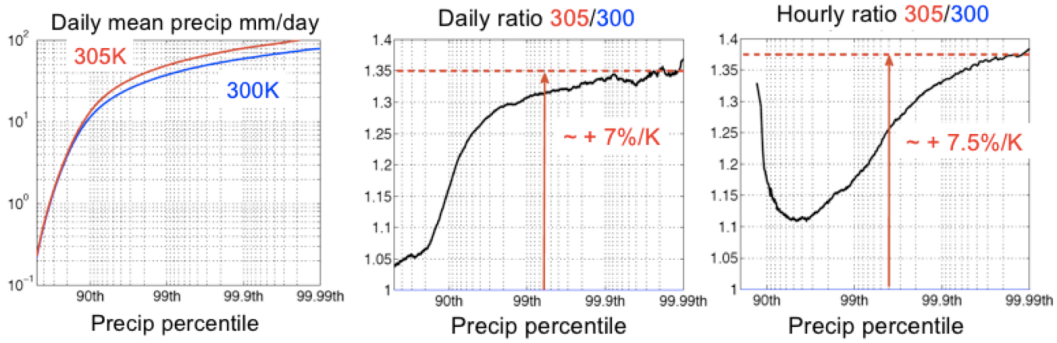

Figure III.6: *Values of daily precipitation extremes (i.e. high percentiles, left panel) in the cold (blue) and warm (red) simulations. The ratio between the warm and cold rainfall rates is shown in the middle panel. Similar results are obtained at hourly time scales (right panel, after [Muller et al., 2011]).*

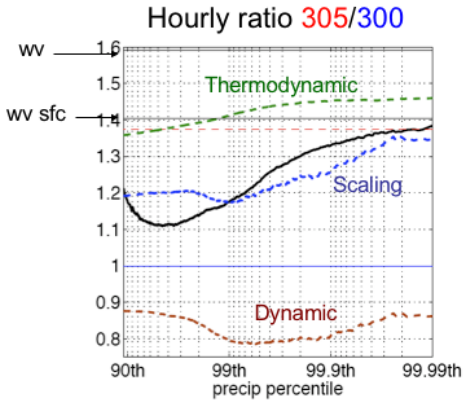

Figure III.7: *Increase in high percentiles (black curve) of hourly mean precipitation when the sea-surface temperature is increased from 300 K to 305 K in cloud-resolving simulations, and comparison with the theoretical scaling (III.14) (blue curve) involving a dynamic and a thermodynamic contribution. The increase in atmospheric water vapor (wv) and low-tropospheric water vapor (wv sfc) are also shown. The amplification of extremes asymptotes $\approx 7\%$ K^{-1} at the highest percentiles (ratio of about 1.35, red line, for a 5 K warming, figure after [Muller et al., 2011]).*

From figure III.7, this increase is remarkably well captured by the scaling (III.13) neglecting changes in precipitation efficiency (i.e. only accounting for the thermodynamic and dynamic contributions). To first order, the amplification of precipitation extremes is well captured by the thermodynamic scaling, which is close to the low-level water vapor increase, and smaller than the atmospheric water vapor increase. The dynamics play a secondary role, and tend to oppose the amplification of extreme rainfall rates with warming.

Simplified scaling and thermodynamic contribution

If the dynamics of convective updrafts do not change with warming, the thermodynamic contribution to precipitation extremes could be expected to scale with the moisture convergence into deep convective updrafts, which would then scale with water vapor following the Clausius-Clapeyron equation (assuming small changes in relative humidity). But these numerical results suggest that we can instead expect tropical precipitation extremes to follow the low-level water vapor, which increases at a smaller pace than atmospheric water vapor (following boundary-layer Clausius-Clapeyron).

The fact that precipitation extremes follow low-tropospheric humidity, and not atmospheric humidity, can be understood using a simplified scaling derived from (III.10) [Muller, 2013]. If we assume that ρw at 500 hPa is a representative value for ρw:

$$\delta P_e \approx \delta\left(\int -\frac{\partial q_{sat}}{\partial z} w\rho dz\right) \quad \text{(III.15)}$$

$$\approx \delta\left((w\rho)_{500hPa}\int -\frac{\partial q_{sat}}{\partial z} dz\right) \quad \text{(III.16)}$$

$$\approx \underbrace{\delta\left((w\rho)_{500hPa}\ q_{sat,BL}\right)}_{\text{simplified scaling}}, \quad \text{(III.17)}$$

where $q_{sat,BL}$ denotes the saturation specific humidity in the boundary layer. If changes in relative humidity are small, the thermodynamic contribution to precipitation extremes is thus expected to follow low-tropospheric water vapor.

Some remarks and implications

Similar increases in precipitation extremes, close to low-tropospheric moisture, have been found in another study using a different cloud-resolving model [Romps, 2011], thus these results seem to be robust to the model used. In the tropics, GCMs predict an increase of water vapor larger than 8% K^{-1} [O'Gorman and Muller, 2010]. If instead precipitation extremes follow low-tropospheric water vapor, the rate of increase is significantly reduced, to less than 6% K^{-1} [O'Gorman and Muller, 2010]. Thus to leading order, at least within the limits of these idealized simulations, precipitation extremes follow this low-tropospheric thermodynamic expectation, consistent with the simplified scaling introduced above.

The dynamics, via increased vertical mass flux in extreme updrafts, and the microphysics, via increased precipitation efficiency, can further amplify the response of precipitation extremes to warming. But without a complete theory for the dynamical and microphysical changes with warming, we can not properly attribute causes for the corresponding contributions to extreme rainfall rates. More work is desirable in particular to clarify the relative roles of convective entrainment [Singh and O'Gorman, 2013], hydrometeor fall speeds [Parodi and Emanuel, 2009] and atmospheric stability [Attema et al., 2014] on the dynamics, as well as the role of cloud-rain autoconversion and rain evaporation [Lutsko and Cronin, 2018] on the microphysics (see also [Muller and Takayabu, 2019] for a more in-depth discussion).

A few studies have found amplification of precipitation extremes exceeding significantly the thermodynamic theoretical expectation, when the warming is uniform in height. In the tropics, one expects the atmosphere to warm following a moist adiabat, with larger warming aloft, as was the case in the cloud-resolving simulations discussed above. If instead the warming is uniform with height, a situation more relevant to the mid latitudes, atmospheric instability is enhanced [Loriaux et al., 2013]. Consistently, faster updrafts contribute positively to the dynamic contribution,

yielding a larger amplification of precipitation extremes with warming than the thermodynamic contribution would entail [Attema et al., 2014, Singleton and Toumi, 2013]. We note though that the link between stability and precipitation extremes is not necessarily straightforward. Differences in atmospheric stability may result in differences in convection, but extremes in precipitation intensity do not necessarily follow the atmospheric stability [Hamada et al., 2015]. Changes in atmospheric stability associated with sub-daily extreme precipitation events, and the corresponding dynamic contribution to precipitation extremes, deserve more investigation.

Note also that a large uncertainty regarding tropical precipitation extremes and their response to warming, is related to convective organization and its response to warming. This is the topic of § III.5 and of the next chapter.

III.4.c Beyond idealized simulations: scaling applied to observations in the Mediterranean region

This section is based on the papers

P. Drobinski, N. Da Silva, G. Panthou, S. Bastin, C. Muller, B. Ahrens, M. Borga, D. Conte, G. Fosser, F. Giorgi, I. Guttler, V. Kotroni, L. Li, E. Morin, B. Onol, P. Quintana-Segui, R. Romera T. Csaba Zsolt
Scaling precipitation extremes with temperature in the Mediterranean: past climate assessment and projection in anthropogenic scenarios
Clim. Dyn. (2016).

P. Drobinski, B. Alonzo, S. Bastin, N. Da Silva, C. Muller
Scaling of precipitation extremes with temperature in the French Mediterranean region: what explains the hook shape?
J. Geophys. Res. - Atmospheres, 121 (2016).

In earlier sections, within the limit of our idealized simulations over tropical oceans, we find that the thermodynamic contribution dominates the response of precipitation extremes to warming, with precipitation extremes increasing at a rate of about 6-7% K^{-1} following the low-tropospheric humidity. But regional specificity, including orography and/or weak moisture advection from oceans, can enhance the dynamic contribution to precipitation extremes, or weaken the thermodynamic contribution. Notably in the south of France, strong seasonal events yield extreme rainfall rates in the fall. These events are known as *événements Cévenoles*.

We quantified, using observations and regional simulations, the dynamic and thermodynamic contributions to extreme precipitation in the south of France. We also analyzed their sensitivity to temperature [Drobinski et al., 2016a]. This allowed us to link precipitation extremes with the intense dynamical convective events of this region in the fall. The precipitation extremes - temperature relationship is found to have a hook shape, with positive slopes at cold temperatures consistent with Clausius-Clapeyron scaling, and negative slope at warm temperatures.

We further analyzed the implications of these results for the response of precipitation extremes to warming in the whole Mediterranean region [Drobinski et al., 2016b], confirming the hook shaped relationship between precipitation extremes and temperature, with positive slopes at cold temperatures and negative slope at warm temperatures. In future climate scenario simulations covering the 2070-2100 period, the temperature at which the slope breaks, shifts to higher temperatures by

a value which is on average the mean regional temperature change due to global warming. Overall, models predict more intense precipitation extremes in the future.

III.5 My research: impact of convective organization and outstanding open questions

III.5.a Impact of convective organization on the amplification of precipitation extremes with warming

This section is based on the paper

C. Muller
Impact of convective organization on the response of tropical precipitation extremes to warming
J. Climate, 26 (2013).

Convective organization is ubiquitous in the tropics, and is associated with extreme weather and strong rainfall rates (as discussed in more detail in the next chapter devoted to convective organization, see for instance §IV.2). A natural question then is how precipitation extremes in organized convection can be expected to change with warming. In this section, we assess the impact of organization on the results of the previous section, addressing the following questions:

- How do precipitation extremes in organized systems respond to warming?
- How sensitive is the amplification of precipitation extremes with warming to the degree of organization?

To that end, we use vertical wind shear to organize the convection into squall lines, using the three simulations illustrated in the right panels of figure IV.3: no shear, critical shear, and supercritical shear. We perform simulations at a control sea-surface temperature value of 300 K, and a warmer simulation at 302 K (see [Muller, 2013] for details). Figure III.8 shows the high percentiles of precipitation in the various simulations, at cold and warm temperatures. As before, precipitation extremes are found to increase with warming, by about 6-7% K^{-1}.

We also see that for a given temperature, precipitation extremes are sensitive to vertical shear and almost double in the presence of shear, but increasing the shear from critical to supercritical shear has very little effect on the rainfall rates. This may not be too surprising since in the supercritical case the squall lines orient themselves so that the line-perpendicular component of the shear is critical. Therefore, one would expect rainfall rates similar to the ones obtained with critical shear as long as the shear is above critical. We will return to this question of the impact of convective organization on precipitation extremes in the next section §III.5.b, but here instead focus on the impact of warming on precipitation extremes, for a given degree of organization.

What is perhaps more surprising is that despite very different organizations, the amplification of precipitation extremes with warming is similar for all shears, though it is slightly larger in the supercritical shear simulation. This behavior is again well captured by the scaling in equation (III.10), as shown in figure III.9. As before, to leading order, the increase in precipitation extremes is determined by the thermodynamic contribution, and dynamics play a secondary role. But interestingly, the dynamic contribution is not robust to the shear: no shear or critical shear yield a negative contribution, opposing the amplification of precipitation extremes with warming.

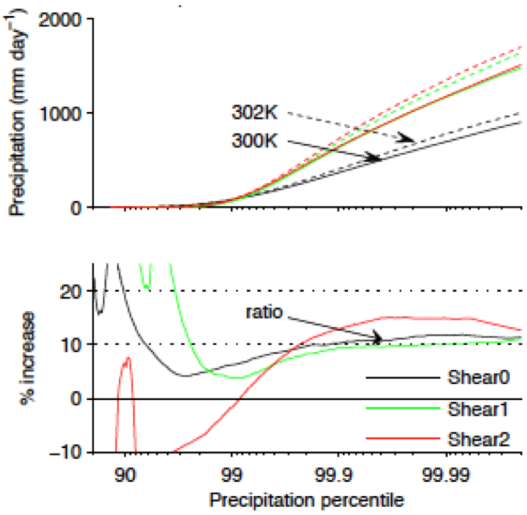

Figure III.8: *Increase in high percentiles of precipitation, in simulations with different shear strengths (after [Muller, 2013]).*

But supercritical shear yields a positive dynamic contribution, which explains the slightly stronger increase of precipitation extremes in that case. As in the previous section, the amplification of precipitation extremes is found to be closer to low-tropospheric humidity increase than to atmospheric humidity increase (not shown). These results thus confirm the conclusions of the previous section, the only difference being the dynamic contribution which can become positive in the presence of strong shear. The fact that precipitation extremes follow low-tropospheric humidity, and not atmospheric humidity, is again consistent with the simplified scaling (III.17).

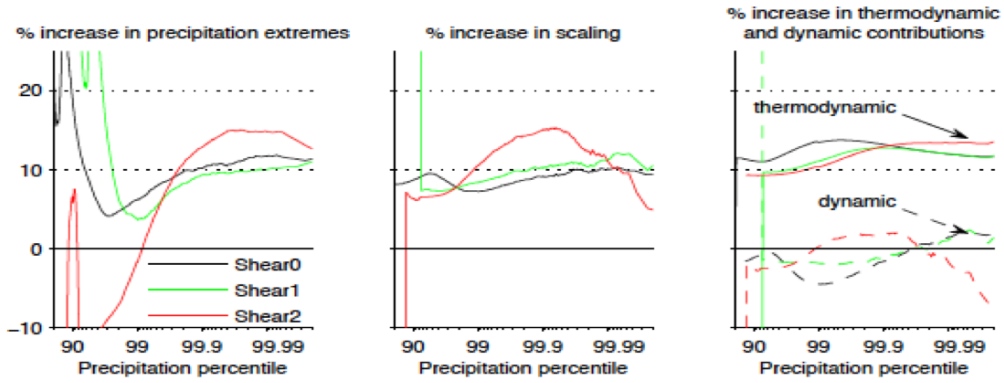

Figure III.9: *Increase in high percentiles of precipitation, and comparison with the theoretical scaling involving a dynamic and a thermodynamic contribution, in simulations with different shear strengths (after [Muller, 2013]).*

The dynamic contribution deserves further investigation, as it is the contribution which is sensitive to the shear and thus the organization. Figure III.10 shows the vertical profiles of ρw and of w in the various simulations. We see that the decrease in vertical mass fluxes with warming

at critical and zero shear, is not observed with supercritical shear. Figure III.10 also shows that the decrease in convective mass flux occurs despite an increase in the maximum updraft velocity (bottom panels). The former is more relevant to precipitation extremes.

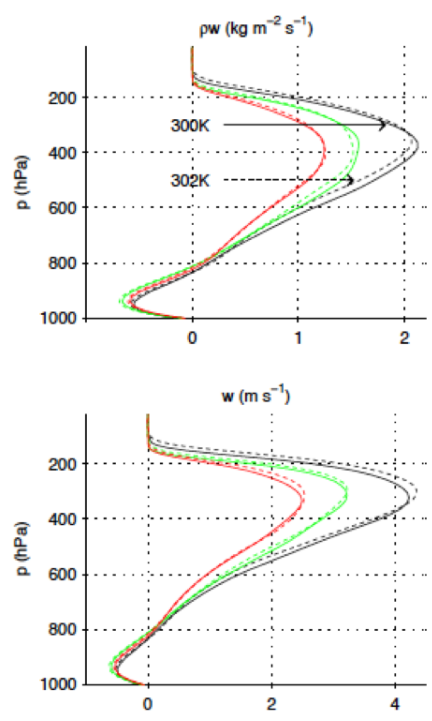

Figure III.10: *Change in vertical velocity and vertical mass flux with warming for the different shears. Despite an increase in vertical velocity, the mass flux decreases with warming (except for the supercritical shear in red). The latter is more relevant to precipitation extremes, explaining the negative dynamic contribution except with the strongest shear (figure III.9, after [Muller, 2013]).*

III.5.b Discussion and outstanding open questions

This section is based on the paper

N. Da Silva, S. Shamekh, C. Muller

Impact of convective self-aggregation on precipitation extremes

Environ. Res. Lett., in preparation (2019).

Note that a large uncertainty regarding tropical precipitation extremes and their response to warming, is related to convective organization and its response to warming. Indeed, in the previous section we investigated the increase of precipitation extremes with warming *for a given degree of organization*. But figure III.8 implies that a change in the degree of organization can lead to up to a doubling of extreme rainfall rates, while, for a given degree of organization precipitation extremes increase at about 7% K^{-1} of warming. Thus the increase of precipitation extremes from a change in convective organization is larger than that associated with warming by several degrees.

In recent work [Da Silva et al., 2019], we investigate the impact of convective self-aggregation on precipitation extremes. Self-aggregation is a particular mode of convective organization due

to internal feedbacks (discussed in more detail in the next chapter). We find that when the atmosphere is more organized into a moist convecting region, and a dry convection-free region, the moister environment of deep convective updrafts, enhances the thermodynamic contribution as well as the microphysic contribution through larger precipitation efficiency (partly due to reduced evaporation of rain falling through a moister near-cloud environment). The dynamics and duration of precipitating events are also affected, thus the amplification of precipitation extremes could be larger than the thermodynamic theoretical expectation. Our results are qualitatively consistent with recent results from [Bao and Sherwood, 2019], using a different model WRF, who find that extreme instantaneous precipitation is more sensitive to microphysical processes while extreme daily precipitation is more linked to the degree of aggregation.

A recent observational study [Tan et al., 2015] finds that recent trends in tropical precipitation can be linked to changes in the frequency of occurrence of organized mesoscale cloud systems. Improved fundamental understanding of convective organization and its sensitivity to warming is hence an area of priority for climate model development to achieve accurate rainfall projections in a warming climate. It is the topic of the next chapter.

Chapter IV

Self-aggregation of tropical deep convection, and implications

"Clouds suit my mood just fine."
Marie Lu (born Xiwei Lu)

IV.1 Summary of key results, main collaborations and relevant supervisions

- *Key results: physical processes responsible for self-aggregation*

  Self-aggregation refers to the spectacular ability of deep clouds to spontaneously cluster in models despite homogeneous boundary conditions and forcing (figure IV.5). More generally, the spatial organization of deep convection at mesoscales, i.e. hundreds of kilometers, is ubiquitous in the tropics. Convective organization can be forced by the large scales (large scales refer to scales similar or larger than mesoscale), for instance vertical wind shear or land-ocean contrasts. But organization can also arise from internal feedbacks linked to the interaction of clouds with their environment. This can lead to the spontaneous inhomogeneous spatial clustering of clouds in otherwise homogeneous unforced environments, e.g. by internal "self-aggregation" feedbacks, still very much an area of active research. This is the topic of this chapter.

  In [**Holloway et al., 2017**], we review the observational evidence that have analyzed observations to look specifically for processes related to self-aggregation in models, and motivate the need for more of this work. Indeed, despite its robust appearance in a hierarchy of models, the relevance of self-aggregation to the real tropics is still debated. Notably, self-aggregation is typically studied in highly idealized settings, including uniform, spatially and temporally constant sea-surface temperature.

  In [**Muller and Bony, 2015**], using idealized simulations with homogeneous sea-surface temperature, we identify radiative longwave feedbacks as being the diabatic feedback responsible for the self-aggregation of convection in cloud-resolving simulations. More precisely, sufficient spatial variability of radiative cooling rates yields a low-level circulation, which induces the upgradient energy transport and radiative-convective instability. In this paper, we also investigate a moisture-memory feedback capable of aggregating convection, even in the absence of diabatic feedbacks, when the evaporation of rain in the subcloud layer is suppressed.

  This expertise on self-aggregation, along with my earlier postdoctoral work on this topic, led to the invitation to participate in two review articles: one [**Wing et al., 2017**] reviewing the self-aggregation of deep convection in idealized simulations, and one [**Zuidema et al., 2017**] reviewing the properties of cold pools below precipitating clouds over oceans, and comparing them with radiatively-driven dry pools, believed to play a crucial role in the onset of self-aggregation.

- *Key results: implications for ocean eddies - convection interaction, and for tropical cyclogenesis*

  As mentioned above, most studies on self-aggregation focused on idealized simulations, in particular radiative-convective equilibrium with homogeneous sea-surface temperature and neglecting Earth's rotation. These two aspects are addressed here.

  In [**Shamekh et al., 2019**], we investigate the impact of sea-surface temperature inhomogeneities on self-aggregation. More precisely, we analyze how a circular hot-spot helps organize convection, and how self-aggregation feedbacks modulate this organization. The hot-spot significantly accelerates aggregation, particularly for warmer/larger hot-spots, and extends the range of domain-mean sea-surface temperatures for which aggregation occurs.

This is because convection over the hot-spot brings the atmosphere towards a warmer moist adiabat, consistent with the hot-spot warmer temperatures. The warmer temperatures are imprinted over the whole domain by gravity waves and subsidence warming. This initial transient warming and concomitant subsidence drying suppress convection outside the hot-spot, thus favoring the aggregation of convection and moisture over the hot-spot.

In **[Muller and Romps, 2018]**, we investigate the impact of the background planetary rotation on self-aggregation and tropical cyclogenesis. Although the prediction of tropical cyclone tracks has improved in recent years, understanding the mechanisms responsible for the genesis and intensification of tropical cyclones remains a major scientific challenge. We show that self-aggregation plays a leading-order role in the genesis of tropical cyclones in cloud-resolving simulations. This suggests that self-aggregation, and the framework developed for its study, could help shed more light into the physical processes leading to cyclogenesis and cyclone intensification. This study adds to the growing literature on the importance of this phenomenon for the tropical atmosphere.

- *Main collaborations and relevant supervisions*

  The hot-spot study [Shamekh et al., 2019] was performed by **Sara Shamekh** during her PhD at LMD (ongoing), supervised by myself and my collaborators **Fabio D'Andrea** and **Jean-Philippe Duvel**, senior scientists at LMD.

  The process study [Muller and Bony, 2015] resulted from a collaboration with **Sandrine Bony**, senior scientist at LMD, and the cyclogenesis study [Muller and Romps, 2018] resulted from a collaboration with **David Romps**, professor at UC Berkely.

  The two invited review articles [Wing et al., 2017] and [Zuidema et al., 2017], as well as the observational paper [Holloway et al., 2017], resulted from a workshop organized by the World Climate Research Program on the Grand Challenge "Clouds, Circulation, and Climate Sensitivity". It is thus the result of a **wide international effort** (lead organizers for this Grand Challenge workshop include Sandrine Bony, LMD/IPSL, Robert Pincus, Colorado University, Bjorn Stevens, Max Planck Institute, David Winker, NASA LRC, Anny Cazenave, ISSI Bern, and Nicolas Champollion, ISSI Bern).

In this chapter, we summarize the key results obtained in these studies, with a particular focus on the cyclogenesis study [Muller and Romps, 2018].

IV.2 Introduction: basics of mesoscale convective organization

This section is based on the book chapter

C. Muller
Clouds in current and in a warming climate
Chapter contribution to the book of lecture notes from
Les Houches 2017 Summer School: Fundamental Aspects of Turbulent Flows in Climate,
Oxford University Press (2019).

IV.2.a Definition

Organized convection refers to convection that is long-lived, i.e. that lasts longer than an individual convective cell (which typically lasts a few hours, < 3 hours), and that grows upscale, i.e. that covers an area larger than an individual convective cell (which typically is < 10 km across). It is well known that clouds often organize at large, planetary and synoptic scales, where they are tightly coupled to the large-scale circulation. In the tropics, there is a clear correlation between cloud fraction and large-scale upward motion, with deep convection in the intertropical convergence zone, or ITCZ, which corresponds to the rising branch of the Hadley cell (e.g., [Muller, 2019]). Clouds are also embedded within the Walker cell, with deep convection occurring above the warm waters of the warm pool, corresponding to the rising branch of the Walker cell. At synoptic scale, it is tightly linked to equatorial waves [Wheeler and Kiladis, 1999] (see e.g. the impact on outgoing longwave radiation of Kelvin waves and equatorial Rossby waves on figure IV.1, as well as that of the Madden-Julian Oscillation).

It is also apparent from figure IV.1 that clouds often organize at smaller, mesoscales (hundreds of kilometers), into what are called mesoscale convective systems. The formation of such systems is still an active area of research, with important societal impacts, as it is associated with extreme weather and strong precipitation. It also has strong climatic impacts, as it affects the large-scale atmospheric radiation budget, by affecting cloud cover and the large-scale thermodynamic profiles (temperature and humidity, [Bony et al., 2015]). In this chapter, we investigate the mesoscale organization of deep convective clouds in the tropics, and review here the basics of mesoscale convective organization and the physical processes involved. We then discuss in more detail a recently discovered phenomenon in idealized simulations of the tropical atmosphere, namely the self-aggregation of convection.

Organized convection at mesoscales takes the form of mesoscale convective systems, or MCS. The American Meteorological Society glossary defines a mesoscale convective system as a "cloud system that occurs in connection with an ensemble of thunderstorms and produces a contiguous precipitation area on the order of 100 km or more in horizontal scale in at least one direction". Mesoscale convective systems include squall lines, mesoscale convective complexes, and tropical cyclones (figure IV.2). Mesoscale convective complexes, or MCC, are a subset of mesoscale convective systems that exhibit a large, circular (eccentricity > 0.7), long-lived (> 6 hours), cold cloud shield. The cloud shield must have an area $> 100\ 000$ km^2 with infrared temperature colder than -32°C, and an area $> 50\ 000$ km^2 with infrared temperature colder than -52°C. Note that these are not mutually exclusive, in fact tropical cyclones can evolve from mesoscale convective complexes, and squall lines can be emitted from tropical cyclones and their outward spiraling bands of precipitation.

The leading physical processes for convective organization are an active area of research. These physical processes include:

- Vertical shear;
- Waves;
- Wind-induced surface heat exchange feedbacks;
- Convective self-aggregation feedbacks.

We describe each process in more detail below.

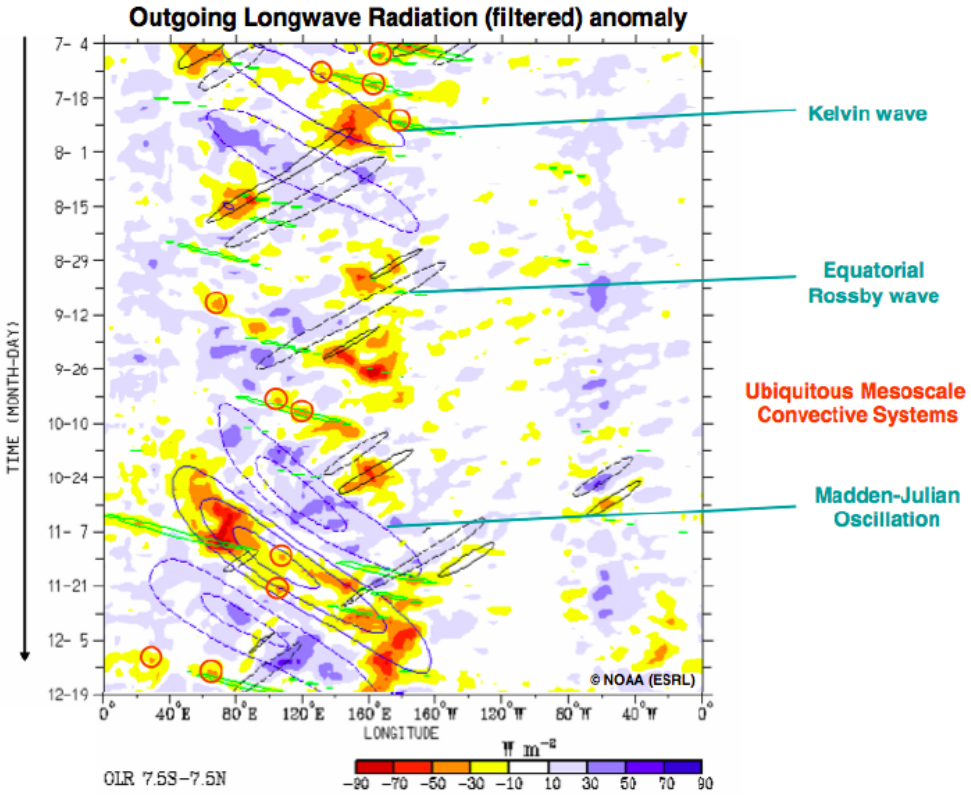

Figure IV.1: *Time-longitude (Hovmoller) section of outgoing longwave radiation anomaly averaged from 7.5S to 7.5N (time-mean and seasons removed, from ESRL-NOAA, courtesy: Gilles Bellon). Contours are anomalies filtered for the total outgoing longwave radiation for specific regions of the wavenumber-frequency domain corresponding to the Madden-Julian Oscillation (blue contours), Kelvin waves (green contours), and equatorial Rossby waves (black contours). Beyond the synoptic equatorial waves, we can also note the numerous smaller-scales (hundreds of kilometers) cloud clusters (red contours); these are mesoscale convective systems, and are the topic of this chapter.*

IV.2.b Role of vertical shear

The presence of background vertical wind shear is known to favor the formation of squall lines. More precisely, the interaction of the shear with cold pools below precipitating clouds, is believed to be key in the formation of squall lines.

One possible explanation (figure IV.3a) is the advection of cold pools away from the convective updraft. Indeed, in the dissipating stage of clouds, the partial evaporation of the falling rain cools the air, creating cold heavy downdrafts, which hit the surface and spread horizontally. These pockets of cold air below clouds are known as cold pools, and inhibit further convection. In the case where the region with downdrafts and cold pools is advected away from the updrafts, as represented schematically in figure IV.3a, the updraft can persist on the upwind side of the cold pool, leading to long-lived convective clouds [Garner and Thorpe, 1992].

Another possible explanation is the interaction of the vorticity of the background shear with the vorticity of the spreading cold pool, which favors the formation of new updrafts and convective

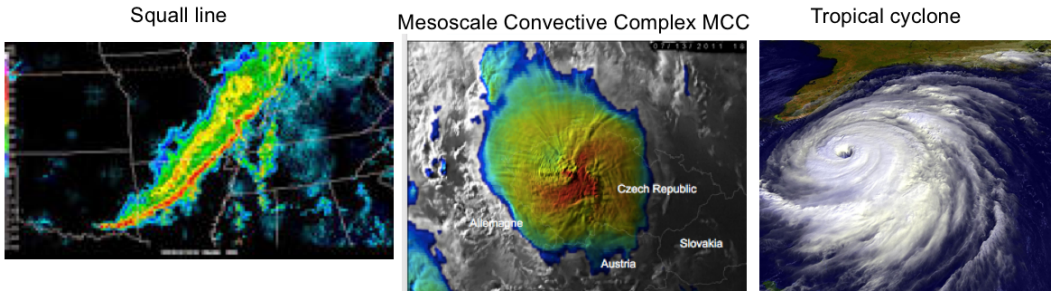

Figure IV.2: *Mesoscale convective systems include squall lines (radar image), mesoscale convective complexes (from EUMETSAT Meteosat-8 satellite), or tropical cyclones (from NOAA-GOES satellite; from [Muller, 2019]).*

cells upshear (figure IV.3b). Note that in the previous theoretical explanation, the squall line is a system of long-lived convective cells, while in this case the squall line is a long-lived system of ordinary cells. [Rotunno et al., 1988] argue that the latter is more consistent with observations, though squall lines can occasionally be composed of long-lived supercell thunderstorms.

Consistently, in cloud-resolving simulations (right panels of figure IV.3), imposing a vertical wind shear, at low levels where cold pools are, yields the organization of clouds into arcs. The top panel shows a simulation without shear, in which the convection is somewhat randomly distributed, resembling "pop-corn" convection. The middle panel shows a simulation with critical shear, defined as the shear yielding squall lines perpendicular to the mean wind (in the x direction in these simulations from left to right). This critical shear was empirically determined in these simulations, decreasing from 10 m s^{-1} at the surface to zero at 1 km. The last panel shows a simulation with supercritical shear (20 m s^{-1} at the surface), in which the squall line orients itself at an angle with the background wind, so that the projection of the shear on the squall line is critical [Muller, 2013].

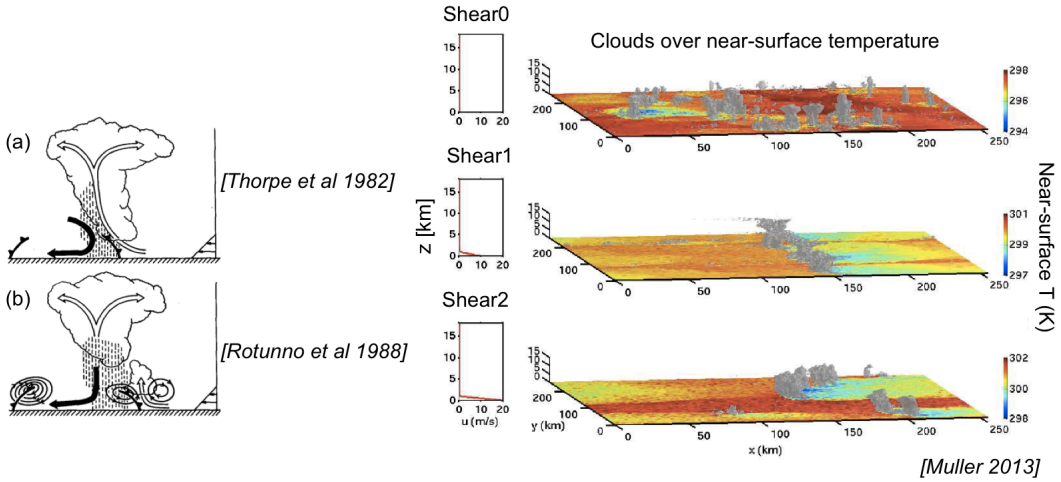

Figure IV.3: *Left: schematic interaction of a vertical wind shear with cold pools below precipitating clouds, adapted from [Rotunno et al., 1988]. Right: 3D view of cloud-resolving simulations with different wind shear, in which convection organizes into arcs, adapted from [Muller, 2013].*

IV.2.c Role of gravity waves

Unlike in mid-latitudes, shear is often weak in the tropics. Thus shear alone can not explain all organized convective systems in the tropics. Additionally, in the tropics, upscale growth is ubiquitous and sometimes rapid, occurring beyond the extent of cold pools, and convective inhibition is small so that small perturbations can easily initiate new convection. Internal feedbacks, independently of a large-scale forcing or a large-scale circulation, are natural candidates to explain the observed organization of tropical clouds.

[Mapes, 1993] proposed that gravity waves, generated by the convection and propagating horizontally away from the convection (located at $x = 0$ on figure IV.4), can destabilize the near-cloud environment and promote new convection nearby. Indeed, the deepest wave which warms and thus stabilizes the atmosphere, propagates the fastest. It is associated with subsidence throughout the troposphere (figure IV.4 $l = 1$ bore). The second mode ($l = 2$ bore on the figure) is a baroclinic mode which propagates slower, and with cooling (through adiabatic ascent) at low levels. This lifting in the lower troposphere encourages convection close to the original cloud, allowing for convection to be "gregarious" [Mapes, 1993].

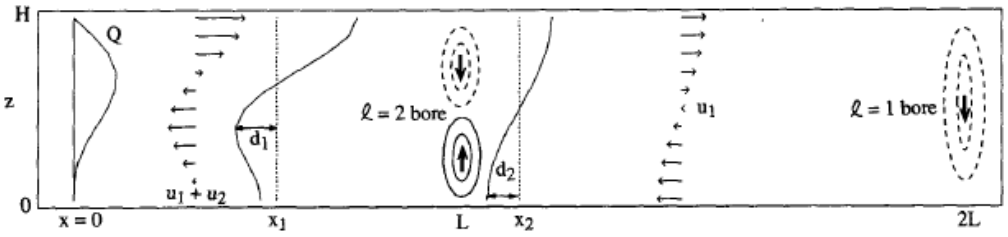

Figure IV.4: *Schematic response to the heating associated with convection and clouds occurring at $x = 0$. The heating profile $Q(z)$ is the sum of a deep mode with heating at all heights and a maximum at mid level, and of a baroclinic mode with cooling at low levels and heating at upper levels. This distribution of heat excites waves that then propagate away from the convection, yielding adiabatic subsidence warming ($l = 1$ bore and $l = 2$ bore at upper levels) and adiabatic cooling through ascent ($l = 2$ bore at lower levels, from [Mapes, 1993]).*

IV.2.d Wind-induced surface heat exchange (WISHE)

The so-called "wind-induced surface heat exchange", or WISHE [Emanuel, 1986], is a positive feedback of convection on itself, related to enhanced surface fluxes in the moist convecting region. This feedback is particularly crucial for tropical cyclones, whose extremely strong surface winds in the eyewall yield enhanced surface fluxes there (mainly in the form of evaporation from the ocean). Thus the eyewall, which is the most energetic region where moisture and clouds are found, is the place where the surface fluxes of energy are strongest. In other words, surface fluxes enhance energy in the high-energy region, thus reinforcing energy gradients and yielding a positive feedback on the convective organization.

IV.2.e Convective self-aggregation

This subsection is based on the paper

C.E. Holloway, A. Wing, S. Bony, C. Muller, H. Masunaga, T. L'Ecuyer, D. Turner, P. Zuidema
Observing convective aggregation
Surv. Geophys., 38 (2017).

An active area of research is linked to the spontaneous self-aggregation of convection. Self-aggregation refers to the spectacular ability of deep clouds to spontaneously cluster in space (see figure IV.5) despite spatially homogeneous conditions and no large-scale forcing, in high-resolution cloud-resolving simulations of the tropical atmosphere. As mentioned in chapter III (see notably §III.3), cloud-resolving models are models with fine, kilometer-scale resolution, i.e. simulations with sufficiently high spatial resolution to explicitly resolve the deep convection and deep clouds, instead of parameterizing them. Self-aggregation was first discovered in idealized settings, namely non-rotating radiative-convective equilibrium (setting further described in §III.3). Since its discovery in cloud-resolving models, the rapidly growing body of literature on self-aggregation confirmed its occurrence in a hierarchy of models, from two- and three-dimensional cloud-resolving models, to regional models and global climate models with parameterized convection, with super-parameterizations or without convective parameterization [Wing et al., 2017].

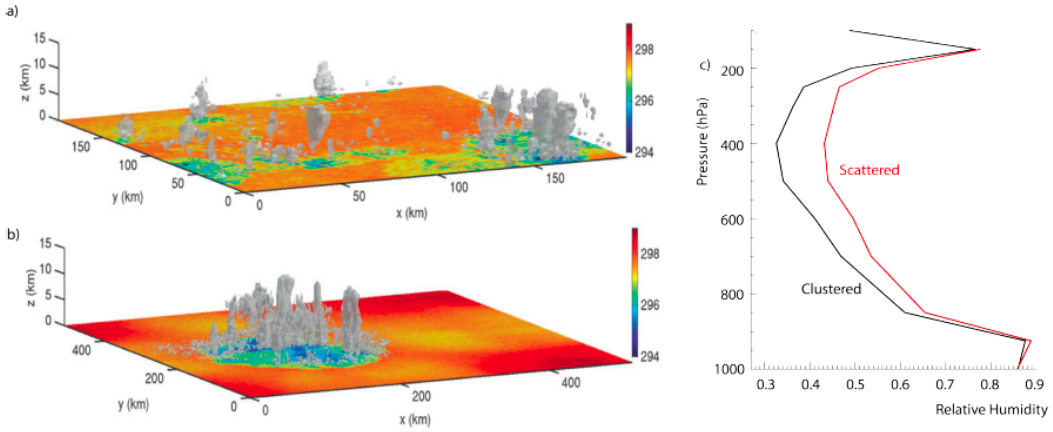

Figure IV.5: *In models, convective self-aggregation (panel b) emerges spontaneously, increasingly so with increasing temperatures. It is associated with a large-scale drying of the atmosphere and enhanced large-scale outgoing radiative cooling to space. In observations (panel c, relative humidity profiles from AIRS satellite measurements) the middle troposphere is drier in an atmosphere in which the same amount of precipitation is concentrated in a smaller number of convective clusters (adapted from [Bony et al., 2015]), consistent with modeled aggregation.*

From the very first studies describing convective self-aggregation [Held et al., 1993, Tompkins, 2001, Bretherton et al., 2005], there has been a recurring question: is this "real"? In other words, is the intriguing clumping behavior representative of actual convective organization in nature, or is it just a model artifact? And, to the extent that the behavior is relevant for understanding real atmospheric convection, what does it tell us about the role of convective organization in weather and climate?

In [Holloway et al., 2017] we argue that this behavior in models does appear to be relevant to real-world convection and climate. Notably, there is agreement between models and observations that, as convection becomes clumped into fewer moist regions, the subsidence regions become drier, resulting in a drier large-scale mean environment (figure IV.5, see also [Tobin et al., 2012]). This

drying, and a reduction of upper-tropospheric stratiform cloud, leads to larger outgoing longwave radiation and stronger atmospheric cooling.

There are also some aspects of self-aggregation in models that conflict with observations, and many aspects that need more observational study. How aggregation and its effects interact with local sea-surface temperature on short time scales and with tropics-wide sea-surface temperatures on long time scales is still uncertain in both models and observations. Initiation processes, such as radiatively driven cold pools and related shallow overturning circulations, are one obvious observational target. Maintenance processes may be even easier to study in observations, since they can be studied in heterogeneous conditions more typical of convection in nature.

Certainly, the study of convective self-aggregation is leading to exciting new insights into processes that allow convection to interact with its environment in models. There are encouraging signs that these processes may operate in nature too, and there is a lot of recent progress arising from the ability to simulate mesoscale systems, requiring large hundreds of kilometers domains, while resolving deep convection, requiring fine kilometric resolution. Thus advances in computer power combined with new discoveries based on idealized frameworks, theory and observational findings, make this the ideal time to determine the fundamental processes governing self-aggregation, and its link to convective organization in nature. In the following sections, we investigate in more detail the physical processes responsible for self-aggregation, and then assess implications for ocean eddies - convection interactions, and for tropical cyclogenesis.

IV.3 My research: physical processes responsible for self-aggregation over homogeneous sea-surface temperatures

This section is based on the papers

C. Muller, S. Bony
What favors convective aggregation and why?
Geophys. Res. Lett., 42 (2015).

A. Wing, K. Emanuel, C. Holloway, C. Muller
Convective self-aggregation in numerical simulations: a review
Surv. Geophys., 38 (2017).

P. Zuidema, G. Torri, C. Muller, A. Chandra
Precipitation-induced atmospheric cold pools over oceans and their interactions with the larger-scale environment
Surv. Geophys., 38 (2017).

In simulations of radiative-convective equilibrium, illustrated in figure IV.5a, convection is somewhat randomly distributed, resembling "pop-corn" convection. Self-aggregation (figure IV.5b) can be seen as an instability of radiative-convective equilibrium, in which random pop-corn convection is replaced by a highly organized state. Convection is confined to a subregion of the domain, and is surrounded by extremely dry air. In this section, we investigate in more detail the physical processes involved. The simulations described here are performed with the cloud-resolving model SAM (see [Khairoutdinov and Randall, 2003] and §III.3 for more details on the model).

IV.3.a Self-aggregation by radiative feedbacks

From sensitivity experiments, i.e. simulations where the various feedbacks are turned on and off (e.g. surface flux feedbacks, radiative feedbacks...), we now know that longwave radiative feedbacks are crucial for self-aggregation, at least at current tropical temperatures [Muller and Held, 2012]. More precisely, the longwave radiative cooling from low clouds in dry regions is found to be necessary for the spontaneous onset of self-aggregation from homogeneous initial conditions. When simulations are initiated from aggregated conditions though, the clear-sky radiative feedback from dry regions and the high-cloud radiative feedback from moist regions are also found to be sufficient to maintain the aggregation.

The importance of longwave radiative feedbacks for convective aggregation can be understood by considering the moist static energy transport between the dry and the moist regions. Note that in the tropics, horizontal temperature gradients are small, so that the variability in moist static energy is largely dominated by the variability of water vapor. Thus high energy regions correspond to moist regions and vice versa. Figure IV.6 shows the circulation (black streamfunctions) in height and moisture space [Bretherton et al., 2005, Muller and Bony, 2015]. The top panels show the circulation along with radiative cooling rates (left) and moist static energy (right). The arrows show the direction of the circulation.

The strong radiative cooling in dry regions at low levels, which is largely due to the presence of low clouds (pink contours top left panel), generates subsidence (blue arrow) in the lowest kilometers of the dry columns. This radiatively-driven subsidence in dry regions further dries those regions, resulting in persistent radiatively-driven "dry pools" [Zuidema et al., 2017], where deep convection is suppressed. The dry subsidence forces a near-surface flow (black arrow) from dry to moist columns. The high moist static energy near the surface (top right panel) is thus exported from the dry regions into the moist regions, yielding an upgradient energy transport. This is the positive feedback believed to be responsible for the strengthening energy gradient and concomitant self-aggregation of convection.

As mentioned above, even without the longwave radiative feedbacks from low clouds, convective aggregation can be maintained from aggregated initial conditions. The bottom panels show the same circulation, but in a simulation without low cloud longwave radiative contributions. The clear-sky low-level cooling in dry regions along with radiative warming from high clouds in the moist columns again yield subsidence in dry (blue arrow) and upward motion (red arrow) in moist regions. The near-surface flow associated with this dynamical response to the radiative cooling distribution (black arrow) again exports energy from dry regions to moist regions, yielding an upgradient energy transport.

In all cases, it is the low-level circulation, forced by differential radiative cooling rates between dry and moist regions, which is responsible for the upgradient energy transport yielding convective aggregation. Note that moist static energy is a strong function of height, thus the altitude of the radiative cooling and heating is important. In fact, [Muller and Bony, 2015] show that imposing enhanced radiative cooling in dry regions in radiative-convective equilibrium simulations can lead to the self-aggregation of convection, if the cooling is applied at low altitudes.

IV.3.b Self-aggregation by moisture-memory feedback

Surprisingly, it is possible to simulate self-aggregation even while suppressing radiation and other diabatic feedbacks [Muller and Bony, 2015], a result later confirmed in another model [Holloway

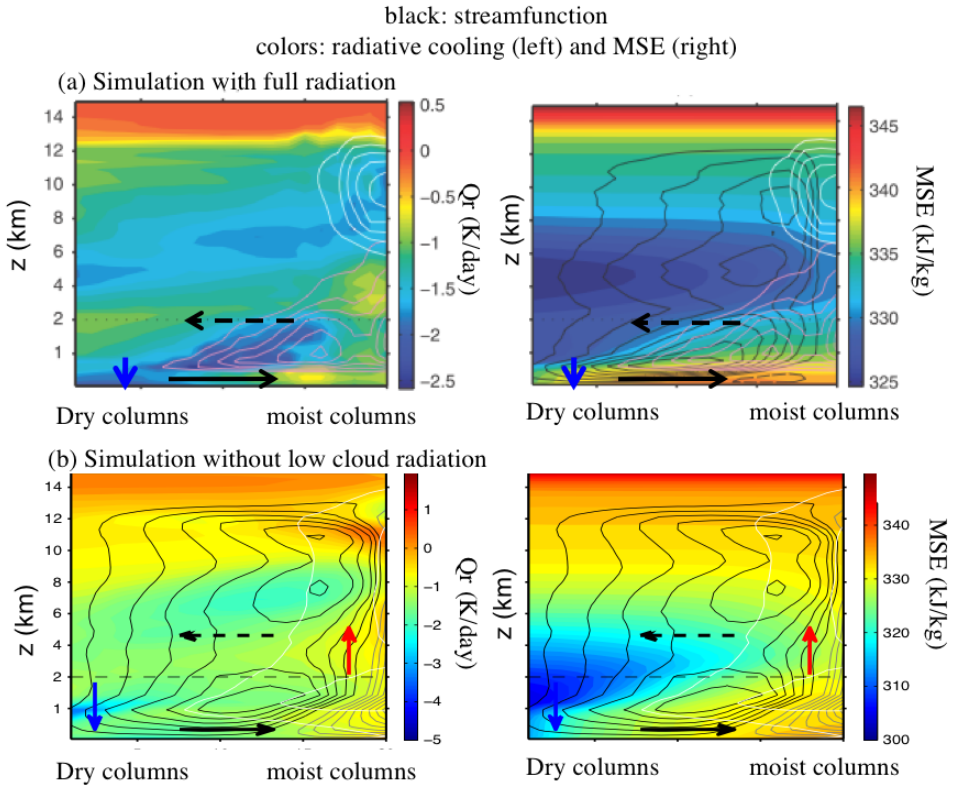

Figure IV.6: *Circulation in height and moisture space (black streamfunction) in simulations that aggregate. The top panels show a simulation with full radiation, while the bottom panels show a simulation where the low-cloud longwave radiative feedback is removed (after [Muller and Bony, 2015]).*

and Woolnough, 2016]. It occurs when the evaporation of falling rain is suppressed in the subcloud layer (below 1 km or so), thus preventing the formation of strong downdrafts and cold pools. In other words, it occurs at unrealistically high precipitation efficiency.

The process leading to self-aggregation seen in these simulations has been called "moisture-memory" feedback, since it relies only on intrinsic interactions between clouds and the water vapor around them to spontaneously organize into clusters. In standard conditions, the cooling associated with the evaporation of rain below deep convecting clouds generates downdrafts, which through their thermodynamical effect oppose the upward motion that generated the cloud. This negative feedback on upward convection suppresses the deep cloud in a few hours. Without the evaporation of rain and the effect of the associated downdrafts, moist areas remain moist (or even get moister by convergence) and thus become even more favorable to convection. This tends to localize the convection, as observed in these simulations.

IV.4 My research: implications for ocean eddies - convection interaction, and for tropical cyclogenesis

IV.4.a Impact of ocean temperature inhomogeneities

This section is based on the paper

S. Shamekh, C. Muller, J.-P. Duvel, F. D'Andrea
How do ocean warm anomalies favor the aggregation of deep convective clouds?
J. Atmos. Sci., in review (2019).

Because of the idealized settings in which self-aggregation was discovered, its relevance to the real world is still debated. Notably, the aforementioned studies used spatially and temporally constant and uniform sea-surface temperature (SST). Here we investigate the impact of ocean SST inhomogeneities on earlier results. More precisely, we investigate how an idealized warm circular SST anomaly, referred to as "hot-spot", helps organize convection, and how self-aggregation feedbacks modulate this organization.

The impact of SST inhomogeneities on deep convection has been widely studied in the literature investigating the response of convection to different surface forcing [Tompkins, 2001, Kuang, 2012, Ramsay and Sobel, 2011] [Tompkins, 2001] finds that flipping the SST anomaly leads to migration of the convective clusters over the warm anomaly. The migration of aggregated convective cluster over warm anomaly has been confirmed by other studies which used a slab ocean in order to have interactive SST [Coppin and Bony, 2017, Grabowski, 2006]. Using a single column model and a cloud-resolving model, [Ramsay and Sobel, 2011] show that precipitation rate increases over local warm SST and is determined by the temperature anomaly rather than mean SST. The SST anomaly, if large enough, can suppress convection in one column and strengthen it in the warmer column. Notably, SST gradients can generate a large-scale circulation that can lead to a migration of deep convection towards the warmest SST.

Ocean mesoscale eddies [Chelton, 2011] can also be associated with SST anomalies reaching a few degrees in cold core cyclonic eddies or warm core anticyclonic eddies. These persistent ocean eddies have typical radius varying with latitude, from a hundred to a few hundreds of kilometers in the tropics ($\pm$ 20° latitude), to around 50 km or less in mid-latitudes. As a surface forcing, eddies can impact the atmosphere locally [Sugimoto et al., 2017] by enhancing low-level convergence and thus convective precipitation. Potentially, the eddies changes the cloudiness and wind field which can impact the large scale circulation. Whether and how such persistent SST anomalies, as an external forcing, can favor or suppress the aggregation of convection is, to our knowledge, still not well covered in the literature and is the topic of this section.

We use the cloud-resolving model SAM as before, and impose an idealized circular hot-spot (radius R and temperature anomaly dT) in the center of the domain (black circle figure IV.7). We find that the presence of a hot-spot significantly accelerates aggregation, particularly for larger domains (figure IV.7) and warmer/larger hot-spots, and extends the range of SSTs for which aggregation occurs (figure IV.8). Indeed in this model, over uniform SST (referred to as "ocean" simulations, figure IV.8a), self-aggregation only occurs for SSTs larger than 295 K. But in the presence of a hot-spot, simulations with domain mean SST as low as 290 K aggregate (figure IV.8b), and the aggregation is significantly faster than warmer constant-SST simulations.

Aggregation even happens without radiative feedbacks for hot-spots sufficiently large/warm [Shamekh et al., 2019]. In that case, the aggregation onset results from a large-scale circulation induced by the hot-spot. Specifically, it is related to an initial transient warming, as convection over the hot-spot brings the atmosphere towards a warmer moist adiabat. The warmer temperatures are imprinted over the whole domain by gravity waves and subsidence warming. The initial

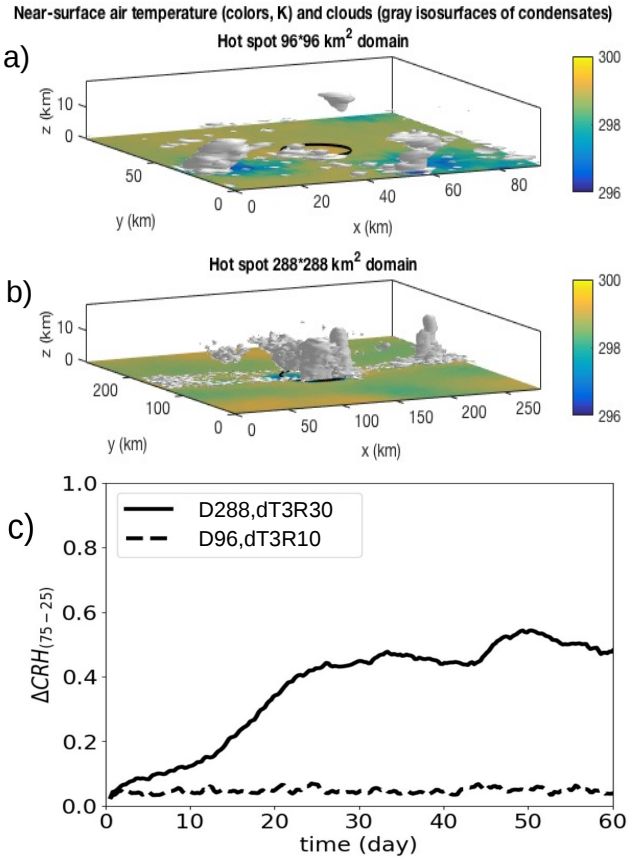

Figure IV.7: *Snapshots of near-surface air temperature (colors, K) and cloud water (grey shades) from two simulations with a hot-spot in the center of the domain (circle) for (a) a domain size 96×96 km^2 and (b) 288×288 km^2. (c) Time evolution of the aggregation index (larger for more organized states) for those two simulations. Larger domains, and larger/warmer hot-spots favor convective aggregation (after [Shamekh et al., 2019]).*

transient warming and concomitant subsidence drying suppress convection outside the hot-spot, thus strengthening the aggregation of convection and moisture over the hot-spot.

Consistently, during the aggregation onset phase, the strength of aggregation is found to nicely correlate with the strength of the large-scale circulation, as measured by the mean subsidence velocity in dry regions. This large-scale circulation is found to be sensitive to the hot-spot fractional area, as can be understood with a simple geometric argument. As the hot-spot becomes larger, the dry region shrinks in our doubly-periodic setting. Therefore stronger compensating subsidence is needed to compensate the upward mass flux over the hot-spot. This strengthening of the large-scale circulation is consistent with the faster aggregation with larger hot-spots.

These results highlight the need to use large domains when investigating convection over inhomogeneous SSTs in similar doubly-periodic geometry, in order to avoid or to control the aggregation of convection over warm temperature anomalies. In reality, with planetary rotation, the scale of the large-scale circulation induced by SST anomalies is likely determined by the Rossby radius of deformation. Our results suggest that for a large enough fractional area of SST anomalies compared to this large-scale circulation, self-aggregation feedbacks could play a role in organizing deep

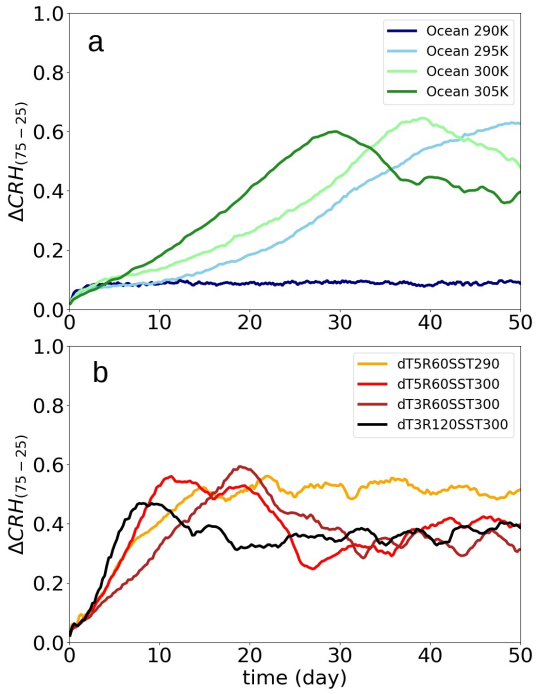

Figure IV.8: *Time evolution of the aggregation index for simulations with full radiative feedback for: (a) simulations with a uniform surface temperature (referred to as "Ocean"; (b) simulations with a hot-spot of different sizes (radius R) and temperature anomalies (dT, with domain-mean SST equal to 290 or 300 K; after [Shamekh et al., 2019]).*

convection over SST anomalies. In the ocean, SST anomalies of the size studied here ($\mathcal{O}$(100 km)) are not uncommon, taking the form of mesoscale eddies (Chelton 2011). Their contribution to convective organization deserves further investigation.

IV.4.b Acceleration of tropical cyclogenesis by self-aggregation feedbacks

This section is based on the paper

C. Muller, D. Romps
Acceleration of tropical cyclogenesis by self-aggregation feedbacks
Proc. Natl. Acad. Sci. (2018).

Few geophysical phenomena are as spectacular as Tropical Cyclones (TCs). The cloud-free eye with weak motion is surrounded by an eyewall with clouds and rotating winds among the strongest on the planet. Though the prediction of cyclone tracks has improved in recent years, understanding the mechanisms responsible for the genesis and intensification of cyclones remains a major scientific challenge [DeMaria et al., 2014]. The present study addresses the following questions: is self-aggregation relevant to the formation of TCs? Or are the feedbacks identified in idealized simulations not robust to planetary rotation? Are they dominated by other processes once rotation is accounted for?

As mentioned above, most studies of self-aggregation focused on idealized simulations, in particular radiative-convective equilibrium with no large-scale forcing and neglecting Earth's rotation. Neglecting Earth's rotation, i.e., setting $f = 0$ s^{-1} where f denotes the Coriolis parameter, is a reasonable approximation near the equator and at small scales, but becomes questionable when the convective aggregate reaches mesoscales. At those scales, the effect of the Earth rotation starts to be appreciable.

Earlier studies of rotating radiative-convective equilibrium, sometimes referred to as a "tropical cyclone world", mainly investigated the properties of the mature cyclones (including the size and the distance between cyclones [Khairoutdinov and Emanuel, 2013, Davis, 2015, Shi and Bretherton, 2014, Wing et al., 2016]). Here, instead, we focus on the onset of cyclone formation, and our goal is to compare in detail cyclogenesis with the onset of convective self-aggregation. To that end, we perform a series of sensitivity runs where various feedbacks are turned on or off. More precisely, we focus on the relative role of the following two feedbacks: radiation feedbacks and surface-flux feedbacks. Radiation feedbacks include low-cloud, high-cloud and clear-sky feedbacks, which have all been shown to contribute positively to self-aggregation [Muller and Bony, 2015]. Surface-flux feedbacks connect enhanced surface winds to enhanced surface fluxes, and this connection, often referred to as a wind-induced surface heat exchange (WISHE, introduced in §IV.2.d) feedback, plays a key role in maintaining tropical cyclones [Emanuel, 1986].

Our work builds upon the recent work of [Davis, 2015, Wing et al., 2016] who investigate the spontaneous generation of tropical cyclones from homogeneous conditions in rotating radiative-convective equilibrium. In particular, [Wing et al., 2016] suggest that radiative feedbacks, known to be key for self-aggregation, could accelerate cyclogenesis, a result that we further investigate and quantify here, in rotating doubly-periodic radiative-convective equilibrium simulations.

Results

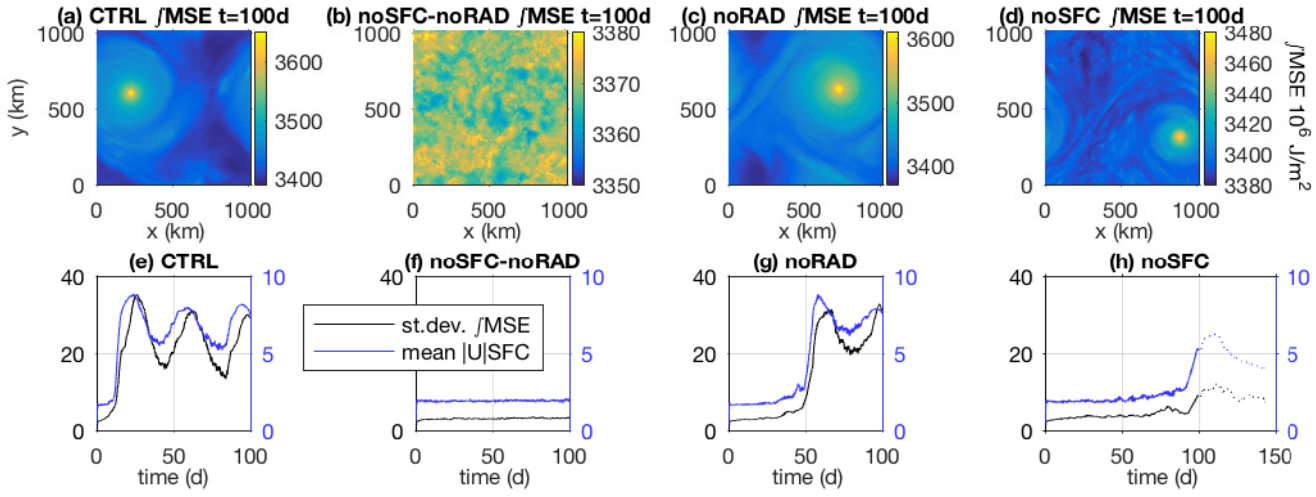

Figure IV.9: *Cyclone evolution in CTRL and sensitivity runs. Top (a-d) Snapshots of ∫MSE at day 100 of the simulations. Bottom (e-h) Time evolution of the standard deviation of ∫MSE, and of the domain-averaged wind speed near the surface in m s^{-1} at the first atmospheric level z = 37.5 m (from [Muller and Romps, 2018]).*

Figure IV.9 shows snapshots from a control simulation and three sensitivity simulations: CTRL

(panel a) with all feedbacks turned on (RAD and SFC); noSFC-noRAD (panel b) with all feedbacks turned off; noRAD (panel c) with interactive radiation turned off; and noSFC (panel d) where feedbacks associated with interactive surface fluxes are turned off (in particular WISHE effects are off). The variable shown is the vertically-integrated moist static energy

$$\int \text{MSE} = \int_0^{z_t} (c_p T + gz + L_v q_v)\ \rho\ dz, \tag{IV.1}$$

where z_t is the tropopause height, c_p the specific heat of air, T temperature, g gravity, L_v latent heat of vaporization, q_v water vapor mixing ratio and ρ density. $\int$MSE is a useful variable since it is conserved during moist adiabatic processes in this model (neglecting subgrid-scale fluxes and latent heat contributions from the ice phase). Hence its mass-weighted vertical integral can only be changed by radiation, surface fluxes, and advection. In the tropics, where horizontal temperature gradients are small, its variability is closely related to that of water vapor. Consistently, snapshots of precipitable water $\int_0^{z_t} q_v\ \rho\ dz$ show a very similar spatial distribution as $\int$MSE, the only difference being that the eye of the cyclone is visible in precipitable water (dry anomaly), while it is not seen in $\int$MSE since the dryness in the eye is largely compensated by warmer conditions due to adiabatic compression. Also shown are the time evolution of the standard deviation of $\int$MSE and of the domain-mean wind speed near the surface (first atmospheric level at 37.5 m, panels e-h), both indicative of the TC intensification. Convective organization in general, is associated with an increase in $\int$MSE variance, as moist regions become moister and dry regions become drier [Wing and Emanuel, 2014, Wing and Cronin, 2016].

The CTRL run develops a cyclone in about 25-30 days, with a minimum surface pressure of about 930 hPa. When all feedbacks are turned off (noSFC-noRAD), no cyclone develops, as expected, since interactive surface fluxes are believed to be key for TCs (this remains true if we run longer; no cyclone develops even after 250 days of simulation). Surprisingly, though, if only radiative feedbacks are removed (noRAD), the cyclogenesis takes about 60 days, which is more than twice as long as in the CTRL run. This suggests that aggregation feedbacks accelerate the cyclogenesis process (at least in the absence of large-scale forcing) by a factor of about two. Perhaps even more surprisingly, if just surface-flux feedbacks are removed (noSFC), the simulation still yields a weak "radiative cyclone". In other words, radiative feedbacks are sufficient to yield a cyclone, even without interactive surface fluxes (i.e., even without WISHE). The TC is still intensifying after 100 days of simulations, but remains weaker than in CTRL even if we run longer (Figure IV.9h). Without the wind-induced enhancement of turbulent surface fluxes, the TC can not reach its full intensity in the mature stage. Yet, the fact that radiative feedbacks on their own are sufficient to initiate even a weak cyclone is remarkable.

Also note that, once the TC is formed, whether radiative feedbacks are turned on or not, the cyclone intensity is to leading order the same, although there is a slight reduction without interactive radiation (7% reduction between CTRL and noRAD of the high percentiles of the standard deviation of $\int$MSE, and 15% reduction of the high percentiles of surface wind speed; similar reductions, between 5 and 15%, are found based on high percentiles of precipitable water and latent heat flux). This is again consistent with our current understanding of TCs, whose main source of energy in the mature stage are interactive surface fluxes [Emanuel, 2003]. But we find here that the radiative feedbacks are responsible for a small but non-negligible contribution to the intensity of the mature cyclone, consistent with an earlier study pointing out the importance of radiation in the maintenance of a cyclone intensity [Wing et al., 2016].

Before moving on, it is interesting to note that the mature cyclone undergoes three periods of

intensification in CTRL. A similar variability was noted in [Wing et al., 2016]. We hypothesize that these periods are related to a vertical wind shear which develops as the TC strengthens.

Role of radiative feedbacks on timing of cyclone formation

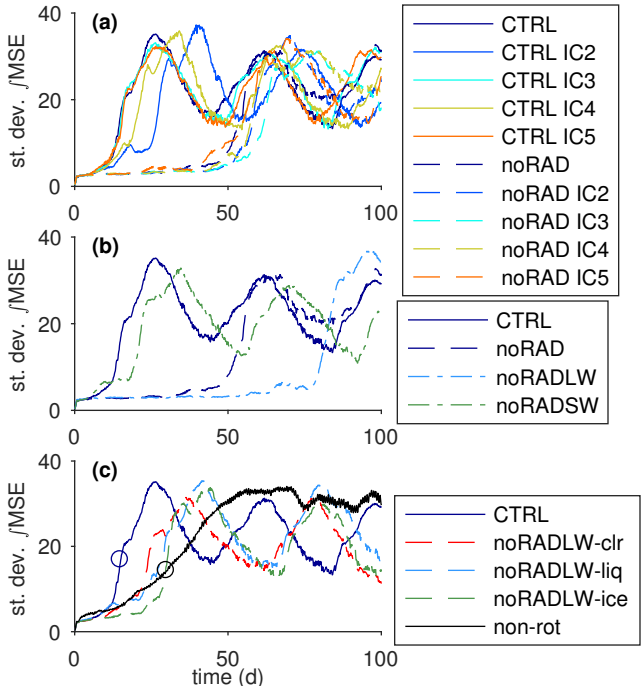

Figure IV.10: *Time evolution of the standard deviation of ∫MSE (10^6 J m^{-2}) (a) for different initial conditions, (b) in sensitivity runs removing separately the SW and LW interactive radiation, and (c) in sensitivity runs removing the LW liquid cloud, ice cloud and clear-sky contributions separately. Open circles in panel c indicate the first 15 days of cyclogenesis and the first 30 days of non-rotating self aggregation (from [Muller and Romps, 2018]).*

Let us now investigate further the impact of radiative feedbacks on the time needed to reach a fully developed cyclone. Both cyclogenesis and self-aggregation have been shown to be sensitive to initial conditions [Khairoutdinov and Emanuel, 2010, Wing et al., 2016]. We verify that the slow down of cyclone formation without radiative feedbacks is robust to initial conditions (Figure IV.10a), with a factor two or larger for all initial conditions. In fact, for all the initial conditions tried here, the control simulation was faster than any sensitivity simulation (noRAD, noSFC, or noSFC-noRAD) that we tried. Also, separately removing the shortwave (SW) and LW contributions to the radiation highlights the key role of LW radiative feedbacks (Figure IV.10b): removing the interactive SW radiation has little impact, while removing the interactive LW radiation slows down the cyclone formation even more than noRAD. This suggests a similarity with the non-rotating self-aggregation process for which LW feedbacks are known to be crucial. Also consistent with self-aggregation is the fact that the three terms in the LW radiative cooling, LW cooling from liquid clouds, ice clouds and clear sky, all contribute positively to the acceleration of the cyclogenesis process (Figure IV.10c). Indeed, removing each separately does not account for the overall slow down of the cyclogenesis.

These results are qualitatively consistent with [Wing et al., 2016] (see their figure 4), who also

find that removing radiative feedbacks delays cyclogenesis. In order to further quantify the impact of radiative feedbacks on the time scale of convective organization, we performed a larger ensemble of CTRL and noRAD simulations, and found that the acceleration of cyclogenesis by radiative feedbacks was extremely robust. Interestingly, the variability of the time scale of convective organization is smaller in our CTRL simulations than in [Wing et al., 2016]. We hypothesize that this is due to the different radiation scheme used (RRTM versus CAM here), since their simulations without radiative feedbacks yield a smaller variability. Other differences in our settings could also play a role (in particular, they use a warmer sea-surface temperature of 305 K compared to 300 K here).

Comparison with nonrotating self-aggregation

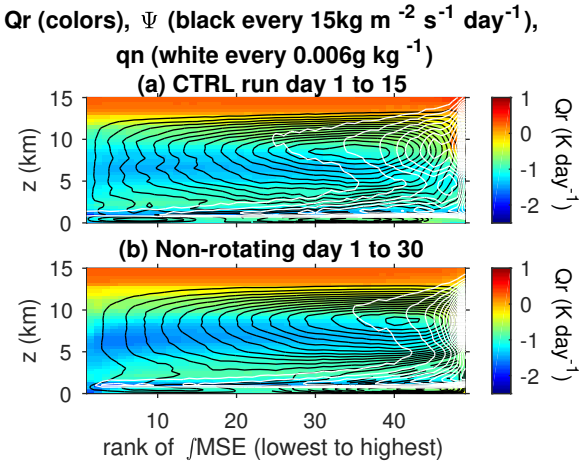

Figure IV.11: *Cyclogenesis versus self-aggregation. Circulation between dry and moist columns during (a) the formation of the tropical cyclone in CTRL and (b) the onset of self-aggregation in a non-rotating simulation. The dry columns are on the left (low ∫MSE rank), and the moist columns are on the right (high rank). Plain black contours indicate counterclockwise circulation, and white contours indicate cloud condensates (from [Muller and Romps, 2018]).*

Figure IV.11 shows similarities between self-aggregation and cyclogenesis. It shows the radiative cooling rates and streamfunctions, as well as cloud content, in the cyclone (a) and self-aggregation (b) runs, as a function of height and rank of vertically-integrated ∫MSE. We focus on the genesis, hence we show day 1 to 15 for the cyclone (see blue open circle in Figure IV.10c, day 15 is about half way to the full cyclone) and day 1 to 30 for self-aggregation (see black open circle Figure IV.10c, where similarly day 30 is about half way to the full aggregation). The self-aggregation plot is slightly less noisy since it contains more days. In both cases, though, there is strong low-level radiative cooling in dry regions (strong cooling between the surface and 2 km in the dry columns below rank 20) from clear-sky and low-level liquid clouds, which promotes aggregation [Muller and Bony, 2015]. We also see the mid-level radiative warming in moist convective regions from middle and high clouds (warming in the moistest columns above 5 km) also known to enhance aggregation [Muller and Bony, 2015].

We can compare the circulation with the one expected from radiative cooling rates only, assuming that radiative cooling is exactly balanced by subsidence warming. This is expected to be true outside of clouds (in cloudy regions however, the latent heat also enters the temperature equation,

and therefore contributes to vertical velocities). Consistently, we find that there is a good agreement in the dry regions away from clouds between the circulation expected from radiative cooling rates only, and the actual circulation (not shown, see [Muller and Romps, 2018] for more details). The differential radiative cooling between dry and moist regions is therefore largely responsible for the low-level subsidence seen in Figure IV.11 below 2 km in the driest columns (up to rank 10 or so). This subsidence is accompanied by a flow from dry to moist columns near the surface (up to rank 20), rising above 2 km in the moister columns (rank 20 or higher). This low-level circulation from dry to moist regions is crucial since it transports MSE upgradient, from dry to moist regions, favoring aggregation [Bretherton et al., 2005, Muller and Bony, 2015].

These results suggest a close similarity between cyclogenesis and the idealized self-aggregation process, which can be quantified further using the moist static energy variance budget to quantify direct diabatic feedbacks, following [Wing and Emanuel, 2014]. Quantitatively, using this budget, the early times of cyclogenesis in the CTRL simulation resemble accelerated self-aggregation (days 1 to 15 for the TC, days 1 to 30 for the self-aggregation), with similar contributions from the various feedbacks to the development of organized convection. The simulations then diverge when interactive surface fluxes become a strong positive feedback in CTRL, due to strong winds and surface fluxes in the flow converging into the cyclone, while they become a small negative feedback in the self-aggregation, due to strong surface latent fluxes in the dry subsidence region, consistent with [Wing et al., 2016] (not shown, see [Muller and Romps, 2018] for more details).

Summary and discussion

The overall picture that emerges is that the feedbacks identified in idealized settings as leading to the spontaneous self-aggregation of convection play an important role in our cyclogenesis simulations. More precisely, the onset of self-aggregation in non-rotating simulations shares qualitative and quantitative properties with tropical cyclogenesis. Radiative feedbacks are found to accelerate the cyclogenesis by a factor two or larger. The longwave radiative feedback is the key contribution to those radiative feedbacks, as in self-aggregation. Surprisingly, radiative feedbacks by themselves are sufficient to yield a cyclone, albeit weak, even in the absence of WISHE effects.

We acknowledge that the simulations used in this study are still idealized, e.g., doubly-periodic and in radiative-convective equilibrium, without large-scale forcing. In the real tropics, the route to tropical cyclogenesis can be quite different, and is influenced by large-scale environmental conditions, such as the passing of an equatorial wave and preexisting favorable moist conditions within a "marsupial pouch" [Dunkerton et al., 2009]. Comparison of the time scale of self-aggregation tendencies investigated here to that of large-scale environmental conditions deserves further investigation using more realistic simulations. Our results suggest that self-aggregation, and the framework developed for its study, can help shed some new light into the physical processes leading to cyclogenesis and cyclone intensification. In particular, our results point out the importance of the longwave radiative cooling at low levels *outside* the cyclone, and the low-level circulation that it entails. Further comparison with data, and analysis of simulations in more realistic settings, are desirable to clarify the precise contribution and location of the longwave radiative feedback.

Chapter V

Perspectives: future research directions

"A ship in port is safe, but that's not what ships are built for."
Grace Hopper

V.1 Summary: scientific and personal objectives

The European Research Council (ERC) Starting grant that I just obtained for the period 2019–2024 will largely shape my research in the coming 5 to 10 years. The topic of this project is convective organization, and implications for tropical cyclones and for the energetics of the tropics, in current and in a warming climate. Indeed, despite its strong societal and climatic impacts, the physical processes behind convective organization are still poorly understood, as discussed in chapter IV. In fact, mesoscale convective organization is typically not accounted for in global climate models used for climate prediction. One of the goals of this project is to lead to improved fundamental understanding of the physical processes at stake. The specific scientific questions addressed are described in more detail in the coming sections.

One of my personal goals is to broaden both my research areas and methodologies. In past work, I have mainly focused on theoretical and idealized numerical tools. In future work, I look forward to investigating observational evidence for the relevance or not of self-aggregation to the observed organization of convection, using both satellite and in-situ observations, as initiated in [Holloway et al., 2017]. I am currently pursuing research in this direction with my colleagues at LMD, and with Allison Wing (Florida State University) and Dave Turner (NOAA).

I am also very excited about my new research on tropical cyclones. I recently started a collaboration with Olivier Pauluis (New York University) on the role of cold pools and shallow circulations on cyclogenesis. I very much hope to continue research in this field. And I hope to continue my existing collaborations on ocean waves, notably with Jean-Marc Chomaz (LadHyX).

Many outstanding open questions remain regarding precipitation extremes and their response to warming. As noted in my recent review paper on precipitation extremes [Muller and Takayabu, 2019], recent decades have seen important fundamental advances on this topic. But without a complete theory for the dynamical and microphysical changes with warming, we can not properly attribute causes for the corresponding contributions to extreme rainfall rates. I hope to pursue research in that theoretical direction as well.

V.2 Perspectives: towards an improved fundamental understanding of convective organization

I first plan to study self-aggregation in simulations in the presence of a large-scale circulation, thus relaxing the radiative-convective equilibrium assumption of earlier work, but still in settings simple enough to allow for quantitative comparison with simple theoretical models that will be developed where possible. The ultimate goal is to derive a simple scaling for the time scale of aggregation, and its dependence on the large-scale circulation and large-scale conditions. Notably, it is well known that self-aggregation is favored at warm sea-surface temperatures in models. This is consistent with theoretical expectations from the effect of clear-sky radiative feedbacks [Emanuel et al., 2014]. But given the importance of cloud radiative feedbacks as well, its inclusion in the theory may help clarify the model behavior.

I also plan to investigate the strength of radiative feedbacks in dry regions in observations. Since the [Tobin et al., 2012] seminal study, other groups have started looking at observational evidence of strong radiative cooling rates in dry regions, but all use satellite data (Hirohiko Masunaga, Sandrine Bony, personal communication). Although this allows to investigate correlations between convective aggregation and radiative cooling rates, the issue with this approach is that the radiative

cooling at low levels is key, and low levels are poorly resolved by satellite.

Instead, we propose to use in-situ data, computing radiative cooling rates from observed tropical thermodynamic profiles, which have high resolutions in the lower troposphere. The question addressed is whether the differential cooling rates consistent with observed dry and moist profiles, are sufficient to yield self-aggregation when imposed in numerical simulations. As mentioned earlier, this project is joint work with Allison Wing (Florida State University) and Dave Turner (NOAA). In a second step, we will then correlate the occurrence of strong differential cooling, with the degree of mesoscale convective organization, derived from satellite, using an index similar to the SCAI index introduced by [Tobin et al., 2012], in collaboration with Addisu Semie and Sandrine Bony (LMD).

V.3 Perspectives: self-aggregation by moisture-memory feedbacks

Little is known about this feedback, which occurs when the evaporation of rain is artificially suppressed in the subcloud layer. It was only recently discovered [Muller and Bony, 2015], and was later confirmed to occur in another model [Holloway and Woolnough, 2016]. The moisture-memory feedback offers a tantalizing framework to investigate the details of the moisture-convection interaction relevant to the organization of convection. In [Muller and Bony, 2015], we hypothesize that low-level moisture is key through its influence on convective available potential energy (hence the buoyancy of near-surface parcels [Muller et al., 2009]). It has also been argued that it could be linked to mid-tropospheric humidity via its impact on entrainment (organized convection leads to entrainment of moister air surrounding updrafts, hence less dilute plumes, [Holloway and Neelin, 2009]). In collaboration with Christopher Holloway (University of Reading), we plan to clarify the atmospheric layer which is key for the moisture-memory interaction, as well as its sensitivity to warming and its interaction with other diabatic feedbacks. We hope in particular to clarify the role of entrainment mixing of rising plumes, known to be a critical parameter in convective parameterizations in climate models, with far-reaching implications beyond the tropics [Tomassini et al., 2015].

This work will hopefully benefit researchers and model developers working on improving the representation of convection and convective organization in models. I will enable these impacts through engagement with modeling centers. I already have strong existing interactions with climate model developers of the French LMDZ model (Laboratoire de Météorologie Dynamique Zoom) and at the Centre National de Recherches Météorologiques (CNRM), and the Met Office in the UK-wide ParaCon project.

V.4 Perspectives: implications for tropical cyclones and for the tropical energetics

Another important aspect of my ERC project is an in-depth analysis of the implications of convective organization and its response to warming, for tropical cyclogenesis and rapid intensification, and for the large-scale tropical hydrological cycle (mean and extreme precipitation) and climate (notably top-of-atmosphere radiation).

In [Muller and Romps, 2018], we show that self-aggregation feedbacks can significantly accelerate cyclogenesis. Our recent work [Shamekh et al., 2019] also indicates that self-aggregation could resonate with a surface hot-spot, i.e. localized warm circular anomalies, with an optimal diameter

around 100 km. Warm anomalies of this size in regions of tropical cyclone formation are not uncommon due to the presence of ocean mesoscale eddies. This work will benefit from an existing collaboration with Sabrina Speich (LMD), using observations of ocean mesoscale eddies and tropical cyclones to assess the role of ocean-atmosphere interactions in observations.

As mentioned earlier, self-aggregation is also associated with increased outgoing longwave radiation at the top of the atmosphere. Given the enhancement of self-aggregation with warming, it could be a key missing ingredient in current estimates of climate sensitivity [Mauritsen and Stevens, 2015]. This also led to the hypothesis that self-aggregation could be a way for the tropical temperatures to regulate themselves [Khairoutdinov and Emanuel, 2010]: increased temperatures yield increased aggregation, which in turn yields increased longwave cooling to space which decreases temperatures, and so on. In observations, [Tobin et al., 2012] confirm that observed aggregation, from satellite brightness temperatures, is correlated with increased top-of-atmosphere longwave cooling. But they also find that this is largely compensated by increased incoming shortwave due to decreased cloud fraction with organization. Whether this behavior holds in cloud-resolving models, and how it may change with warming, is unknown and is of primary global importance.

Overall, these projects are all part of an international ongoing effort aimed at clarifying the impact of convective organization in our current, and in a warming climate.

Appendices

.1 Curriculum vitae

CONTACT

Laboratoire de Météorologie Dynamique
École Normale Supérieure — 06 50 13 56 40
24 rue Lhomond — carolinemuller123@gmail.com
75005 Paris — www.lmd.ens.fr/muller/

RESEARCH TOPICS

Hydrological cycle (mean and extreme precipitation), spatial organization of tropical clouds, cyclogenesis, ocean circulation, internal waves.

RESEARCH EXPERIENCE

2015–present **CNRS, Laboratoire de Météorologie Dynamique (LMD), École Normale Supérieure (ENS) Paris**
CNRS researcher *Chargée de recherche CNRS*
& joint appointment as ENS lecturer *Maître de conférence attachée à l'ENS*

2012–2015 **CNRS, Laboratoire d'Hydrodynamique (LadHyX), École Polytechnique, France**
CNRS researcher *Chargée de recherche CNRS*

2010–2012 **Princeton University/GFDL** Atmosphere Ocean Science Dept.
Associate Research Scholar, with Isaac Held

2008–2010 **Massachusetts Institute of Technology (MIT)** Earth, Atmospheric and Planetary Sciences Dept.
Postdoctoral Associate, with Paul O'Gorman

Summers of 2004, 2005 and 2006 **NASA** Goddard Institute for Space Studies
Summer research intern, with Vittorio Canuto and Armando Howard

EDUCATION

Courant Institute of Mathematical Sciences, New York University
PhD Applied Mathematics, May 2008
MS Mathematics, May 2005
- PhD title: Wave-induced mixing in the abyssal ocean
- Advisor: Oliver Bühler

Georgia Institute of Technology
MS Aerospace Engineering, March 2003 - selective dual degree program with Supaéro
- Master's thesis topic: A wavelet method for solving optimal control problems
- Advisor: Panagiotis Tsiotras

Supaéro, École Nationale Supérieure de l'Aéronautique et de l'Espace, France
Engineering degree, March 2003
- Ranked first on the competitive entrance exam for Supaéro, Math major

Distinctions	2019–2024	**ERC Starting Grant** *European Research Council (ERC)*
	2019	**Invited professor - Spring semester** *New York University - Abu Dhabi campus*
	2012–2017	**Director of the graduate summer school** "Fluid Dynamics of Sustainability and the Environment" (FDSE): annual summer school co-organized by École Polytechnique & the University of Cambridge `fdse.org`
	2016	**Invited professor - Spring semester** *New York University - Shanghai campus*
	2015	**Joint appointment as ENS lecturer** *École Normale Supérieure, Paris*
	2009	**Publication selected to be an "Editor's Highlight"** *Geophysical Research Letter*
	2007	**"Sandra Bleistein" Prize** for notable achievement in applied math *Courant Institute of Mathematical Sciences*
	2007	**Nominated for Outstanding Teaching Award** *New York University, College of Arts and Sciences*
	2007	**Best poster presentation award** *AMS* 16^{th} *Conference on Atmospheric and Oceanic Fluid Dynamics*
	2003–2008	**Henry MacCracken Fellowship** *New York University Graduate School of Arts and Sciences*
	1999	**Ranked first** on the entrance exam for Supaéro, Math major *Supaéro, École Nationale Supérieure de l'Aéronautique et de l'Espace*
Outreach	2017–present	**Public seminars** on tropical cyclones and on climate change *Les Houches City Hall (2017); L'Institut des Hautes Études pour la Science et la Technologie (IHEST, 2018); La Direction Générale de l'Armement (2017)*
	2017–present	**Appearances in the media** on hurricanes and on climate change *Television (France Info - France télévision; BFMTV; LCI television; M6 including their famous scientific TV show E=M6; France O); Radio (AFP; France culture); Written press (Newspaper 20 minutes)*
	2015–present	**Scientific popularization** participation and scientific presentations at numerous events *Open doors days at ENS; Alumni visits at ENS; High-school students days; science for kids events*

Organization of scientific meetings and graduate schools

2019	Co-organizer of the ICTP graduate summer school on cloud organization and climate sensitivity, Trieste Italy (2 week school)
2012–present	Co-organizer of the graduate summer school FDSE (2 week school)
2018	Co-organizer of the graduate summer school "Cloud Modeling" at ENS Paris (1 week school)
2017	Co-organizer of the conference AMA - "Ateliers de Modélisation de l'Atmosphère" (1 week workshop)
2015	Co-organizer of the conference "NewWave" on internal waves (3 day workshop)

PhD committees	2019	Member of the PhD committee (reviewer) of Jiawei Bao *The University of New South Wales, Australia; advisor Steven Sherwood*
	2018	Member of the PhD committee of Antoine Renaud *ENS Lyon, advisor Antoine Venaille*
	2018	Member of the PhD committee of Maxence Lefevre *Sorbonne Université, advisor Sébastien Lebonnois*
	2018	Member of the PhD committee of Grimaud Pillet *ENS Lyon, advisor Thierry Dauxois*
	2018	Member of the PhD committee of Keshav Raja *LEGI, advisor Joël Sommeria*
	2017	Member of the PhD committee of Jessica Loriaux *KNMI, De Bilt, The Netherlands, advisor Pier Siebesma*
	2017	Member of the PhD committee of David Coppin *LMD, advisor Sandrine Bony*
	2015	Member of the PhD committee of Tamara Beitzel-Barriquand *LOCEAN, advisor Pascale Bouruet-Aubertot*
Administration	2018–present	**Editor** for the journal *Current Climate Change Reports*
	2016–present	**Elected member of the laboratory committee** of *LMD*
	2018	**Vice-president of the search committee** for an assistant professor position at *ENS Paris*
	2017	Member of the search committee for an assistant professor position, *Université de la Polynésie Française*
	2012–2017	**Director of the FDSE graduate summer school**
	2016–2017	Organizer of laboratory (LMD) seminars at *ENS*
	2014–2015	Organizer of laboratory (LadHyX) seminars at *École Polytechnique*
	2010–2012	Organizer of the climate dynamics seminar at *Princeton University*
	2008–2010	**Created and ran** a journal club to discuss papers on climate science *MIT*
	2003–present	**Reviewer for several journals**, including *Nature, Nature Geoscience, Nature Climate Change, Proceedings of the National Academy of Sciences, Reviews of Geophysics, Geophysical Research Letters, Journal of Geophysical Research - Atmospheres, Journal of Geophysical Research - Oceans, Journal of Climate, Journal of the Atmospheric Sciences, Journal of Physical Oceanography, Environmental Research Letters, Journal of Advances in Modeling Earth Systems, Journal of Fluid Mechanics, Quarterly Journal of the Royal Meteorological Society*

Main fundings & participation in national and international projects

2019–2024 **PI**, ERC Starting Grant, funded by ERC:
organisation of CLoUdS, and implications for Tropical cyclones and for the Energetics of the tropics, in current and in a waRming climate

2018–2019 **PI**, PSL/NYU international collaborative project, funded by PSL (consortium of French universities and research institutions) and NYU (New York University):
New perspectives on tropical cyclone formation and intensification

2018–2021 **PI**, LMD collaborative project, funded by LEFE (French national funding program from CNRS-INSU):
Robustness Of the Self-Aggregation of convection to Large-scale forcing, and implications for precipitation over tropical Islands

2017–2018 **co-PI**, PI: B. Legras, PSL collaborative project, funded by PSL (consortium of French universities and research institutions):
Analyse de la croissance et morphologie des amas nuageux par méthodes variationnelles d'imagerie et de dynamique des fluides

2017–2019 **co-PI**, PI: L.Oruba, collaborative project, funded by LEFE (French national funding program from CNRS-INSU):
Ocean-Atmosphere interactions: oceanic mesoscale eddies and tropical cyclones

2016–2017 **PI**, ENS collaborative project, funded by ENS Actions Incitatives:
Role of small-scale Ocean dynamics in the large-scale Oceanic and atmospheric Circulation

2016–2017 **PI**, LadHyX collaborative project, funded by Chaire DDX-EDF (Chair for Sustainable Development) at Ecole Polytechnique:
Role of ocean Internal waves in the ocean Circulation

2016–2017 **PI**, France-Berkeley international collaborative project, funded by the France-Berkeley fund:
Impact of Self- Aggregation on Cyclogenesis

2015–2016 **PI**, LadHyX/LMD collaborative project, funded by Chaire DDX-EDF:
Modeled Aggregation of Convection And Cyclogenesis

2014–2015 **PI**, LadHyX/LMD collaborative project, funded by Chaire DDX-EDF:
Organization of Convection in the Tropical Atmosphere

2013–2017 **PI**, PhD funding, funded by Direction Générale de l'Armement (DGA):
Dissipation Of Tidal Energy in the Deep Ocean

Teaching activities

2017-present	Lecturer	Clouds and Atmospheric Convection, ENS Paris
2015-present	Lecturer	Linear Algebra for Geosciences, ENS Paris
2015-present	Lecturer	Meteorology, ENS Paris
2014&16&18	Lecturer	Clouds and Climate, FDSE graduate summer school, University of Cambridge UK
2013&15&17	Lecturer	Numerical methods for fluid dynamics and applications, FDSE graduate summer school, Ecole Polytechnique
2016	Lecturer	Calculus, New York University in Shanghai
2013&14&15	Teaching Assistant	Fluid Dynamics, ENSTA
2014	Teaching Assistant	Turbulence, Ecole Polytechnique
2013	Lecturer	Physical Oceanography, ENSTA
2005&06&07&08	Lecturer	PreCalculus, Calculus II and Calculus III, NYU
2003&04&05	Teaching Assistant	Business Calculus and Quantitative Reasoning, NYU

.2 Supervisions

The superscript * indicates supervisions with publications, and those publications are listed below.

POSTDOCS

2019 (ongoing)	Nicolas Da Silva*, **main supervisor**
2017–2018 (1 year)	Jean-Baptiste Courbot, **co-supervisor** (main supervisor Bernard Legras LMD) *Now maître de conférences at the Université de Haute Alsace*

PHD

2017–2020 (ongoing)	Sara Shamekh*, **co-supervisor** (main supervisor Fabio D'Andrea LMD)
2014–2017 (3 years)	Océane Richet*, **main supervisor** (co-supervisor Jean-Marc Chomaz LadHyX) *Now postdoctoral researcher on a 3-year fellowship at the university of Tasmania*

MASTERS

2017 (2 months)	Phuong Nguyen, **main supervisor** Masters 1 internship
2016 (6 months)	Marius Guerard, **main supervisor** Masters 2 internship (co-supervisors Sandrine Bony and Thomas Dubos LMD)
2014 (2 months)	Bastien Alonzo*, **co-supervisor** Masters 1 internship (main supervisor Philippe Drobinski LMD)
2014 (4 months)	Nicolas Da Silva*, **co-supervisor** Masters 1 internship (main supervisor Philippe Drobinski LMD)
2014 (6 months)	Keshav Raja, **main supervisor** Masters 2 internship
2014 (6 months)	Adrien Lefauve*, **main supervisor** Masters 2 internship
2013 (6 months)	Francois Lefeuvre, **main supervisor** Masters 2 internship (co-supervisor Jean-Marc Chomaz LadHyX)
2013 (6 months)	Jonathan Morgan, **main supervisor** Masters 2 internship (co-supervisor Jean-Marc Chomaz LadHyX)

LICENCES (UNDERGRADUATES)

2018 (1 month)	Basile Poujol, **main supervisor** L3 internship
2018 (1 month)	Victoria Etonno, **main supervisor** L3 internship
2017 (1 month)	Octave Tessiot, **main supervisor** L3 internship
2016 (4 months)	Hugo Cui, **main supervisor** L3 research project (one day per week, co-supervisor Bernard Legras LMD)
2014 (3 months)	Tom Beucler, **main supervisor** L3 research project (one day per week)
2013 (3 months)	Adrien Boch, **main supervisor** L3 research project (one day per week)

Publications from those supervisions:

1. Da Silva N. *, S. Shamekh*, C. Muller, 2019, *Impact of convective self-aggregation on precipitation extremes*, in preparation

2. Shamekh S.*, C. Muller, J.-P. Duvel, F. D'Andrea, 2019 *How do ocean warm anomalies favor the aggregation of deep convective clouds?*, in review

3. Richet O.*, J.-M. Chomaz, C. Muller, 2018, *Internal tide dissipation at topography: triadic*

resonant instability equatorward and evanescent waves poleward of the critical latitude J. Geophys. Res. - Oceans, **123**

4. Richet O.*, C. Muller, J.-M. Chomaz, 2017, *Impact of a mean current on the internal tide energy dissipation at the critical latitude* J. Phys. Oceanogr., doi: 10.1175/JPO-D-16-0197.1.

5. Drobinski P., N. Da Silva*, G. Panthou, S. Bastin, C. Muller, B. Ahrens, M. Borga, D. Conte, G. Fosser, F. Giorgi, I. Guttler, V. Kotroni, L. Li, E. Morin, B. Onol, P. Quintana-Segui, R. Romera T. Csaba Zsolt, 2016, *Scaling precipitation extremes with temperature in the Mediterranean: past climate assessment and projection in anthropogenic scenarios* Clim. Dyn., doi:10.1007/s00382-016-3083-x

6. Drobinski P., B. Alonzo*, S. Bastin, N. Da Silva*, C. Muller, 2016, *Scaling of precipitation extremes with temperature in the French Mediterranean region: what explains the hook shape?* J. Geophys. Res. - Atmospheres, **121**

7. Lefauve* A., C. Muller, A. Melet, 2015, *A three-dimensional map of tidal dissipation over abyssal hills* J. Geophys. Res. - Oceans, **120**

.3 List of publications and talks

Peer-reviewed publications

(my updated list of publications is available at http://www.lmd.ens.fr/muller/pub.html)

1. Da Silva N., S. Shamekh, C. Muller, 2019, *Impact of convective self-aggregation on precipitation extremes* Environmental Research Letters, in preparation.

2. Muller C., Y. Takayabu, 2019, *Response of precipitation extremes to warming: what have we learned from theory and idealized cloud-resolving simulations?* Environmental Research Letters, to be submitted.
Review paper

3. Shamekh S., C. Muller, J.-P. Duvel, F. D'Andrea, 2019, *How do ocean warm anomalies favor the aggregation of deep convective clouds?* in review.

4. Muller C., 2019, *Clouds in current and in a warming climate* Chapter contribution to the book of lecture notes, from the Les Houches Summer School: Fundamental Aspects of Turbulent Flows in Climate, Volume 108, August 2017 Oxford University Press, in review.

5. Richet O., J.-M. Chomaz, C. Muller, 2018, *Internal tide dissipation at topography: triadic resonant instability equatorward and evanescent waves poleward of the critical latitude* Journal of Geophysical Research - Oceans, **123**.

6. Muller C., D. Romps, 2018, *Amplification of tropical cyclogenesis by self-aggregation feedbacks* Proceedings of the National Academy of Sciences, 201719967; DOI: 10.1073/pnas.1719967115.

7. Zuidema P., G. Torri, C. Muller, 2017, *Precipitation-induced atmospheric cold pools over oceans and their interactions with the larger-scale environment* Surveys in Geophysics, **38**
Review paper

8. Holloway C. , A. Wing, S. Bony, C. Muller, H. Masunaga, T. L'Ecuyer, D. Turner, P. Zuidema, 2017, *Observing Convective Aggregation* Surveys in Geophysics, **38**

9. Wing A., K. Emanuel, C. Holloway, C. Muller, 2017, *Convective self-aggregation in numerical simulations : a review* Surveys in Geophysics, **38**
Review paper

10. Richet O., C. Muller, J.-M. Chomaz, 2017, *Impact of a mean current on the internal tide energy dissipation at the critical latitude* Journal of Physical Oceanography, doi: 10.1175/JPO-D-16-0197.1.

11. Drobinski P., N. Da Silva, G. Panthou, S. Bastin, C. Muller, B. Ahrens, M. Borga, D. Conte, G. Fosser, F. Giorgi, I. Guttler, V. Kotroni, L. Li, E. Morin, B. Onol, P. Quintana-Segui, R. Romera T. Csaba Zsolt, 2016, *Scaling precipitation extremes with temperature in the Mediterranean: past climate assessment and projection in anthropogenic scenarios* Climate Dynamics, doi:10.1007/s00382-016-3083-x

12. Drobinski P., B. Alonzo, S. Bastin, N. Da Silva, C. Muller, 2016, *Scaling of precipitation extremes with temperature in the French Mediterranean region: what explains the hook shape?* Journal of Geophysical Research - Atmospheres, **121**

13. Lefauve A., C. Muller, A. Melet, 2015, *A three-dimensional map of tidal dissipation over abyssal hills* Journal of Geophysical Research - Oceans, **120**

14. Muller C., S. Bony 2015, *What favors convective aggregation, and why?* Geophysical Research Letters, **42**

15. Melet A., M. Nikurashin, C. Muller, S. Falahat, J. Nycander, P. Timko, B. Arbic, J. Goff, 2013, *Internal tide generation by abyssal hills using analytical theory* Journal of Geophysical Research - Oceans, **118**

16. Muller C., 2013, *Impact of convective organization on the response of tropical precipitation extremes to warming,* Journal of Climate, **26**

17. Muller C., I.M. Held, 2012, *Detailed investigation of the self-aggregation of convection in cloud-resolving simulations* Journal of the Atmospheric Sciences, **69**

18. Muller C., P.A. O'Gorman, 2011, *An energetic perspective on the regional response of precipitation to climate change* Nature Climate Change, **1**

19. Muller C., P.A. O'Gorman, L.E. Back, 2011, *Intensification of precipitation extremes with warming in a cloud-resolving model* Journal of Climate, **24**

20. O'Gorman P.A., C. Muller, 2010, *How closely do changes in surface and column water vapor follow Clausius-Clapeyron scaling in climate-change simulations?* Environmental Research Letters, **5**
ERL news article about this paper

21. Canuto V., A.M. Howard, Y. Cheng, C. Muller, A. Leboissetier and S.R. Jayne, 2010, *Ocean turbulence III: New GISS vertical mixing scheme* Ocean Modelling, **34**

22. Muller C., L.E. Back, P.A. O'Gorman, and K.A. Emanuel, 2009, *A model for the relationship between tropical precipitation and column water vapor* Geophysical Research Letters, **36**
Chosen to be an editor's highlight

23. Muller C. and O. Buhler, 2009, *Saturation of the internal tides and induced mixing in the abyssal ocean* Journal of Physical Oceanography, **39**

24. Buhler O. and C. Muller, 2007, *Instability and focusing of internal tides in the deep ocean* Journal of Fluid Mechanics, **588**

Other publications

1. Muller C., S. Bony, 2016, *Self-Aggregation of atmospheric convection in idealized simulations*, Workshop report, Oberwolfach Workshop Multiscale Interactions in Geophysical Fluids

2. Muller C., 2016, *Dynamique des fluides géophysiques, l'expérience Chinoise*, News article, Journal du Bureau du CNRS en Chine

3. Muller C., A. Lefauve, 2014, *A worldwide map of tidal dissipation* Scientific contribution for the exhibition Lost in Fathoms by A. Tondeur & J.M. Chomaz, GV Art gallery London.

4. Muller C., A. Melet, M. Nikurashin, 2013, *Abyssal Hill Roughness Impact on Internal Tide Generation: Linear Theory* Communication for the workshop OGOA "Ondes de Gravité dans l'Océan et l'Atmosphère" 23-24 may 2013 ENS Lyon

5. Muller C.J., 2008, *Wave-induced mixing above the abyssal seafloor* Ph.D. Thesis, New York University

6. Muller C.J., 2007. Communications from CFM2007 18è congrès français de mécanique à Grenoble, august 2007 http://irevues.inist.fr/cfm2007

Invited talks

(my updated list of talks is available at http://www.lmd.ens.fr/muller/talks.html)

1. **Géopolitique du risque** seminar series, Oct 2018, ENS Paris

2. **Journée Géosciences et Sociétés** for professors of "classes préparatoires", Oct 2018, ENS Paris

3. **Workshop on Non-Hydrostatic Ocean Modeling**, Oct 2018, Brest

4. **WCRP workshop** WCRP Grand Challenge on Weather and Climate Extremes/GEWEX Global Data and Analysis Panel workshop, Offenbach, Germany, July 2018

5. **EGU meeting** (European Geophysical Union), Understanding past, present and future changes in the hydrological cycle session, Vienna, Austria, Apr 2018

6. **University of Cambridge**, Fluid Mechanics Seminar - Department of Applied Mathematics and Theoretical Physics DAMTP, Mar 2018

7. **Journée thématique Institut Pierre Simon Laplace IPSL**. Seminar Cyclones and climate change, Feb 2018

8. **Institut des Hautes Études pour la Science et la Technologie (IHEST)**; Ministère de l'Enseignement supérieur, de la Recherche et de l'Innovation, Séminaire et table ronde, Tropical cyclones, Jan 2018

9. **Direction Générale de l'Armement (DGA)**, Seminar, Dans l'oeil du cyclone, Dec 2017

10. **Réunion du Groupement De Recherche (GDR) Megha-Tropiques** Self-aggregation of atmospheric convection in idealized simulations, Nov 2017

11. **Les Houches city hall**, public seminar, Le changement climatique vu des nuages, France, Aug 2017

12. **Les Houches école de physique**, graduate-level courses. Fundamental aspects of turbulent flows in climate dynamics, France, Aug 2017

13. **Gordon Research Conference on Radiation & Climate**, Connecting Observations to Global Circulation Modeling Challenges, Portland, USA, July 2017

14. **Minisymposium KNMI**, Convective extreme precipitation at mid-latitudes, Netherlands, Jan 2017
15. **AGU Fall Meeting** (American Geophysical Union), San Francisco, USA, Dec 2016
16. **Oberwolfach meeting**, Multiscale interactions in geophysical fluids, Germany, Aug 2016
17. **University of Edinburgh**, Trapped Waves and wave radiation in fluid mechanics workshop, Scotland, July 2016
18. **Imperial College**, Atmospheric Physics Seminar, UK, June 2016
19. **ETH Zurich**, Workshop Cloud and boundary layer dynamics: the next decade, Switzerland, June 2016
20. **Conference on Mathematical Geophysics**, Paris, France, June 2016
21. **New York University - Shanghai**, Partial Differential Equations Seminar, Shanghai, China, May 2016
22. **EGU meeting** (European Geophysical Union), Hydrological cycle session (invitation declinée), Vienna, Austria, Apr 2016
23. **International Space Science Institute Workshop**, Bern, Switzerland, Feb 2016
24. **University of Reading**, Meteorology Departmental Seminars, Oct 2015
25. **University of Reading**, Mathematics of Planet Earth, London Mathematical Society (LMS), Sept 2015
26. **UC Berkeley**, Atmospheric Sciences Center seminar, USA, Aug 2015
27. **ESPCI Paris** Bifurcations and Instabilities in Fluid Dynamics, France July 2015
28. **Les Houches école de physique**, Theoretical advances in planetary flows and climate dynamics, France, Mar 2015
29. **Geophysical Fluid Dynamics (GFD) summer school**, Climate physics and dynamics, Woods Hole MA, USA, Aug 2014
30. **Latsis Symposium** Atmosphere and Climate Dynamics: From Clouds to Global Circulations, Zurich, Switzerland, June 2014
31. **Grand Challenge Workshop** Clouds, circulation and climate sensitivity, Germany, Mar 2014
32. **Lorenz center workshop MIT** Cambridge MA, USA, Feb 2014
33. **Max Planck Institute for Meteorology** KlimaCampus Seminar, Hamburg, Germany, Nov 2013
34. **National Oceanic & Atmospheric Administration (NOAA)** Physical Sciences Division Seminar, Boulder CO, USA, Oct 2013
35. **Texas Tech University** Red Raider Mini-Symposium, Lubbock TX, USA, Oct 2013

.4 List of 5 selected publications attached with this document

1. Richet O., J.-M. Chomaz, C. Muller, 2018, *Internal tide dissipation at topography: triadic resonant instability equatorward and evanescent waves poleward of the critical latitude* Journal of Geophysical Research - Oceans, **123**.

2. Muller C., D. Romps, 2018, *Amplification of tropical cyclogenesis by self-aggregation feedbacks* Proceedings of the National Academy of Sciences, 201719967; DOI: 10.1073/pnas.1719967115.

3. Wing A., K. Emanuel, C. Holloway, C. Muller, 2017, *Convective self-aggregation in numerical simulations : a review* Surveys in Geophysics, **38**
Review paper

4. Muller C., S. Bony 2015, *What favors convective aggregation, and why?* Geophysical Research Letters, **42**

5. Muller C., 2013, *Impact of convective organization on the response of tropical precipitation extremes to warming,* Journal of Climate, **26**

Bibliography

[Attema et al., 2014] Attema, J. J., Loriaux, J. M., and Lenderink, G. (2014). Extreme precipitation response to climate perturbations in an atmospheric mesoscale model. *Environ. Res. Lett.*, 9(1):014003.

[Bao and Sherwood, 2019] Bao, J. and Sherwood, S. C. (2019). The role of convective self-aggregation in extreme instantaneous versus daily precipitation. *J. Adv. Model. Earth Syst.*, 11(1):19–33.

[Bell, 1975] Bell, T. H. (1975). Lee waves in stratified flows with simple harmonic time dependence. *J. Fluid Mech.*, 67:705–722.

[Betts and Harshvardhan, 1987] Betts, A. K. and Harshvardhan (1987). Thermodynamic constraint on the cloud liquid water feedback in climate models. *J. Geophys. Res.*, 92(7):8483–8485.

[Bony et al., 2015] Bony, S., Stevens, B., and Coauthors (2015). Clouds, circulation and climate sensitivity. *Nature Geosci.*

[Bourget et al., 2013] Bourget, B., Dauxois, T., Joubaud, S., and Odier, P. (2013). Experimental study of parametric subharmonic instability for internal plane waves. *J. Fluid Mech.*, 723:1–20.

[Bretherton et al., 2005] Bretherton, C. S., Blossey, P. N., and Khairoutdinov, M. (2005). An energy-balance analysis of deep convective self-aggregation above uniform SST. *J. Atmos. Sci.*, 62(12):4273–4292.

[Bühler and Muller, 2007] Bühler, O. and Muller, C. J. (2007). Instability and focusing of internal tides in the deep ocean. *J. Fluid Mech.*, 588:1–28.

[Chelton, 2011] Chelton, D. (2011). Global observations of nonlinear mesoscale eddies. *Prog. Oceanogr.*

[Coppin and Bony, 2017] Coppin, D. and Bony, S. (2017). Internal variability in a coupled general circulation model in radiative-convective equilibrium. *Geophys. Res. Lett.*, 44.

[Da Silva et al., 2019] Da Silva, N., Shamekh, S., and Muller, C. J. (2019). Impact of convective self-aggregation on precipitation extremes. *Environ. Res. Lett.*, (to be submitted).

[Davis, 2015] Davis, C. A. (2015). The formation of moist vortices and tropical cyclones in idealized simulations. *J. Atmos. Sci.*, 72(9):3499–3516.

[De Lavergne et al., 2016] De Lavergne, C., Madec, G., Le Sommer, J., Nurser, A. J. C., and Naveira Garabato, A. C. (2016). On the consumption of antarctic bottom water in the abyssal ocean. *J. Phys. Oceanogr.*, 46:635?661.

[DeMaria et al., 2014] DeMaria, M., Sampson, C. R., Knaff, J. A., and Musgrave, K. D. (2014). Is tropical cyclone intensity guidance improving? *Bull. Amer. Meteor. Soc.*, 95(3):387–398.

[Drobinski et al., 2016a] Drobinski, P., Alonzo, B., Bastin, S., Da Silva, N., and Muller, C. (2016a). Scaling of precipitation extremes with temperature in the french mediterranean region: What explains the hook shape? *J. Geophys. Res.*, 121(7):3100–3119.

[Drobinski et al., 2016b] Drobinski, P., Da Silva, N., Panthou, G., Bastin, S., Muller, C., Ahrens, B., Borga, M., Conte, D., Fosser, G., Giorgi, F., et al. (2016b). Scaling precipitation extremes with temperature in the mediterranean: past climate assessment and projection in anthropogenic scenarios. *Clim. Dynam.*, 51(3):1237–1257.

[Dunkerton et al., 2009] Dunkerton, T. J., Montgomery, M., and Wang, Z. (2009). Tropical cyclogenesis in a tropical wave critical layer: Easterly waves. *Atmos. Chem. Phys.*, 9(15).

[Emanuel, 2003] Emanuel, K. (2003). Tropical cyclones. *Annu. Rev. Earth Planet. Sci.*, 31(1):75–104.

[Emanuel, 1986] Emanuel, K. A. (1986). An air-sea interaction theory for tropical cyclones. part 1: Steady-state maintenance. *J. Atmos. Sci.*, 43(6):585–604.

[Emanuel, 1994] Emanuel, K. A. (1994). *Atmospheric convection*. Oxford University Press, USA.

[Emanuel et al., 2014] Emanuel, K. A., Wing, A. A., and Vincent, E. M. (2014). Radiative-convective instability. *J. Adv. Model. Earth Syst.*, 6(1):75–90.

[Ferrari, 2014] Ferrari, R. (2014). Oceanography: What goes down must come up. *Nature*, 513(7517):179.

[Garner and Thorpe, 1992] Garner, S. T. and Thorpe, A. J. (1992). The development of organized convection in a simplified squall-line model. *Quart. J. Roy. Meteor. Soc.*, 118(503):101–124.

[Garrett and Kunze, 2007] Garrett, C. and Kunze, E. (2007). Internal tide generation in the deep ocean. *Annu. Rev. Fluid Mech.*, 39:57–87.

[Grabowski, 2006] Grabowski, W. W. (2006). Impact of explicit atmosphere-ocean coupling on mjo-like coherent structures in idealized aquaplanet simulations. *J. Atmos. Sci.*, 63:2289–2306.

[Hamada et al., 2015] Hamada, A., Takayabu, Y. N., Liu, C., and Zipser, E. J. (2015). Weak linkage between the heaviest rainfall and tallest storms. 6:6213.

[Held et al., 1993] Held, I. M., Hemler, R. S., and Ramaswamy, V. (1993). Radiative-convective equilibrium with explicit two-dimensional moist convection. *J. Atmos. Sci.*, 50(23):3909–3909.

[Held and Soden, 2006] Held, I. M. and Soden, B. J. (2006). Robust Responses of the Hydrological Cycle to Global Warming. *J. Climate*, 19:5686–5699.

[Holloway et al., 2017] Holloway, C., Wing, A. A., Bony, S., Muller, C., Masunaga, H., L'Ecuyer, T., Turner, D., and Zuidema, P. (2017). Observing convective aggregation. *Surv. Geophys.*, 38.

[Holloway and Neelin, 2009] Holloway, C. E. and Neelin, J. D. (2009). Moisture vertical structure, column water vapor, and tropical deep convection. *J. Atmos. Sci.*, 66(6):1665–1683.

[Holloway and Woolnough, 2016] Holloway, C. E. and Woolnough, S. J. (2016). The sensitivity of convective aggregation to diabatic processes in idealized radiative-convective equilibrium simulations. *J. Adv. Model. Earth Syst.*, 8(1):166–195.

[Iribarne and Godson, 1981] Iribarne, J. V. and Godson, W. L. (1981). *Atmospheric thermodynamics*. Springer. Section 9.14.

[Khairoutdinov and Emanuel, 2013] Khairoutdinov, M. and Emanuel, K. (2013). Rotating radiative-convective equilibrium simulated by a cloud-resolving model. *J. Adv. Model. Earth Syst.*, 5(4):816–825.

[Khairoutdinov and Emanuel, 2010] Khairoutdinov, M. F. and Emanuel, K. A. (2010). Aggregated convection and the regulation of tropical climate. *Preprints, 29th conference on Hurricanes and Tropical Meteorology, Tucson, AZ, Amer. Meteor. Soc.*, P2.69.

[Khairoutdinov and Randall, 2003] Khairoutdinov, M. F. and Randall, D. A. (2003). Cloud-resolving modeling of the arm summer 1997 iop: Model formulation, results, uncertainties and sensitivities. *J. Atmos. Sci.*, 60:607–625.

[Kharin et al., 2007] Kharin, V. V., Zwiers, F. W., Zhang, X., and Hegerl, G. C. (2007). Changes in temperature and precipitation extremes in the ipcc ensemble of global coupled model simulations. *J. Climate*, 20:1419–1444.

[Kuang, 2012] Kuang, Z. (2012). Weakly forced mock walker cells. *J. Atmos. Sci.*, 69:2759–2786.

[Lefauve et al., 2015] Lefauve, A., Muller, C., and Melet, A. (2015). A three-dimensional map of tidal dissipation over abyssal hills. *J. Geophys. Res.*, 120(7):4760–4777.

[Legg, 2014] Legg, S. (2014). Scattering of low-mode internal waves at finite isolated topography. *J. Phys. Oceanogr.*, 44(1):359–383.

[Loriaux et al., 2013] Loriaux, J. M., Lenderink, G., De Roode, S. R., and Siebesma, A. P. (2013). Understanding convective extreme precipitation scaling using observations and an entraining plume model. *J. Atmos. Sci.*, 70(11):3641–3655.

[Lutsko and Cronin, 2018] Lutsko, N. J. and Cronin, T. W. (2018). Increase in precipitation efficiency with surface warming in radiative-convective equilibrium. *J. Adv. Model. Earth Syst.*, 10(11):2992–3010.

[MacKinnon et al., 2013] MacKinnon, J. A., Alford, M. H., Sun, O., Pinkel, R., Zhao, Z., and Klymak, J. (2013). Parametric subharmonic instability of the internal tide at 29°N. *J. Phys. Oceanogr.*, 43(1):17–28.

[MacKinnon and Winters, 2005] MacKinnon, J. A. and Winters, K. B. (2005). Subtropical catastrophe: Significant loss of low-mode tidal energy at 28.9°N. *Geophys. Res. Lett.*, 32(15).

[Manabe and Strickler, 1964] Manabe, S. and Strickler, R. F. (1964). Thermal equilibrium of the atmosphere with a convective adjustment. *J. Atmos. Sci.*, 21(4):361–385.

[Mapes, 1993] Mapes, B. E. (1993). Gregarious tropical convection. *J. Atmos. Sci.*, 50(13):2026–2037.

[Marshall et al., 1997] Marshall, J., Adcroft, A., Hill, C., Perelman, L., and Heisey, C. (1997). A finite-volume, incompressible navier stokes model for studies of the ocean on parallel computers. *J. Geophys. Res.*, 102(C3):5753–5766.

[Maurer et al., 2016] Maurer, P., Joubaud, S., and Odier, P. (2016). Generation and stability of inertia–gravity waves. *J. Fluid Mech.*, 808:539–561.

[Mauritsen and Stevens, 2015] Mauritsen, T. and Stevens, B. (2015). Missing iris effect as a possible cause of muted hydrological change and high climate sensitivity in models. *Nature Geosci.*, 8(5):346.

[Melet et al., 2013a] Melet, A., Hallberg, R., Legg, S., and Polzin, K. (2013a). Sensitivity of the ocean state to the vertical distribution of internal-tide-driven mixing. *J. Phys. Oceanogr.*, 43(3):602–615.

[Melet et al., 2013b] Melet, A., Nikurashin, M., Muller, C., Falahat, S., J., N., G., T. P., K., A. B., and A., G. J. (2013b). Internal tide generation by abyssal hills using analytical theory. *J. Geophys. Res.*, 118:6303–6318.

[Muller, 2019] Muller, C. (2019). *Clouds in current and in a warming climate*. Chapter contribution to the book of lecture notes from "Les Houches 2017 Summer School: Fundamental Aspects of Turbulent Flows in Climate". Editors: F. Bouchet, C. Salomon, T. Schneider, A. Venaille. Oxford University Press.

[Muller, 2013] Muller, C. J. (2013). Impact of convective organization on the response of tropical precipitation extremes to warming. *J. Climate*, 26:5028–5043.

[Muller et al., 2009] Muller, C. J., Back, L. E., O'Gorman, P. A., and Emanuel, K. A. (2009). A model for the relationship between tropical precipitation and column water vapor. *Geophys. Res. Lett.*, 36:L16804.

[Muller and Bony, 2015] Muller, C. J. and Bony, S. (2015). What favors convective aggregation and why? *Geophys. Res. Lett.*, 42.

[Muller and Bühler, 2009] Muller, C. J. and Bühler, O. (2009). Saturation of the internal tides and induced mixing in the abyssal ocean. *J. Phys. Oceanogr.*, 39:2077–2096.

[Muller and Held, 2012] Muller, C. J. and Held, I. M. (2012). Detailed investigation of the self-aggregation of convection in cloud-resolving simulations. *J. Atmos. Sci.*, 69:2551–2565.

[Muller and O'Gorman, 2011] Muller, C. J. and O'Gorman, P. A. (2011). An energetic perspective on the regional response of precipitation to climate change. *Nature Climate Change*, 1(5):266–271.

[Muller et al., 2011] Muller, C. J., O'Gorman, P. A., and Back, L. E. (2011). Intensification of precipitation extremes with warming in a cloud-resolving model. *J. Climate*, 24(11):2784–2800.

[Muller and Romps, 2018] Muller, C. J. and Romps, D. M. (2018). Acceleration of tropical cyclogenesis by self-aggregation feedbacks. *Proc. Natl. Acad. Sci. (USA)*, page 201719967.

[Muller and Takayabu, 2019] Muller, C. J. and Takayabu, Y. (2019). Response of precipitation extremes to warming: what have we learned from theory and idealized cloud-resolving simulations? *Environ. Res. Lett.*, (to be submitted).

[Munk and Wunsch, 1998] Munk, W. and Wunsch, C. (1998). Abyssal recipes II: energetics of tidal and wind mixing. *Deep-Sea Res. Part I: Oceanogr. Res. Papers*, 45:1977–2010.

[Nikurashin and Legg, 2011] Nikurashin, M. and Legg, S. (2011). A mechanism for local dissipation of internal tides generated at rough topography. *J. Phys. Oceanogr.*, 41(2):378–395.

[Nikurashin and Vallis, 2012] Nikurashin, M. and Vallis, G. (2012). A theory of the interhemispheric meridional overturning circulation and associated stratification. *J. Phys. Oceanogr.*, 42(10):1652–1667.

[Nikurashin et al., 2013] Nikurashin, M., Vallis, G. K., and Adcroft, A. (2013). Routes to energy dissipation for geostrophic flows in the southern ocean. *Nature Geosci.*, 6(1):48.

[O'Gorman, 2015] O'Gorman, P. A. (2015). Precipitation extremes under climate change. *Curr. Clim. Change Rep.*, 1(2):49–59.

[O'Gorman and Muller, 2010] O'Gorman, P. A. and Muller, C. J. (2010). How closely do changes in surface and column water vapor follow Clausius-Clapeyron scaling in climate-change simulations? *Environ. Res. Lett.*, 5:025207.

[O'Gorman and Schneider, 2009] O'Gorman, P. A. and Schneider, T. (2009). The physical basis for increases in precipitation extremes in simulations of 21st-century climate change. *Proc. Natl. Acad. Sci. (USA)*, 106:14773–14777.

[Parodi and Emanuel, 2009] Parodi, A. and Emanuel, K. A. (2009). A theory for buoyancy and velocity scales in deep moist convection. *J. Atmos. Sci.*, 66:3449–3463.

[Polzin et al., 1997] Polzin, K. L., Toole, J. M., Ledwell, J. R., and Schmitt, R. W. (1997). Spatial variability of turbulent mixing in the abyssal ocean. *Science*, 276(5309):93–96.

[Ramsay and Sobel, 2011] Ramsay, H. A. and Sobel, A. H. (2011). Effects of relative and absolute sea surface temperature on tropical cyclone potential intensity using a single-column model. *J. Climate*, 24(1):183–193.

[Richet et al., 2018] Richet, O., Chomaz, J.-M., and Muller, C. (2018). Internal tide dissipation at topography: Triadic resonant instability equatorward and evanescent waves poleward of the critical latitude. *J. Geophys. Res.*, 123(9):6136–6155.

[Richet et al., 2017] Richet, O., Muller, C., and Chomaz, J.-M. (2017). Impact of a mean current on the internal tide energy dissipation at the critical latitude. *J. Phys. Oceanogr.*, 47(6):1457–1472.

[Romps, 2011] Romps, D. M. (2011). Response of tropical precipitation to global warming. *J. Atmos. Sci.*, 68(1):123–138.

[Rotunno et al., 1988] Rotunno, R., Klemp, J. B., and Weisman, M. L. (1988). A theory for strong, long-lived squall lines. *J. Atmos. Sci.*, 45(3):463–4.

[Shamekh et al., 2019] Shamekh, S., Muller, C., Duvel, J.-P., and D'Andrea, F. (2019). How do ocean warm anomalies favor the aggregation of deep convective clouds? *J. Atmos. Sci.*, (in review).

[Shi and Bretherton, 2014] Shi, X. and Bretherton, C. S. (2014). Large-scale character of an atmosphere in rotating radiative-convective equilibrium. *J. Adv. Model. Earth Syst.*

[Singh and O'Gorman, 2013] Singh, M. S. and O'Gorman, P. A. (2013). Influence of entrainment on the thermal stratification in simulations of radiative-convective equilibrium. *Geophys. Res. Lett.*, 40(16):4398–4403.

[Singleton and Toumi, 2013] Singleton, A. and Toumi, R. (2013). Super clausius–clapeyron scaling of rainfall in a model squall line. *Quart. J. Roy. Meteor. Soc.*, page doi:10.1002/qj.1919.

[Smith and Sandwell, 1997] Smith, W. H. F. and Sandwell, D. T. (1997). Global Sea Floor Topography from Satellite Altimetry and Ship Depth Soundings. *Science*, 277:1956–1962.

[Sommeria et al., 2016] Sommeria, J., Ajayi, A.-O., Raja, K., Staquet, C., Viboud, S., and Voisin, B. (2016). Laboratory modelling of momentum transport by internal gravity waves and eddies in the antarctic circumpolar current. In *VIIIth International Symposium on Stratified Flows (ISSF)*.

[Staquet and Sommeria, 2002] Staquet, C. and Sommeria, J. (2002). Internal gravity waves: from instabilities to turbulence. *Annu. Rev. Fluid Mech.*, 34(1):559–593.

[Sugimoto et al., 2017] Sugimoto, S., Aono, K., and Fukui, S. (2017). Local atmospheric response to warm mesoscale ocean eddies in the kuroshio–oyashio confluence region. *Scientific reports*, 7(1):11871.

[Sugiyama et al., 2010] Sugiyama, M., Shiogama, H., and Emori, S. (2010). Precipitation extreme changes exceeding moisture content increases in MIROC and IPCC climate models. *Proc. Natl. Acad. Sci. (USA)*, 107:571–575.

[Tan et al., 2015] Tan, J., Jakob, C., Rossow, W. B., and Tselioudis, G. (2015). Increases in tropical rainfall driven by changes in frequency of organized deep convection. *Nature*, 519(7544):451.

[Thorpe, 2005] Thorpe, S. A. (2005). *The Turbulent Ocean*. Cambridge University Press.

[Tobin et al., 2012] Tobin, I., Bony, S., and Roca, R. (2012). Observational evidence for relationships between the degree of aggregation of deep convection, water vapor, surface fluxes, and radiation. *J. Climate*, 25:6885–6904.

[Tomassini et al., 2015] Tomassini, L., Voigt, A., and Stevens, B. (2015). On the connection between tropical circulation, convective mixing, and climate sensitivity. *Quart. J. Roy. Meteor. Soc.*, 141(689):1404–1416.

[Tompkins, 2001] Tompkins, A. M. (2001). Organization of tropical convection in low vertical wind shears: The role of water vapor. *J. Atmos. Sci.*

[Trenberth, 1999] Trenberth, K. E. (1999). Conceptual framework for changes of extremes of the hydrological cycle with climate change. *Climatic Change*, 42:327–339.

[Waterhouse et al., 2014] Waterhouse, A. F., MacKinnon, J. A., Nash, J. D., Alford, M. H., Kunze, E., Simmons, H. L., Polzin, K. L., St. Laurent, L. C., Sun, O. M., Pinkel, R., Talley, L. D., Whalen, C. B., Huussen, T. N., Carter, G. S., Fer, I., Waterman, S., Naveira Garabato, A. C., Sanford, T. B., and Lee, C. M. (2014). Global patterns of diapycnal mixing from measurements of the turbulent dissipation rate. *J. Phys. Oceanogr.*, 44:1854–1872.

[Wheeler and Kiladis, 1999] Wheeler, M. and Kiladis, G. N. (1999). Convectively coupled equatorial waves: Analysis of clouds and temperature in the wavenumber–frequency domain. *J. Atmos. Sci.*, 56(3):374–399.

[Wing et al., 2017] Wing, A., Emanuel, K., Holloway, C., and Muller, C. (2017). Convective self-aggregation in numerical simulations: A review. *Surv. Geophys.*, 38.

[Wing et al., 2016] Wing, A. A., Camargo, S. J., and Sobel, A. H. (2016). Role of radiative–convective feedbacks in spontaneous tropical cyclogenesis in idealized numerical simulations. *J. Atmos. Sci.*, 73(7):2633–2642.

[Wing and Cronin, 2016] Wing, A. A. and Cronin, T. W. (2016). Self-aggregation of convection in long channel geometry. *Quart. J. Roy. Meteor. Soc.*

[Wing and Emanuel, 2014] Wing, A. A. and Emanuel, K. A. (2014). Physical mechanisms controlling self-aggregation of convection in idealized numerical modeling simulations. *Journal of Advances in Modeling Earth Systems*.

[Wunsch, 2000] Wunsch, C. (2000). Moon, tides and climate. *Nature*, 405:743–4.

[Wunsch and Ferrari, 2004] Wunsch, C. and Ferrari, R. (2004). Vertical mixing, energy, and the general circulation of the oceans. *Annu. Rev. Fluid Mech.*, 36(1):281–314.

[Young et al., 2008] Young, W. R., Tsang, Y.-K., and Balmforth, N. J. (2008). Near-inertial parametric subharmonic instability. *J. Fluid Mech.*, 607:25–49.

[Zuidema et al., 2017] Zuidema, P., Torri, G., Muller, C., and Chandra, A. (2017). Precipitation-induced atmospheric cold pools over oceans and their interactions with the larger-scale environment. *Surv. Geophys.*, 38.